

AD-A275 777



2

Global Acoustic Mapping of Ocean Temperatures

GAMOT



DTIC
ELECTE
FEB 14 1994
A

Woods Hole Oceanographic Institution
The Pennsylvania State University
Naval Research Laboratory-Stennis
The Florida State University
University of Alaska
University of Texas at Austin

This document has been approved
for public release and sale; its
distribution is unlimited.

*Original contains color
plates: All DTIC reproductions
will be in black and
white*

QUARTERLY PROGRESS REPORT

October-December 1993

94 2 10 178

94-04854



DISCLAIMER NOTICE



THIS DOCUMENT IS BEST QUALITY AVAILABLE. THE COPY FURNISHED TO DTIC CONTAINED A SIGNIFICANT NUMBER OF COLOR PAGES WHICH DO NOT REPRODUCE LEGIBLY ON BLACK AND WHITE MICROFICHE.

GAMOT



January 31, 1994

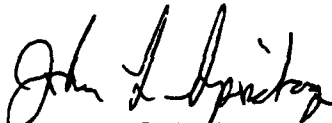
Dr. Ralph Alewine
Advanced Research Projects Agency
3701 North Fairfax Drive
Arlington, VA 22203-1714

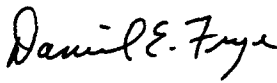
Dear Dr. Alewine,

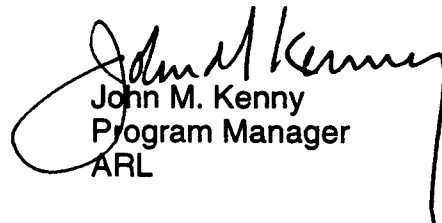
The attached report fulfills the third quarterly progress report requirement for the period from October 1, 1993 to December 31, 1993 as contained in the ARPA Grant No: MDA972-93-1-0004 entitled "Real Time System for Practical Acoustic Monitoring of Global Ocean Temperature" issued by the Contracts Management Office. The United States Government has a royalty-free license throughout the world in all copy rightable material contained herein. This report is approved for unlimited distribution and public release. Additional copies of this report will be mailed to the distribution list contained in Attachment Number 2 of the Grant.

Financial status reports will be submitted separately from this report. Woods Hole Oceanographic Institution, as the Grantee, will submit all financial reports directly to you.

The information contained in this report represents the inputs and opinions of the entire GAMOT team; the Woods Hole Oceanographic Institution, the Pennsylvania State University, the Applied Research Laboratory, the Florida State University, University of Alaska, University of Texas at Austin and NRL-Stennis. If this report generates any questions, please do not hesitate to direct your questions or comments to the Principal Investigators or the Program Manager.


John L. Spiesberger
Principal Investigator
WHOI/PSU


Daniel E. Frye
Principle Investigator
WHOI


John M. Kenny
Program Manager
ARL

Dist	Avail a d/or Special
A-1	

January 15, 1994

GAMOT EXECUTIVE SUMMARY

Work continues on all GAMOT Tasks as described in ARPA Grant No: MDA972-93-1-0004.

- **Task A.** Task A work is on schedule. GAMOT is investigating the acoustic thermometry data taken in 1987 along fifteen basin scale sections in the northeast Pacific. Multipaths along 13 of the 15 sections have been successfully interpreted using ray theory. Of particular note is that the temperatures in the northeast Pacific were colder in the summer of 1987 than climatological data compiled by Levitus.

Work continues on the development of the signal processing package for the SSAR.

We are computing travel times of rays through the ocean models of the Pacific. These travel times are being compared with acoustic travel time data taken in the 1980's. We are also developing theoretical extensions to classical ray theory that may allow us to extend the accuracy of travel times for acoustic multipaths below 100 Hz. Classical ray theory alone has too large an error for mapping global ocean temperatures below 100 Hz.

- **Task B.** The FSU tasks and deliverables are on schedule. Model runs of the northeast Pacific Ocean for 1961-1991 driven by equatorial Kelvin waves and real winds have been completed. Estimated acoustic travel time anomalies vary over periods from months to a decade. Travel time anomaly due to variations in upper layer thickness are shown to compare favorably to published variations in August 1987. Interannual phenomenon such as El Nino are seen to have significant effect on travel times, depending on the particular path.

- **Task C.** Development of the SSAR is proceeding on schedule with no significant delays or problems. The follow-on test of the Standard SSAR design was conducted in early November and the prototype was then deployed for a long-term, free drifting test. The buoy initially drifted away from Bermuda (approximately 100 miles south) but then drifted back to the south coast of the island. To keep it from going aground, a retrieval cruise was conducted in early December. The buoy was retrieved, examined for any mechanical degradation and re deployed 70 miles east of Bermuda. It is presently located about 180 miles southeast of the island. Laboratory testing is continuing at Tension Member Technology. Two short hoses have been tested to destruction and two more hoses are being built for additional tests. Analysis of the data collected with the Standard prototype in November is underway. Final mechanical and electrical designs are nearing completion and parts are being ordered for the ten operational units. Schedules for system tests at the AUTEC range and off the coast of California are tentatively set for March and early April, respectively.

- **Task D.** Last quarter ARPA directed the GAMOT Principal Investigators to submit a proposal to increase the scope of Task D (procure a 70 Hz source which

could be moored autonomously). Seven contractors responded to the RFP. Site visits were conducted and additional question asked to ensure that there was sufficient information available to fairly evaluate all of the responses.

At a meeting at WHOI in December 1993, the responses were weighted and the field of contenders was reduced to the two most promising responses. The procurement specifications and statements of work are being finalized. The proposal will be presented in early February 1994.

- **Meetings.** . An Ocean Modeling meeting was conducted by Dr. J. O'Brien on October 8 at Florida State University. The second Executive Committee meeting was held on October 15 in Washington DC. The next Program Review will be hosted by Dr. O'Brien and GAMOT at Florida State University on March 18, 1994.

- **Issues and Concerns.** In the previous quarterly reports, two issues were addressed:

- Acoustic interaction of cabled sources with the bottom slope, and
- Identification of a source for the autonomous mooring.

These issues have not been resolved and there is no new information to report.

There are no new issues.

TASK A

TOMOGRAPHIC DATA ANALYSIS

All Task A work is on schedule.

GAMOT is investigating the acoustic thermometry data taken in 1987 along fifteen basin scale sections in the northeast Pacific. At this time, multipaths along 13 of the 15 sections have been successfully interpreted using ray theory. Identification of the multipaths is a crucial step in solving the inverse problem. The program ZRAY, developed on this project, was used to implement the ray calculations. The importance of the program ZRAY is discussed in depth in Appendix A.

Of particular note is that the temperatures in the northeast Pacific were colder in the summer of 1987 than climatological data compiled by Levitus. This result is easy to see with sound because the acoustic multipaths arrived between 0.3 and 1.5 s later than the travel times of rays traced through Levitus' climatological data. Since the data are late, the speed of sound is slower and the ocean is colder than Levitus' data. The acoustic technique is straightforward.

GAMOT continues to develop the signal processing package for the SSAR. The software development is on schedule.

We are computing travel times of rays through the ocean models of the Pacific. These travel times are being compared with acoustic travel time data taken in the 1980's. Work is still in progress.

We are developing theoretical extensions to classical ray theory that may allow us to extend the accuracy of travel times for acoustic multipaths below 100 Hz. Classical ray theory alone has too large an error for mapping global ocean temperatures below 100 Hz.

Figures

Fig. 1 Task A Schedule

Appendix A: Successful Modelling of Acoustic Multipaths over a 3000 km
Section in the Pacific with Rays

[illegible]

Successful modelling of acoustic multipaths over a 3000 km section in the Pacific with
rays

John L. Spiesberger

Department of Meteorology and the Applied Research Laboratory 512 Walker
Building, Pennsylvania State University University Park, PA 16802

Eugene Terray and Ken Prada

Department of Applied Ocean Physics and Engineering, Bigelow 2, Woods Hole
Oceanographic Institution, Woods Hole, MA. 02543

ABSTRACT

A new ray model is compared with tomographic data from basin-scale transmissions in the northeast Pacific (250 Hz, 0.016 ms resolution, ~ 3000 km). Model calculations resemble the arrival pattern of the acoustic multipaths quite well. To date, this is the longest distance in the ocean over which ray theory has been shown to accurately predict the acoustic impulse response of the ocean. The new ray model confirms previous analysis, based on the MPP ray model, that basin-scale tomography is feasible and that the international algorithm for the speed of sound in seawater is too fast. However, the new ray model looks much more like the data than MPP because the new model has a more realistic bottom and a more realistic sound speed field. At 3000 km, there is no evidence that ray theory suffers from any lack of predictability due to chaotic behavior in this particular experiment. The new model is suitable for automating the identification of acoustic multipaths over basin scales.

Technical Area: Underwater Acoustics

(PACS) Subject Classification numbers: 43.30Cq, 43.30Pc

INTRODUCTION

In 1986 and 1987, acoustic transmissions were broadcast over 3000 km in the northeast Pacific¹ (Fig. 1). The transmissions had a center frequency of 250 Hz and a temporal resolution of 0.016 s (Fig. 2). The source was mounted at about 0.86 km depth on a mooring² and the signals were detected on a U.S. Navy SOSUS station. The precise location and depth of the receiver are classified.

Previous analysis of these data with the MPP ray model provided evidence that basin-scale tomography was practical¹ and that the international standard algorithm for the speed of sound was too fast at pressures found below about 1 km (Refs. 3-6). We are confident of the ray modelling done with MPP because further experiments also found the international standard algorithm for the speed of sound was too fast⁷.

It is not obvious, on first look, that the MPP ray modelling is correct because it generates rays which do not appear in the data (Fig. 2). Indeed, MPP generates spurious arrivals because it unrealistically puts corners both in the sound speed field and in the bottom topography. These deficiencies have been appreciated since the 1960's (Ref. 8). Another possibility exists for the spurious arrivals generated by MPP; they could arise from an inherent unpredictability of ray theory related to chaotic behavior⁹⁻¹². Chaotic rays can occur when the sound speed field varies in both depth and range. Do the spurious arrivals originate from MPP's implementation of ray theory or do they originate from limitations of ray theory per se? The maximum distance over which ray theory can be used to model acoustic multipaths is unknown.

The new ray model discussed here, ZRAY, has no new physics but implements ray theory more realistically than MPP for applications in acoustic propagation in the ocean. In ZRAY, the sound speed field and the bottom topography are smoothed realistically. Thus, ZRAY's implementation yields a set of rays which looks like the data (Fig. 2). ZRAY gives a simpler and more accurate prediction than MPP.

ZRAY was developed so that an ocean acoustic tomography system for global ocean

monitoring and mapping could be automated^{13,14}. This is the only ray trace program we are aware of that realistically models sound speed fields in the ocean, accounts for variable bottom depths, and can be run without manually intensive preparation and post-analysis work. Ray theory is suitable for global monitoring networks at acoustic frequencies above 100 Hz (Ref. 15). Below 100 Hz, the travel time errors associated with ray theory are unacceptably large for mapping climatic temperature changes¹⁵.

I. NEW RAY MODEL

ZRAY is based on the algorithm by *Bowlin et al.*¹⁶. Sound speed is computed as a function of depth from *Levitus's*¹⁷ summertime values of temperature, salinity, and pressure. These data are converted to sound speed using *Del Grosso's*¹⁸ algorithm because the international standard algorithm, based on *Chen and Millero's* results¹⁹, yields speeds that are too fast³⁻⁷. Sound speed profiles are taken at about 400 km intervals along the section¹. The vertical spacing of sound speed data are taken at the standard depths compiled by *Levitus*¹⁷.

At each depth where the speed of sound is specified, the speed of sound would have a discontinuity if linear segments were used to interpolate between the sound speed data. ZRAY smoothes out these corners using quadratic splines so that the derivative of the speed of sound is continuous in the vertical direction. This quadratic spline is constrained to pass through the data points exactly and not exhibit any overshoot phenomenon (Fig. 3). In ZRAY, the quadratic spline is constrained to pass through

the input data points by setting the control variables to,

$$\text{factor} = 1 \quad \text{iteration} = 10 \quad ,$$

(p. 43 of Ref. 16). There is no reason to make the quadratic spline miss the input data points, and introduce a bias, since our best guess of the sound speed field is derived from *Levitus'* data¹⁷.

The sound speed field between the stations is a linear function of horizontal distance. Consequently, there is a discontinuity in the horizontal derivative of the speed of sound at each station. This discontinuity is found to be so small that no false caustics are created for the 3000 km section examined here.

The bathymetry along the geodesic between the source and the receiver comes from ETOPO5 (Ref. 20) and from classified bathymetry taken by the U.S. Navy. The geodesic distance between the source and receiver was computed in the WGS-84 coordinate system. Quadratic splines are used to smooth out the corners of the bathymetric data along the geodesic. Thus, the horizontal derivative of the bottom depth is continuous. Rays reflect specularly from the bottom and the surface. Some of the early arrivals reflect from the surface many times¹.

The impulse response of ZRAY is convolved with a Gaussian pulse 0.016 s wide to mimic the ideal pulse shape from the acoustic source. The amplitudes of these pulses are computed for geometric and diffracted energy. A so called "diffracted eigenray" approaches, but does not hit, the receiver. Energy leaks into the receiver in the shadow zone of the caustic. The travel times of the diffracted eigenrays are computed by

calculating when a plane wave, perpendicular to the caustic, would cross the receiver (Fig. B3 of Ref. 1). Amplitudes for geometric and diffracted eigenrays are estimated using equations (2.5.3) and (2.5.6) of Ref. 21.

ZRAY, and its eigenray finder, have been verified using the procedures given in Ref. 16 and in the Appendix.

II. Comparison with data

ZRAY predicts only one more multipath than observed (Fig. 2 (b), between rays 1 and 2). That extra weak arrival is diffracted and it is predicted to miss the receiver by hundreds of meters. ZRAY predicts other arrivals which cannot be resolved with 0.016 s pulses, but the unresolved pulses are very weak. The rays from MPP contain many spurious arrivals. There is a correspondence between the rays from ZRAY and most of the rays from MPP (Table I). The inclination angles from the new ray model and MPP are within $\pm 0.07^\circ$ respectively.

The travel times from ZRAY and MPP are within 0.08 s (Table I). Since the travel time is about 1800 s, the fractional difference in travel time is only about $\frac{0.08 \text{ s}}{1800 \text{ s}} \sim 4 \times 10^{-5}$. The travel times from both ray traces are about 0.5 s earlier than observed³⁻⁶. This difference is due to many phenomenon, the most important of which is an error in the climatological temperatures⁴⁻⁶.

None of the rays from ZRAY interact with the bottom of the ocean, in contrast to the predictions from MPP where four rays interact with the bottom. Results from ZRAY are more credible than from MPP because ZRAY's output looks more like the

data than the output from MPP.

Perhaps the eigenrays from ZRAY resemble observations better than eigenrays from MPP because the sound speed profile in ZRAY is smooth, like the ocean, while the sound speed profile in MPP has corners, unlike the ocean. Previous calculations with a full-wave solution to the acoustic wave equation show a multipath structure that has more arrivals than observed in the data, but not as many spurious arrivals as from MPP (Fig. 3 in Ref. 22). Because the full-wave solution was computed using a sound speed profile with corners in the sound speed field, like MPP, it is possible that the extra arrivals would disappear from the full-wave model if the corners were smoothed as in ZRAY.

III. DISCUSSION

Ray theory can be implemented to successfully predict the travel times of acoustic multipaths over a 3000 km distance in the northeast Pacific. To date, this is the longest distance where ray theory has been shown to be a good model for predicting the travel times of multipaths in the ocean.

There is no evidence that ray theory is limited by an inherent unpredictability related to chaos at 3000 km along this section of the Pacific. The rays are traced through sound speed profiles based on historically averaged values of temperature, salinity, and depth as compiled by *Levitus*¹⁷. Furthermore, geometric rays traced from the source to the receiver and vice-versa are nearly identical. This implies that ray trajectories are insensitive to the initial conditions and that there is no evidence of

chaotic behavior. The predictability of the rays may be related to the fact that they are inclined at about ten degrees with respect to the horizontal. Multipaths with flatter inclination angles may be more unpredictable but they are not studied here because they are not observed in this experiment.

Previous tomographic analysis of this section only used the twelve multipaths for which the MPP ray model predicted no bottom interaction¹. ZRAY confirms that those twelve rays do not interact with the bottom. In fact, ZRAY indicates that none of the sixteen observed multipaths interacts with the bottom. Tomographic analysis of this section could be extended to include all sixteen multipaths with an attendant improvement in the tomographic maps.

It would be interesting to use other implementations of ray theory to see whether they yield a set of travel times which resembles the data for this section. This remains for the future.

ZRAY and its eigenray finder requires 22.5 hours of CPU time on a SUN SPARC station 2 workstation in this application. Ray tracing is amenable to massively parallel processing, and the algorithm could be used for real-time applications. ZRAY does not generate spurious arrivals, thus the potential exists for automating the modelling of the multipaths for tomography at frequencies above 100 Hz.

ACKNOWLEDGMENTS. For more than 14 years, I (Spiesberger) have had the privilege of using the U.S. Navy's SOSUS stations to study the ocean using tomography. Until late 1993, I have been unable to acknowledge my gratitude to the

many U.S. Navy personnel who I have had the great pleasure to work with, because of security constraints. The fact that I can now acknowledge them is due to CAPT Hearst Coen (Ret.) who led the policy change leading to a public announcement of the mission of these stations. CAPT Coen was perhaps the first Navy person to recognize the great potential of the SOSUS stations for scientific use. In this experiment, he allowed us access and facilitated our research along with ADM Craig Dorman, ADM Ray Witter, Dr. Joel Sinsky, CDR John Reid, Dr. Dennis Conlon, and AT&T personnel Al Burrows and Henry Grenier. The ZRAY code used to produce the some of the results published here is derived from the ray code written by James Bowlin and discussed in Ref. 16. This research was supported by the Office of Naval Research grant N00014-92-J-1222 and by the Advanced Research Projects Agency grant MDA972-93-1-0004.

REFERENCES

- ¹J. L. Spiesberger and K. Metzger, "Basin-scale tomography: a new tool for studying weather and climate," *J. Geophys. Res.*, **96**, 4869-4889 (1990).
- ²P.F. Worcester, B.D. Dushaw, and B.M. Howe, "Proc. IEEE Fourth Working Conference on Current Measurements, Clinton, Maryland, 65-70, (1990).
- ³J.L. Spiesberger and K. Metzger, "A basin-scale (3000 km) tomographic section of temperature and sound speed in the northeast Pacific," *Trans. Am. Geophys. Union*, **71**, 157, (1990).
- ⁴J.L. Spiesberger and K. Metzger, "New estimates of sound-speed in water," *J. Acoust. Soc. Am.*, **89**, 1697-1700, (1991).
- ⁵J.L. Spiesberger and K. Metzger, "A new algorithm for sound speed in seawater," *J. Acoust. Soc. Am.*, **89**, 2677-2688, (1991).
- ⁶J.L. Spiesberger, "Is Del Grosso's sound-speed algorithm correct?" *J. Acoust. Soc. Am.*, **93**, 2235-2237, (1993).
- ⁷B.D. Dushaw, P.F. Worcester, B.D. Cornuelle, and B.M. Howe, "On equations for the speed of sound in seawater," **93**, 255-275, (1993).
- ⁸M.A. Pedersen, "Acoustic intensity anomalies introduced by constant velocity gradients," *J. Acoust. Soc. Am.*, **33**, 465-474 (1961).

⁹D.R. Palmer, M.G. Brown, F.D. Tappert, and H.F. Bezdek, "Classical chaos in nonseparable wave propagation problems," *Geophys. Res. Letters*, **15**, 569-572, (1988).

¹⁰F.D. Tappert, M.G. Brown, and G. Goni, "Weak chaos in an area-preserving mapping for sound ray propagation," *Physics Letters A*, **153**, 181-185, (1991).

¹¹M.G. Brown, F.D. Tappert, and G. Goni, "An investigation of sound ray dynamics in the ocean volume using an area preserving mapping," *Wave Motion*, **14**, 93-99, (1991).

¹²D.R. Palmer, T.M. Georges, and R.M. Jones, "Classical chaos and the sensitivity of the acoustic field to small-scale ocean structure," *Computer Physics Comm.* **65**, 219-223, (1991).

¹³J.L. Spiesberger and J.B. Bowlin, A telemetry scheme for ocean acoustic tomography: Real time monitoring, *J. Marine Environmental Engineering*, **1**, 1-22, (1993).

¹⁴J.L. Spiesberger, Is it cheaper to map Rossby waves in the global ocean than in the global atmosphere?, *J. Marine Environmental Engineering*, **1**, 83-90, (1993).

¹⁵L. Boden, J.B. Bowlin, and J.L. Spiesberger, "Time domain analysis of normal mode, parabolic, and ray solutions of the wave equation," *J. Acoust. Soc. Am.*, **90**, 954-958 (1991).

¹⁶J. B., Bowlin, J.L. Spiesberger, T.F. Duda, and L. Freitag, "Ocean acoustical ray-tracing software RAY", Woods Hole Oceanographic Technical Report, WHOI-93-10, (1993).

¹⁷S. Levitus, "Climatological atlas of the world ocean," NOAA Prof. Pap. 13, (U.S. Government Printing Office, Washington, DC, 1982).

¹⁸V.A. Del Grosso, "New equation for the speed of sound in natural waters (with comparisons to other equations," *J. Acoust. Soc. Am.*, 56, 1084-1091 (1974).

¹⁹ C. Chen and F.J. Millero, "Speed of sound in seawater at high pressures, *J. Acoust. Soc. Am.*, 62, 1129-11135 (1977).

²⁰ National Geophysical Data Center, ETOPO5, 5 minute gridded world elevations and bathymetry - a digital data base, Boulder, Colo., (1987).

²¹L.M. Brekhovskikh and Y. Lysanov, *Fundamentals of Ocean Acoustics*, (Springer-Verlag, New York, 1982).

²² L. R. Boden and J. L. Spiesberger, "Comparison of observed and simulated acoustic multipaths for a 3000 km section in the Pacific" submitted to *J. Acoust. Soc. Am.*, (1993).

²³A. Ben-Menahem, and J. S. Sarva, *Seismic waves and sources*, 1108pp., Springer-Verlag, New York, (1981).

APPENDIX. ZRAY and the Eigenray Finder

Ray geometry and travel times compare favorably with analytical and other ray trace programs as described in Ref. 16. These cases did not test three other portions of ZRAY, namely specular reflection from a non-flat bottom, the Earth flattening transformation²³, and treatment of range dependent sound speed profiles.

Cases where rays reflect specularly from non-flat bottoms were compared with analytical solutions for a simple case. The speed of sound was taken as constant, and a bottom profile was built by joining linear segments. The corners of the linear segments were smoothed with a parabola over a 1 m scale with ZRAY. Because the speed of sound is constant, ray paths are linear segments, and a separate program was written to compute these paths and their travel times. Rays were traced over thousands of kilometers using variable depth bottoms composed of about 50 linear segments. The ray paths and travel times from ZRAY were within 0.001 m and 0.001 s of the exact solutions. The analytical test case is only valid if the rays do not reflect within 1 m of the original corners of the bottom profile because the bottom is parabolic in those regions. In each comparison, none of the rays reflected within 1 m of those corners.

The Earth-flattening transformation was checked by applying the transformation to a sound speed profile that was constant in space. The transformed sound speed profile increases almost linearly with depth and analytical expressions are available for the resultant travel time and geometry of the ray path (p. 112-115 of Ref. 21). At distances of about 1100 km, the travel time from ZRAY was within 4 μ s of the travel

time computed analytically.

The best check to date that ZRAY correctly handles horizontal variations of sound speed is perhaps the comparison with MPP given in Table I. Over a 3000 km section, travel times from ZRAY and MPP are within about ± 0.03 s. This difference is ascribed to the slightly different ways that the sound speed profiles are interpolated.

Table I. Comparison of the ZRAY and MPP raytrace programs. Differences are taken as values from ZRAY minus values from MPP. Geometric and diffracted arrivals are denoted by G and D respectively. None of these rays from ZRAY interact with the bottom of the ocean. Ray 16 from MPP and ZRAY are different. In MPP, ray 16 interacts with the bottom, and in ZRAY, it does not interact with the bottom.

Arrival number	Angular difference (deg)	Arrival time difference (ms)	Type
1	-0.036	+0.036	G
2	0.	+0.036	G
3	-0.031	+0.035	G
4	+0.019	+0.035	G
6	-0.045	+0.037	G
7	+0.033	+0.046	G
8	+0.033	+0.047	G
9	+0.006	+0.044	G
10	+0.013	+0.044	G
11	-0.072	+0.048	G
12	+0.049	+0.079	D
13	+0.009	+0.050	D
14	-0.022	+0.050	D
15	-0.043	+0.045	D

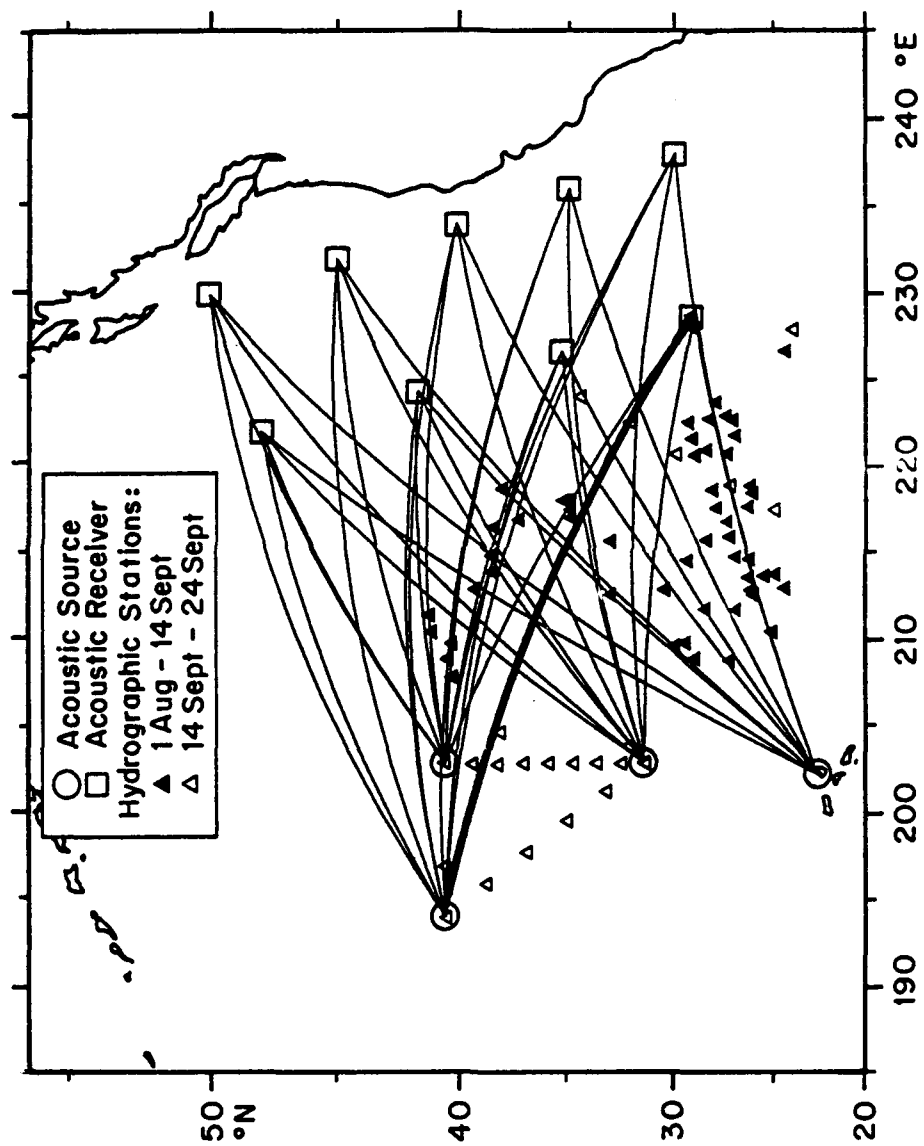
FIGURE CAPTIONS

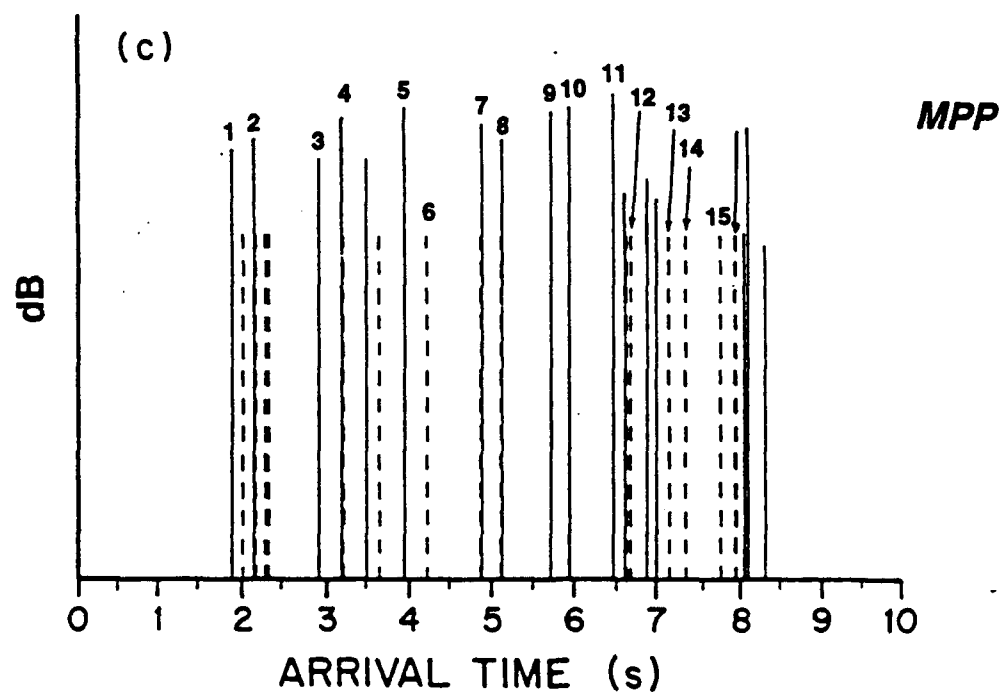
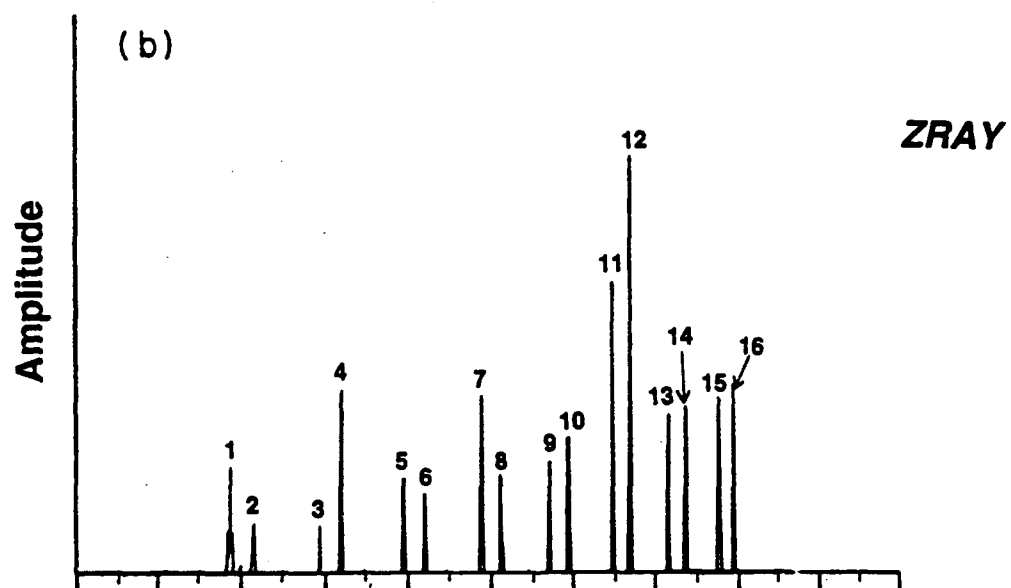
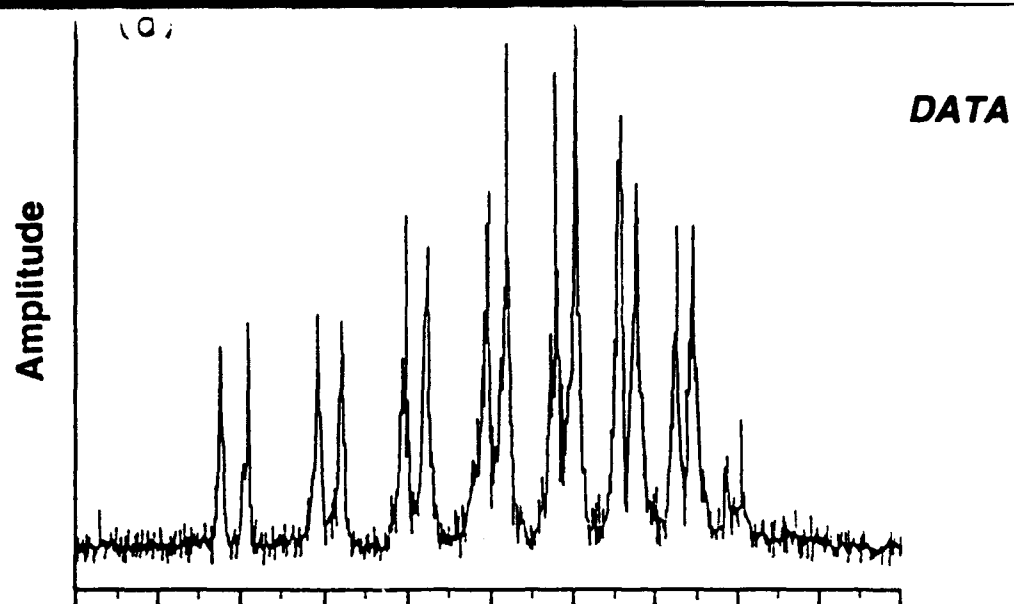
Figure 1. Plan view of the ocean acoustic tomography experiment with the approximate positions of four acoustic sources and nine receivers indicated. The tomographic section studied here is indicated by the heavy line. The three sources north of 30° N are moored about 0.86 km depth in about 5.5 km of water². Figure adapted from Ref. 1.

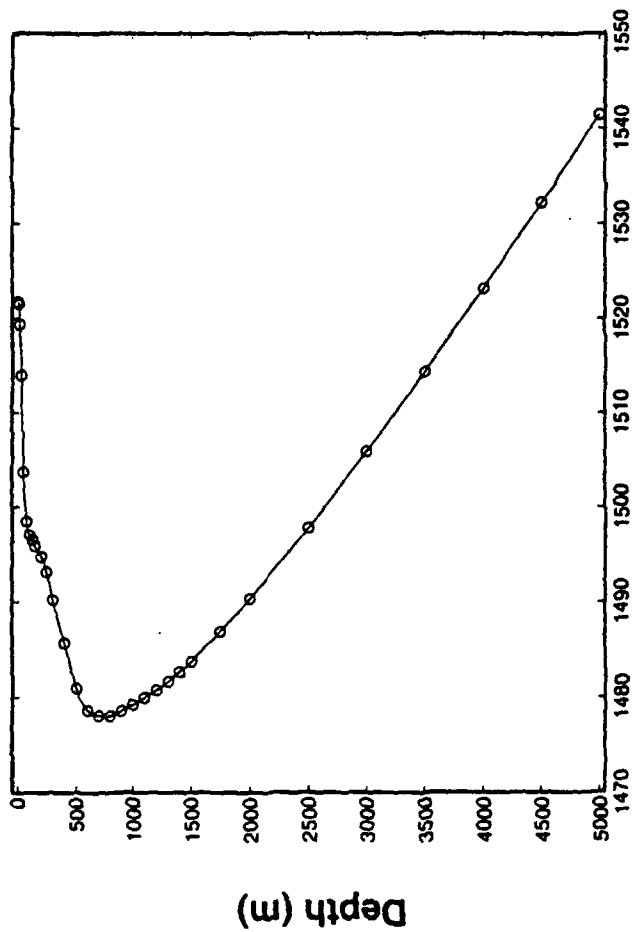
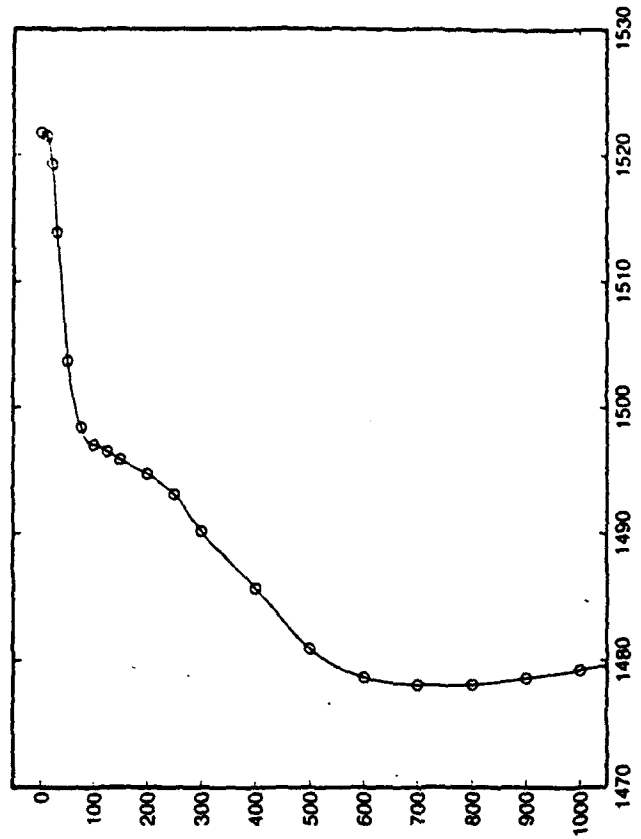
Figure 2. (a) Daily averaged multipath record for 10 September 1987 with the horizontal axis denoting arrival time and the vertical axis denoting amplitude. (b) The arrival times from the new ray model with 16 arrivals numbered. Arrival times are shifted by a constant to align with the top panel. The vertical axis is amplitude. Sound speeds are computed from *Levitus's* summer climatology¹⁷ using the algorithm derived by *Del Grosso*¹⁸. The ray arrivals are convoluted with a Gaussian pulse about 0.016 s wide to mimic the shape of an ideal bandlimited pulse. (c) The arrival times from the MPP ray trace with 16 arrivals numbered as in the middle panel. Arrival times are shifted by a constant to align with the top panel. The vertical axis is in dB. Sound-speeds are computed as in (b). Signal-to-noise ratios are computed for geometric rays (solid vertical lines), while the signal-to-noise ratios for non-geometric pulses (dashed vertical lines) are set to an arbitrary constant because the algorithm does not compute their magnitude.

Figure 3. Quadratic splines (solid lines) fitted to the sound speed data (circles) near the source. (Right) A blow-up of the features in the main thermocline. Note that the

spline goes through the original data without exhibiting overshoot phenomenon.







Sound Speed (m/s)

TASK B OCEAN MODELING

Model solutions of the NEP for 1961-1989 are complete. Four model runs with different inputs at the southeastern boundary were described in the previous report. The four forcing mechanisms were (i) a Kelvin wave with period 1 year and no (flat) bottom topography. All other runs had realistic topography. (ii) a Kelvin wave with period 1 year; (iii) a Kelvin wave with period four years; (iv) the Kelvin wave from the equatorial model. The fifth and most recently completed model run (which was behind schedule as of the previous quarterly report) is identical to (iv) but with the addition of observational (COADS) winds. The model was spun-up for 20 years with climatological winds and a climatological Kelvin wave from the equatorial model. Observed winds and the raw Kelvin signal were then used to run the model from 1961-1989.

The mean circulation for this model has been generated (Fig. 1). Since model years in the 1960s are influenced by a spin-up effect due to the replacement of climatological winds with observed (COADS) winds, the mean is based on model years 1970-1989. In the eastern part of the basin, upper layer thickness (ULT) anomalies due to the Kelvin wave forcing are usually very similar to the ULT without winds as shown in Fig. 2. The western part of the basin is dominated by the wind-driven large-scale gyre and does not have the same similarity.

Figure 2 shows a deep ULT anomaly of about 35 m in a region where the mean ULT is 100-150 m. Thus the Kelvin signal propagating off the coast as a Rossby wave has a significant effect on the circulation in the eastern Pacific Ocean. The effect of this signal on acoustic travel times is measurable and described below.

Comparison of our model results to observations (Task B4) involves computing travel time anomalies as described in the last report. Total travel times from acoustic source to receiver along a great-circle path is estimated using a sound speed estimate (Roed 1993)

$$c = c_0 - \beta \Delta \rho (\alpha D)^{-1} (h-H)$$

where c_0 is the mean sound speed, β is the local derivative of the Coriolis term, $\Delta \rho$ is the density difference between upper and lower layer, α is a thermal expansion coefficient, D is a geometric constant, h is the upper layer thickness (ULT), and H is its mean thickness. Travel time anomaly is then

$$T = \int [\beta \Delta \rho (\alpha D)^{-1} (h-H)]^{-1} ds \quad (1)$$

where ds is the segment along the great circle path from source to receiver. In the calculations below, H is the mean ULT along each path during 1970-1989. All the paths used in this calculation originate near 18.4N, 206.2E as shown in Fig. 3. Their final coordinates are:

Path #	latitude	longitude
1	21.2	254.1
2	18.4	106.2
3	24.6	247.7
4	26.5	246.6
5	28.5	245.2
6	30.8	243.7
7	33.2	241.7
8	35.9	238.1
9	40.0	235.4
10	47.1	235.2

Travel times for the new model run are shown in the Figs. 4 and 5. There is an adjustable factor (D) in the calculation of T which controls the magnitude of these results. For these calculations $D=1000$ meters.

A direct comparison of acoustic travel time changes obtained from the model and field observations is now possible. The travel time anomalies for all the paths for 1987-1989 are shown in Fig. 6. These can be compared to the data in Fig. 8 of Spiesberger et al. (1992). It appears our estimated travel time anomalies are similar to their observations. The advantage of using these models in conjunction with tomography is they further the understanding of the ocean dynamics underlying the results from acoustic tomography. These models capture variations over a range of weeks to decades and can be used to study ocean behavior on broad range of time scales.

Design of new models (Task B5). This work is being done in collaboration with researchers at the Naval Research Laboratories (NRL). Ocean models very similar to the FSU model have been developed, but with additional complexity. The NRL ocean models are high horizontal resolution layered models driven by observed winds. Unlike the FSU model, they have high vertical resolution (typically 14 vertical layers), allowing for the occurrence of additional baroclinic modes in the model, and include thermodynamics processes.

Unlike the FSU model, one of the primary requirements for reliability of the NRL model results is good thermodynamic input quantities. Accurate observations or estimations of winds, fluxes of solar, specific and sensible heat, humidity, air and sea-surface temperatures are needed for forcing these ocean models. The FSU model only requires winds. This added complexity

greatly increases the computation requirements. The NRL global ocean model requires about 100 hours of Cray YMP CPU time for one model year compared to about 40 minutes CPU time for the FSU model. The use of a massively parallel machine would probably decrease this time requirement, but would require a nontrivial rewriting of the model software.

FIGURES

- Fig. 1 Mean ULT for the wind-driven, remote-forced model. 1970-1989.
- Fig. 2 (a) ULT in the coupled model without winds. (b) ULT anomaly in the coupled model with observed winds. The deep band near the eastern part of the basin is due to the 1982-1983 El Nino.
- Fig. 3 Great circle paths used for calculations of travel time.
- Fig. 4 Travel time anomalies for new model run based on Eq. (1).
- Fig. 5 Travel time anomaly contours. (a) 1970-1979. (b) 1980-1989. Solid (dashed contours are positive (negative) indicating faster (slower) average sound speed and warmer (colder) average water temperatures.
- Fig. 6. Travel time anomalies, 1987-1989.
- Fig. 7. Task B Schedule

REFERENCES

- Roed, L.P., 1993: personal communication.
- Spiesberger, J.L. and K. Metzger, 1991: Basin-scale tomography: A new tool for studying weather and climate. *J. Geophys. Res.*, 96C, 4869-4889.
- Spiesberger, J.L., K. Metzger and J.A. Furgeson, 1992: Listening for climatic temperature change in the northeast Pacific: 1983-1989. *J. Acoust. Soc. Am.*, 92, 384-399.

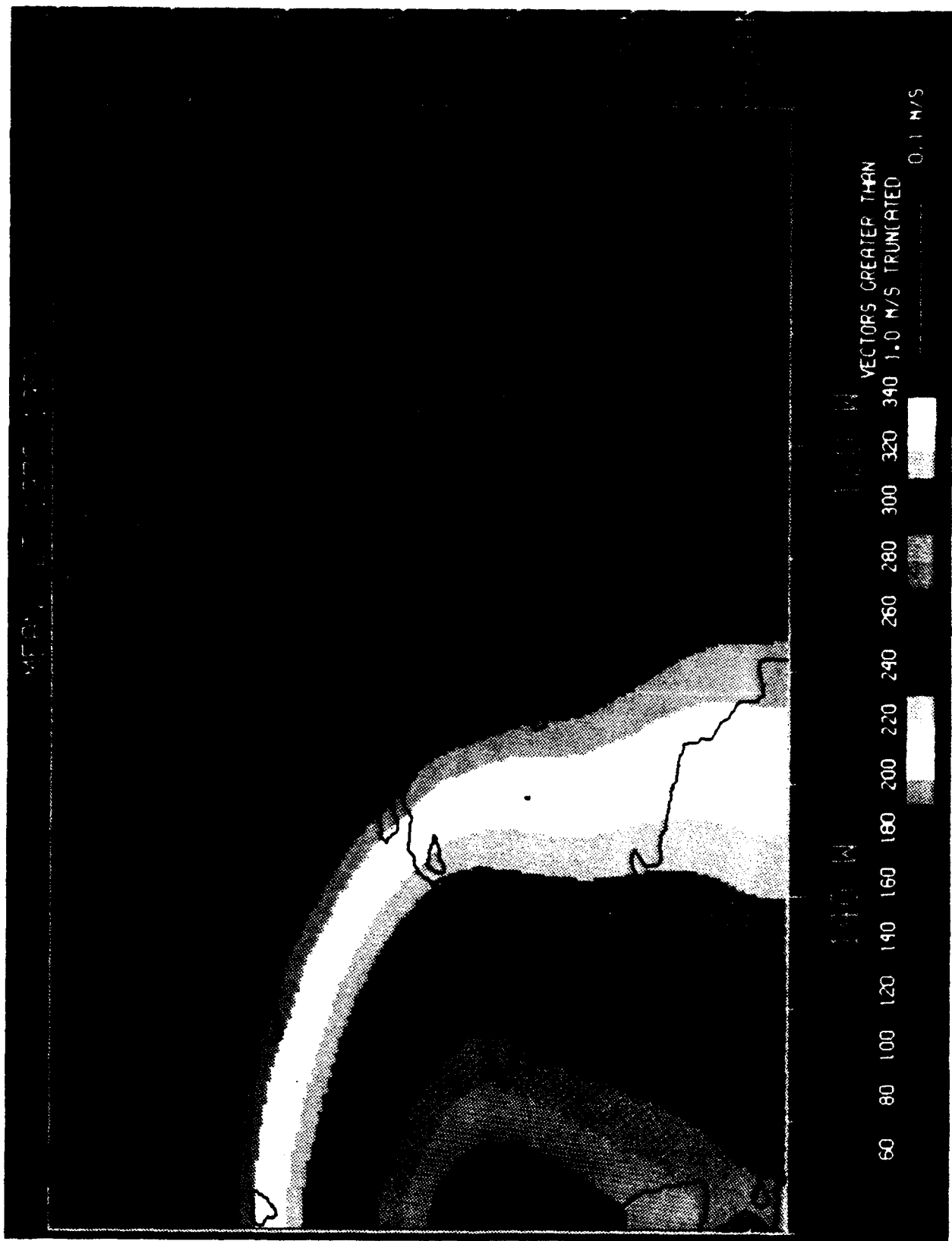


Figure 1

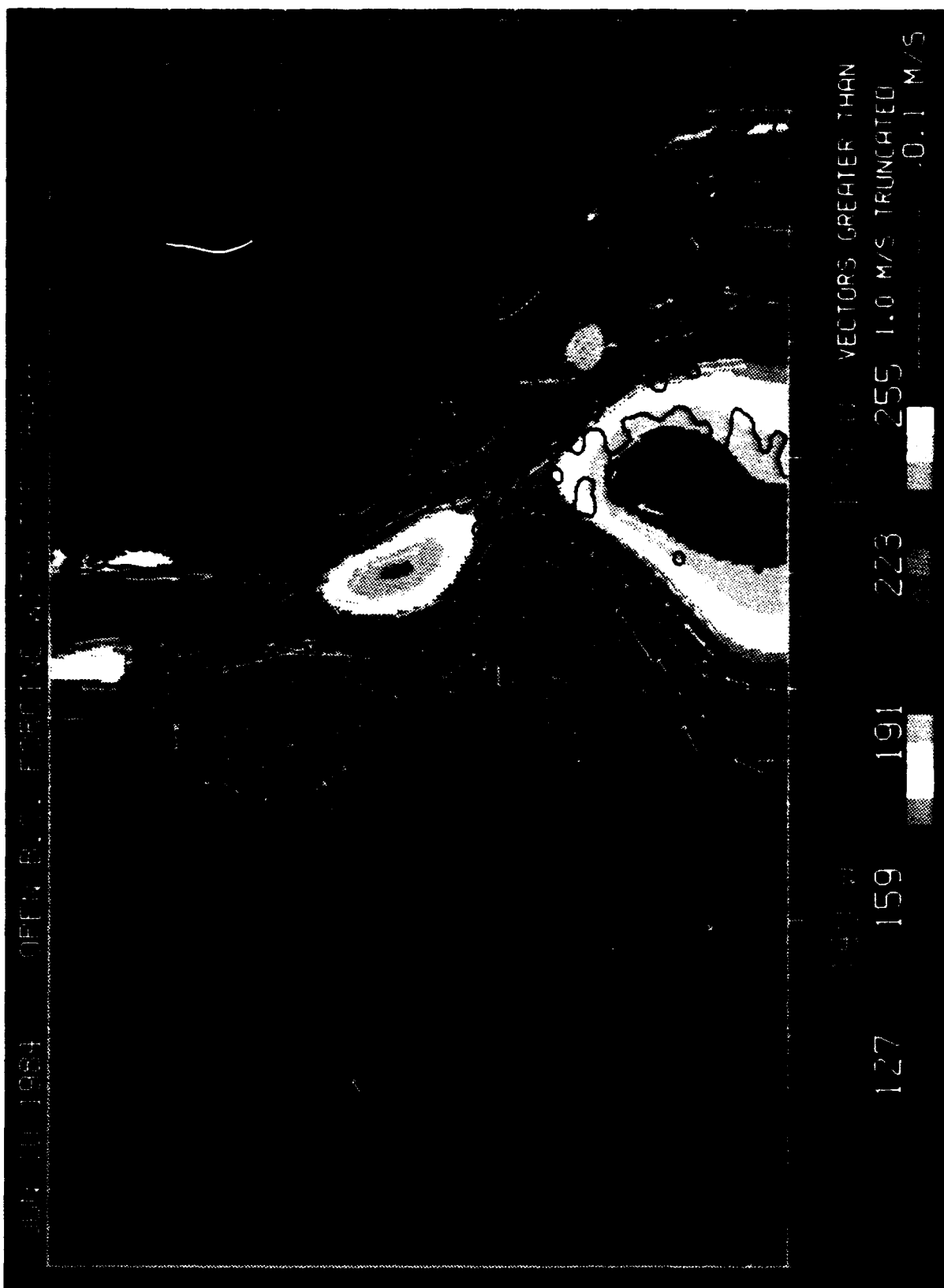


Figure 2a

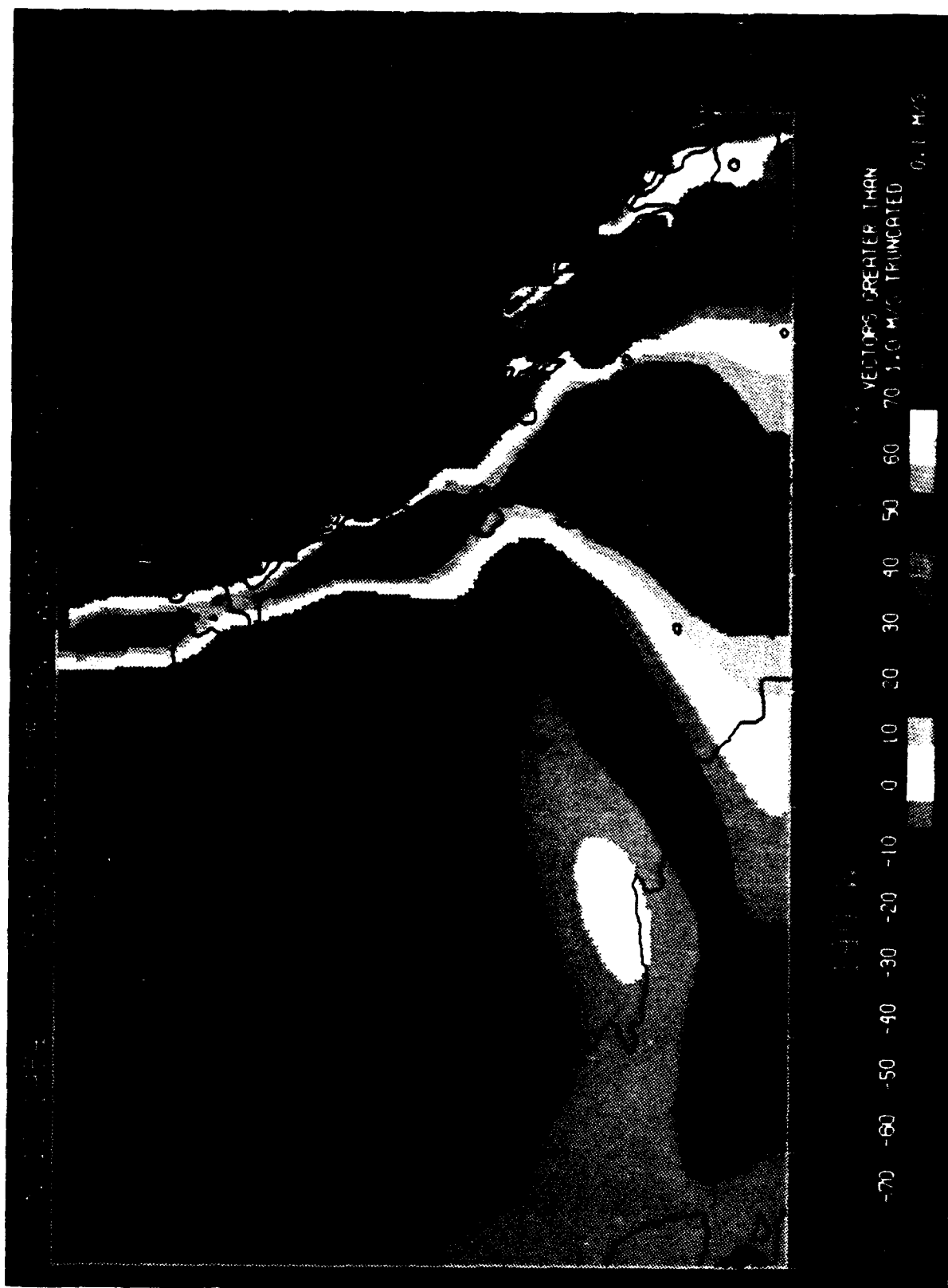


Figure 2b

Great Circle Paths

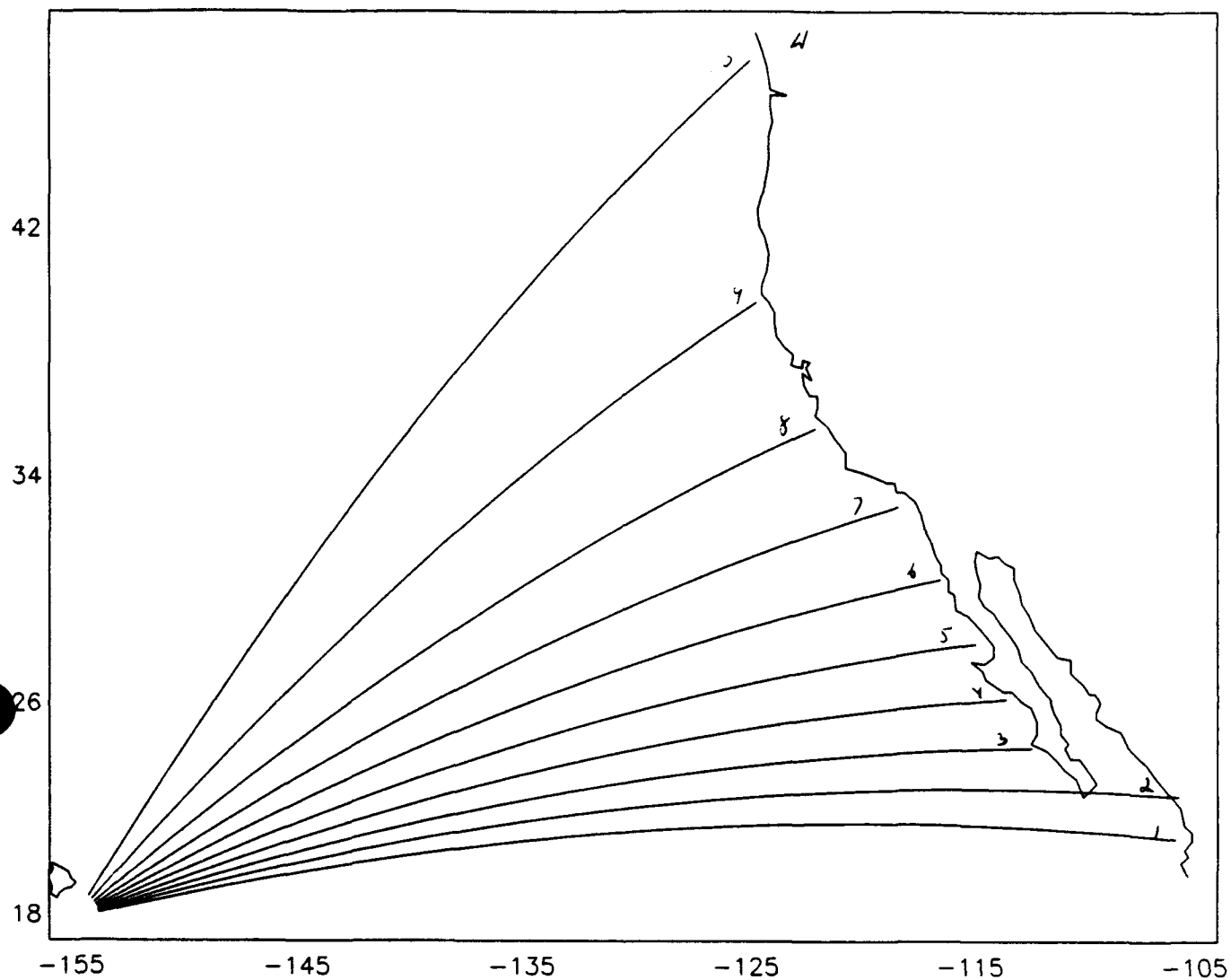


Figure 3

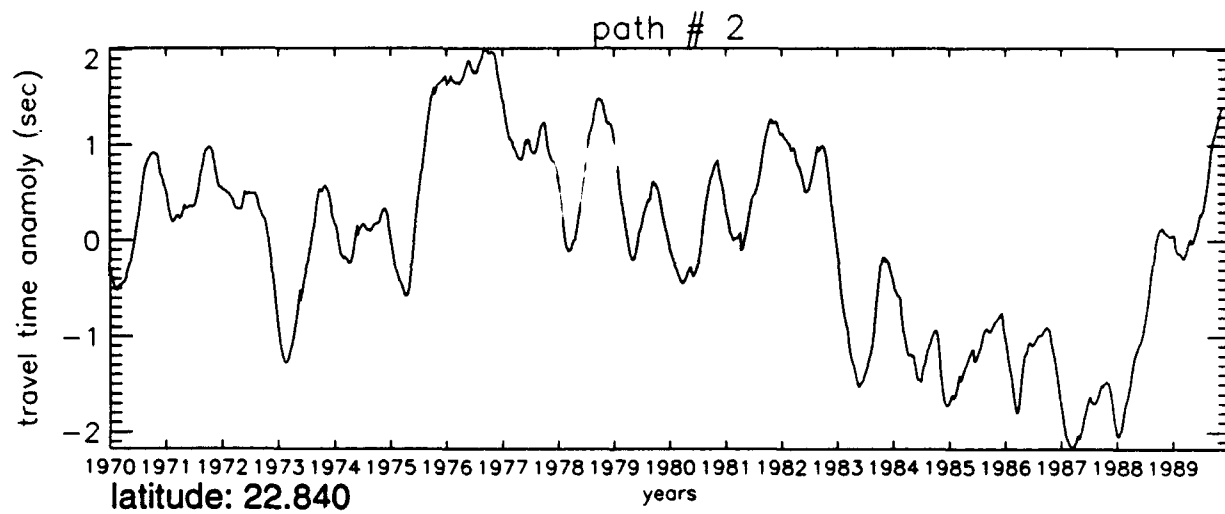
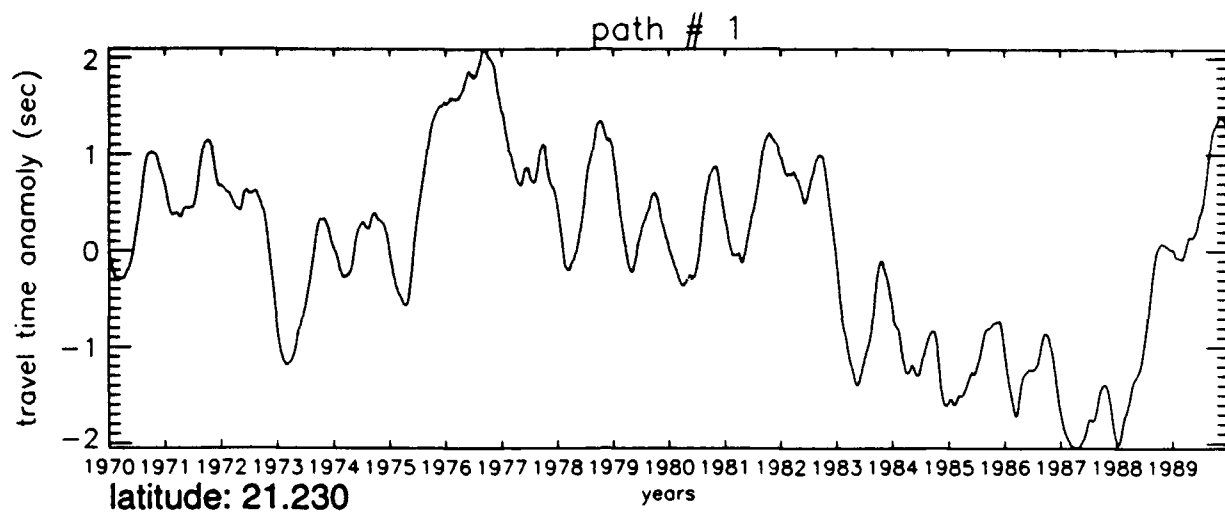


Figure 4

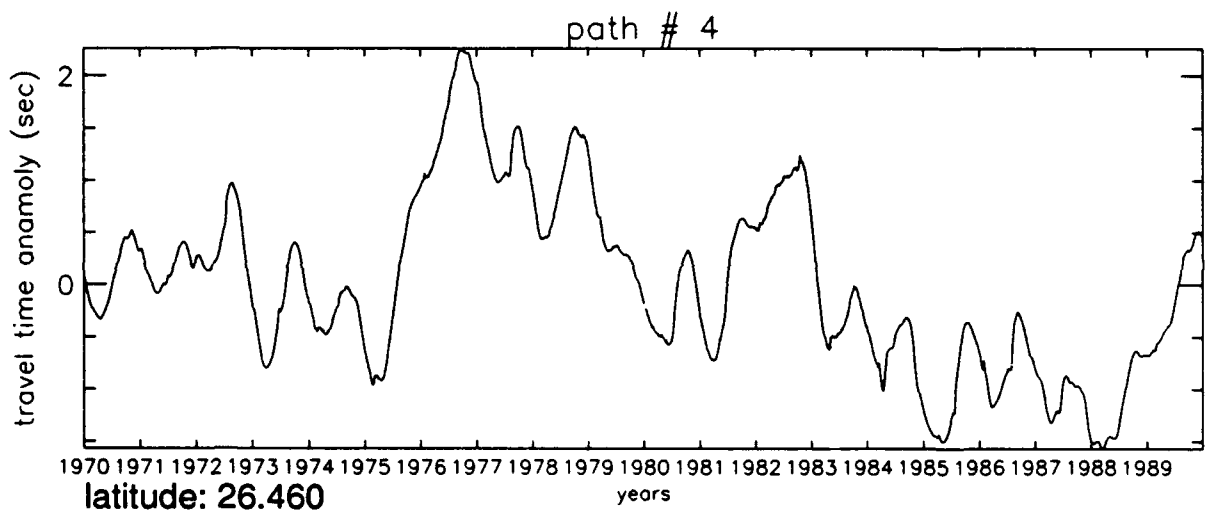
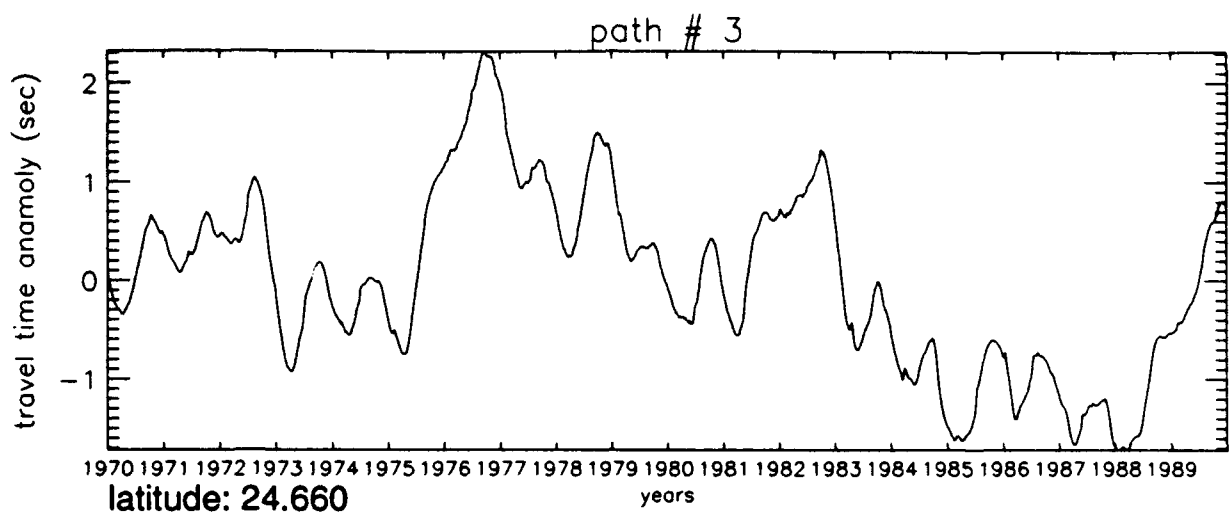


Figure 4

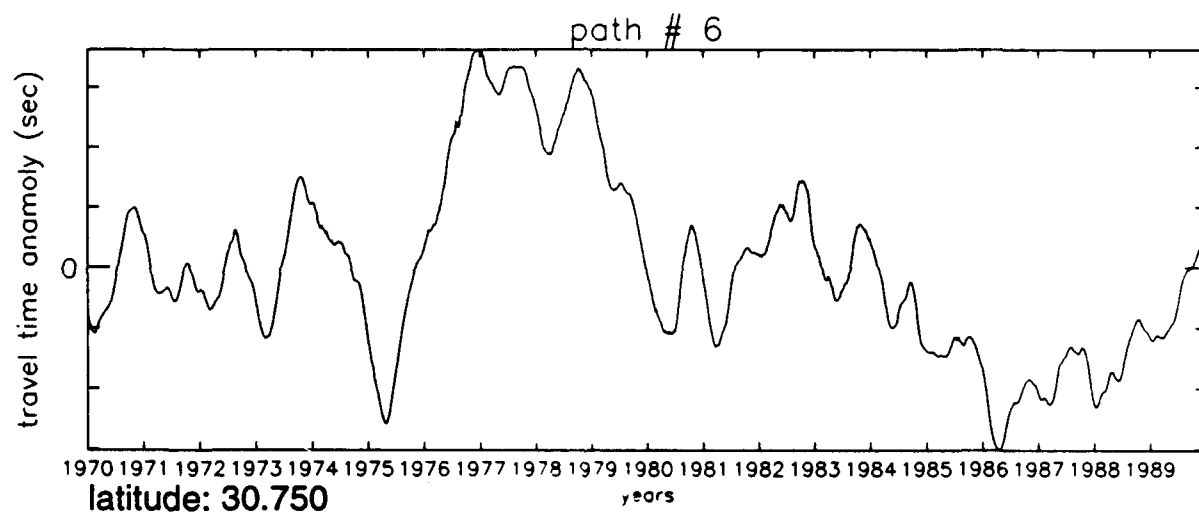
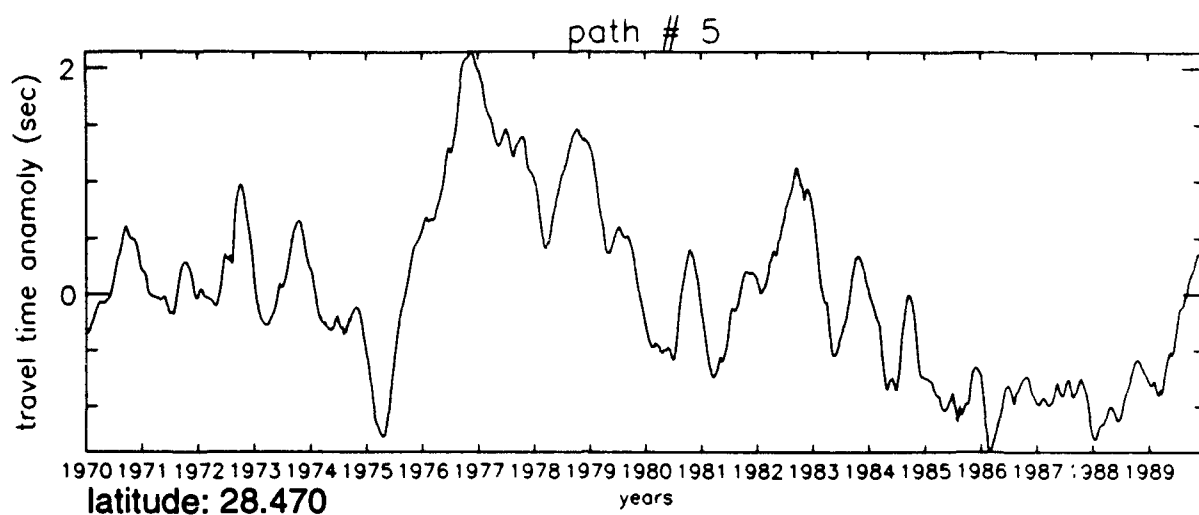


Figure 4

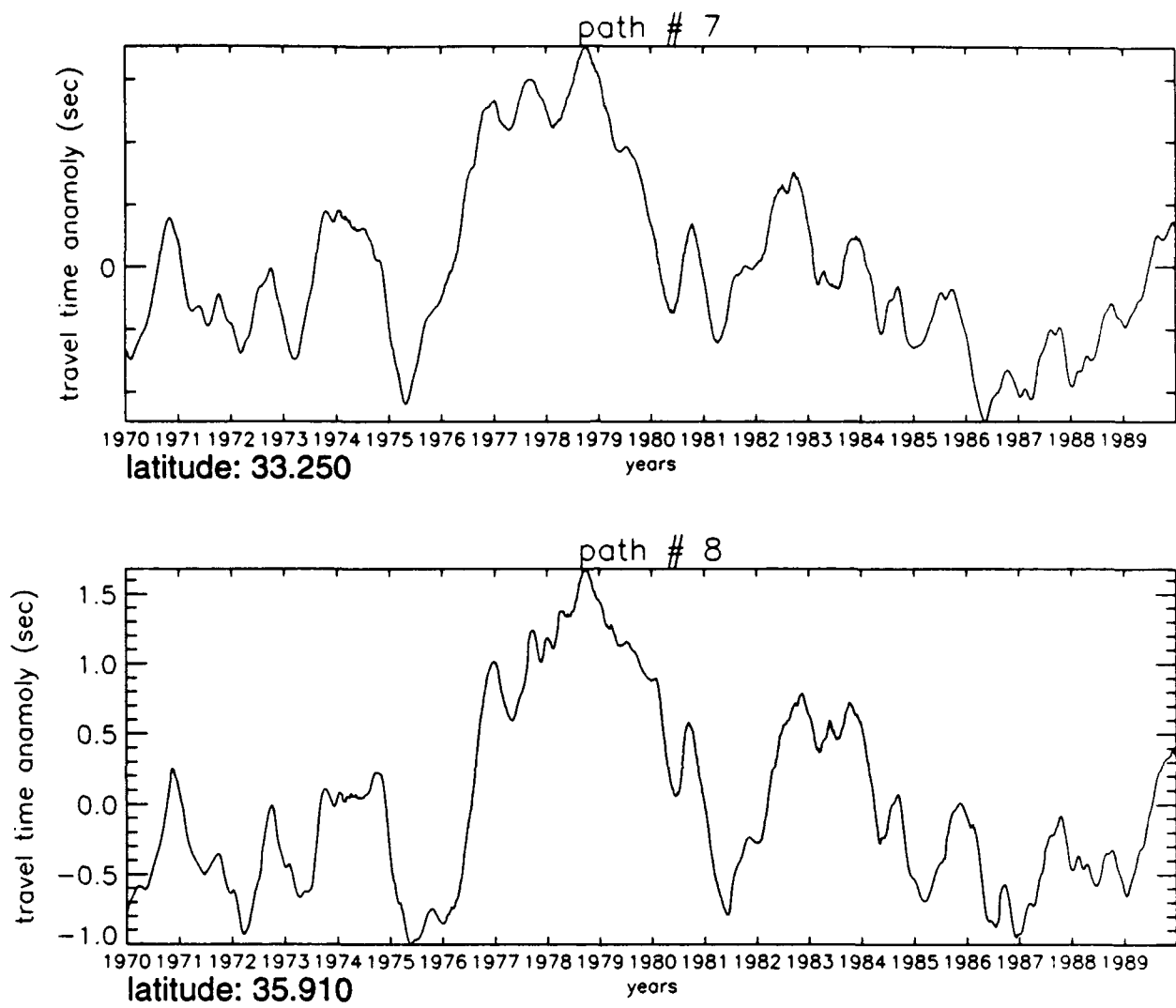


Figure 4

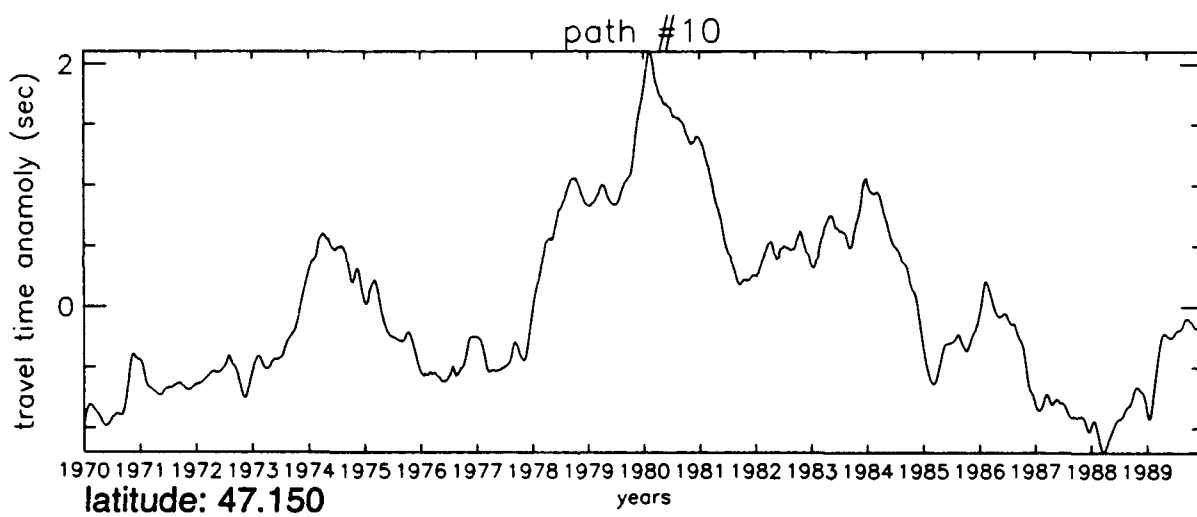
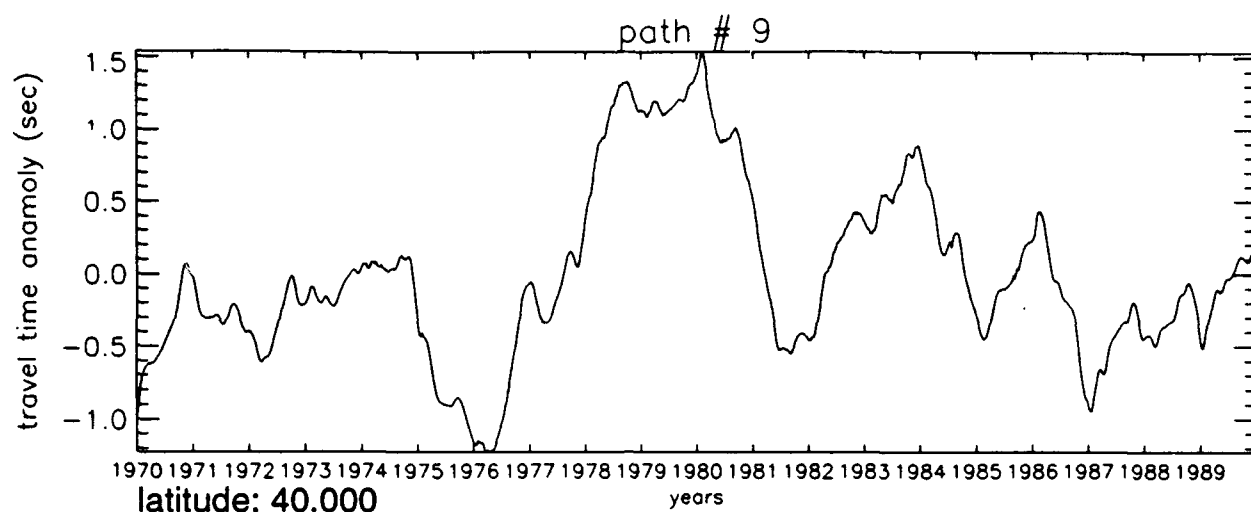


Figure 4

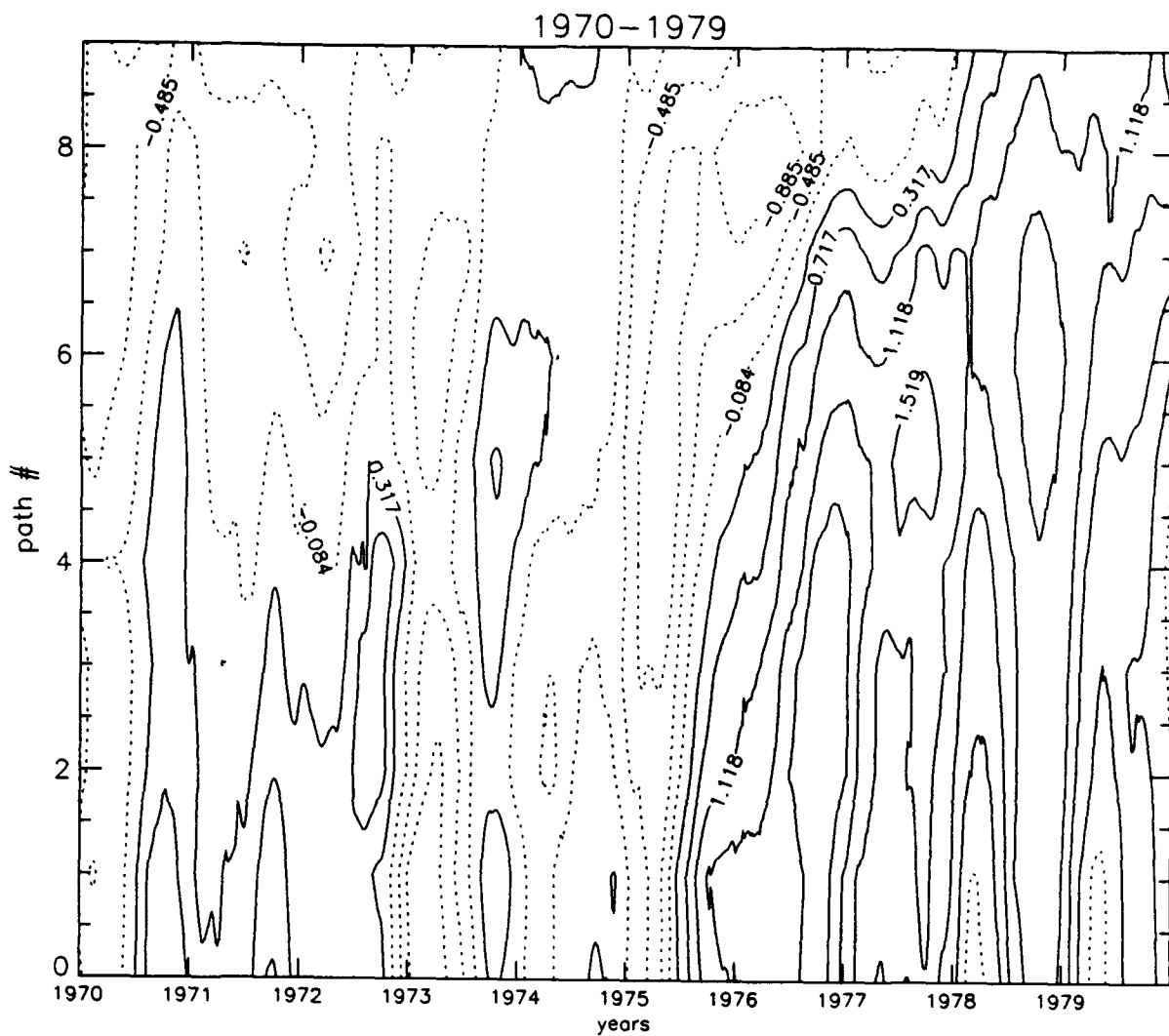


Figure 5a

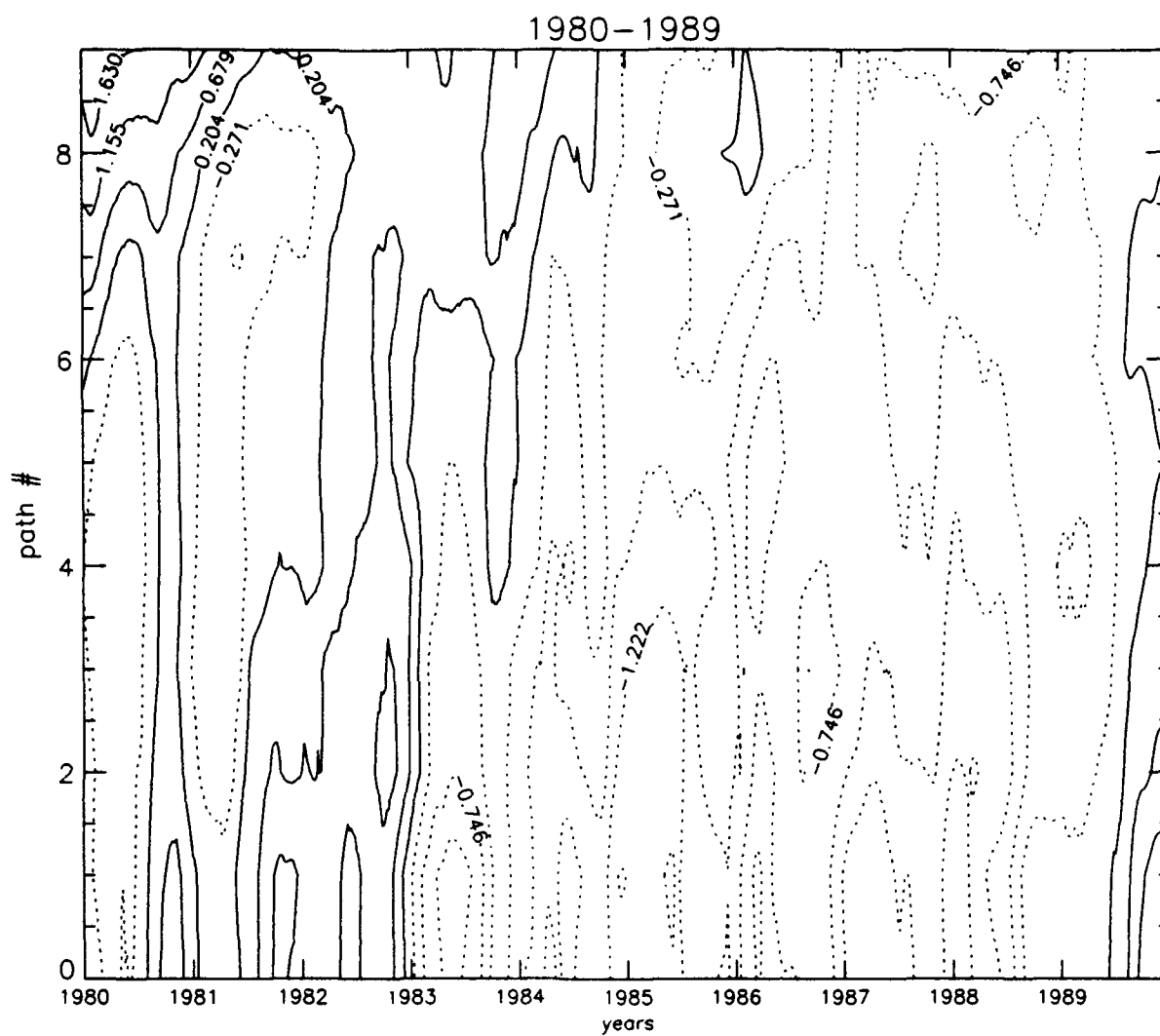


Figure 5b

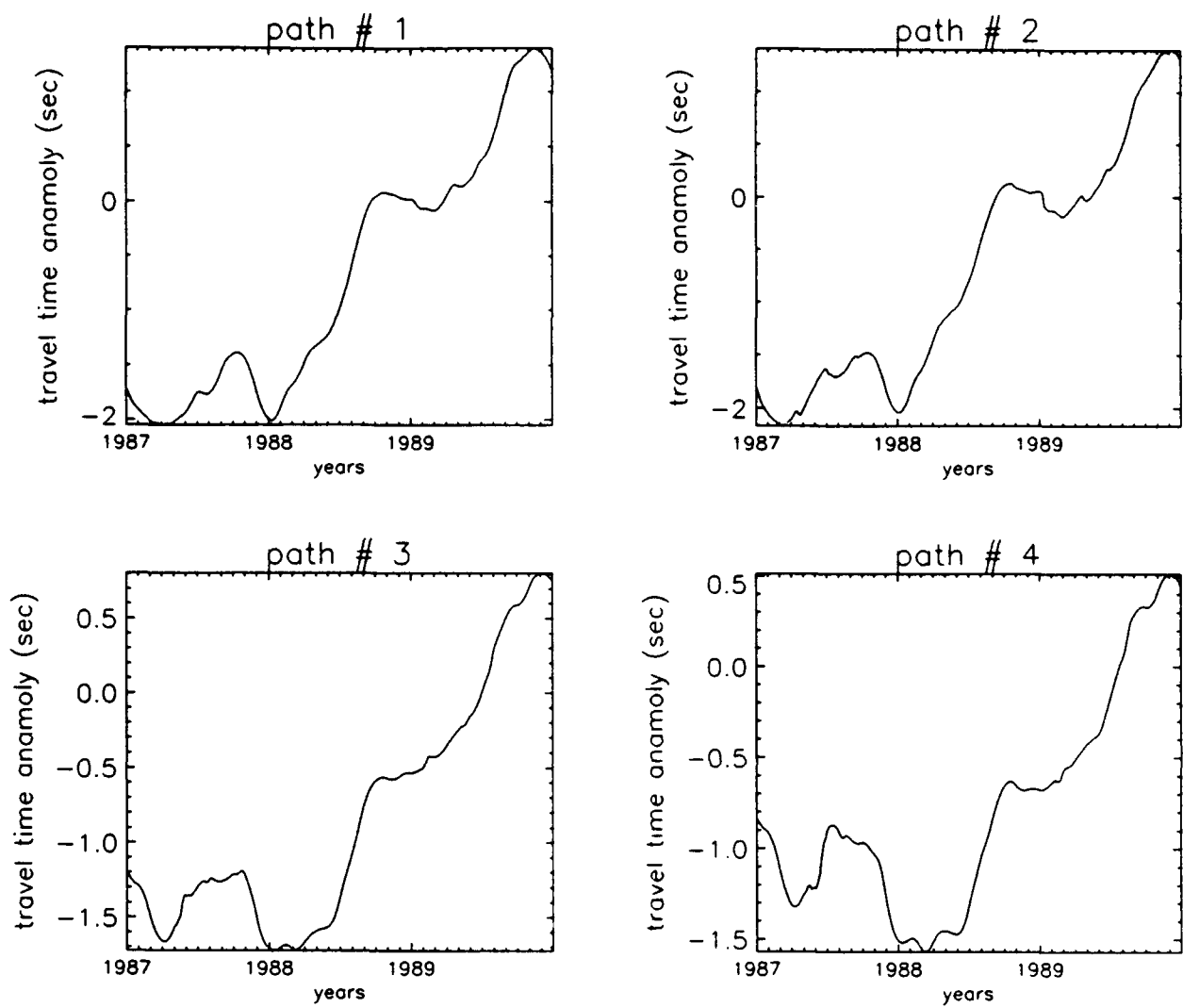


Figure 6

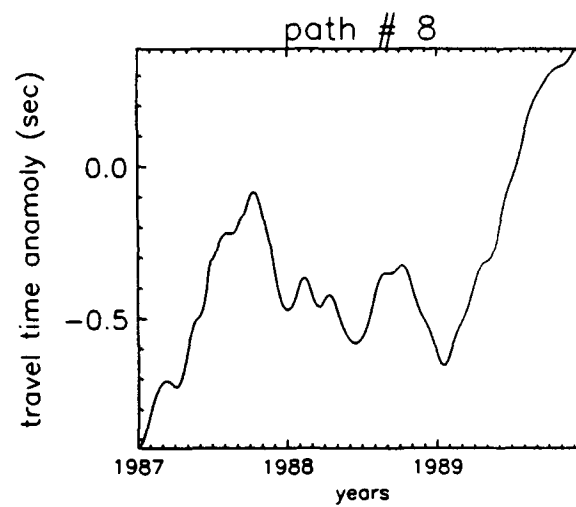
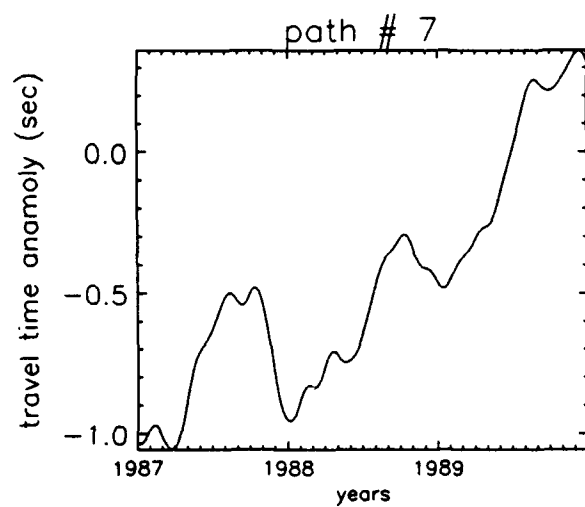
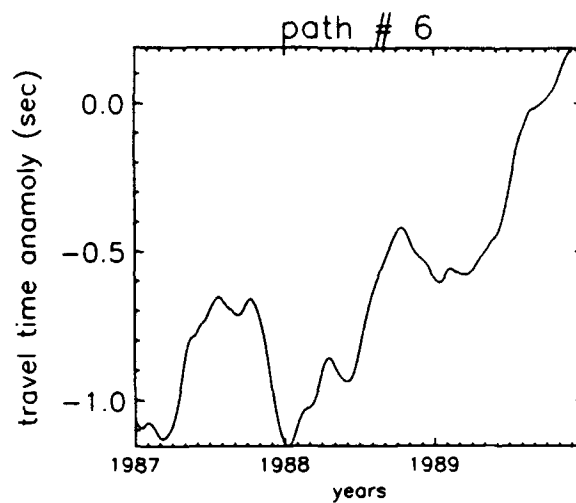
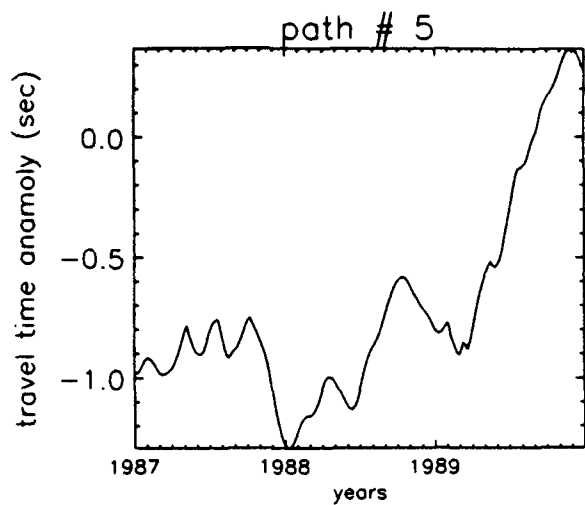


Figure 6

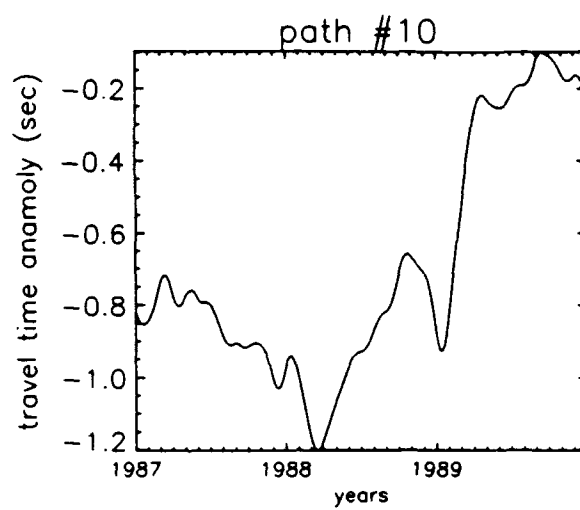
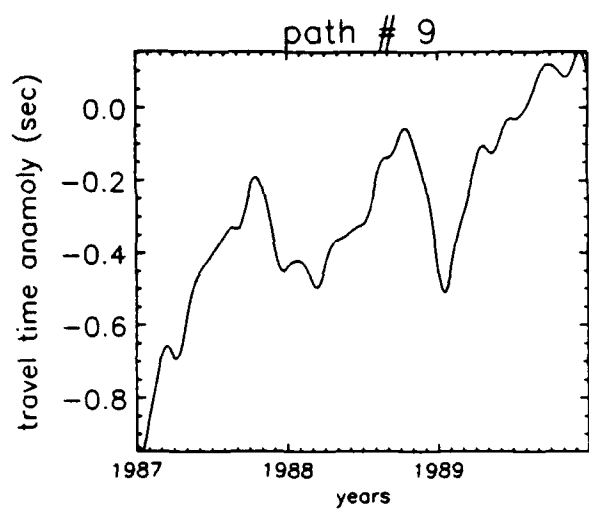


Figure 6

N.M	TASK B	Start Date	Finish Date	1993												1994												1995											
				A	M	J	J	A	S	O	N	D	J	F	M	A	M	J	J	A	S	O	N	D	J	F	M	A	M	J	J								
B.1	OBTAIN EQUATORIAL PAC WIND FIELDS FROM 80-91 AND DRIVE THE EQUATOR MODEL	4/14/93	5/31/93																																				
B.2	EXTRACT THE COASTAL KELVIN SIGNAL FROM THE EQUATOR MODEL AND DRIVE THE MID LATITUDE MODEL	6/1/93	6/30/93																																				
B.3	INTEGRATE THE MODEL SOLUTIONS BETWEEN HAWAII AND WEST COAST RCVRS	6/1/93	6/30/93																																				
B.4	COMPARE WITH OBSERVATIONS AND IDENTIFY VARIABILITY IN ACOUSTIC TRAVEL TIMES	7/1/93	9/1/93																																				
B.5	DESIGN FUTURE EXPERIMENTS	9/15/93	4/1/94																																				
B.6	ADD MODEL COMPLEXITY AND VERTICAL STRUCTURE TO IMPROVE ESTIMATES OF TRAVEL TIME	4/15/94	9/1/94																																				
B.7	RUN NRL MODELS	9/15/94	4/1/95																																				
B.8	USE REAL DATA TO ASSIMILATE INTO OCEAN MODELS OF THE NORTH PACIFIC	9/15/94	4/1/95																																				
B.9	SUBMIT FINAL REPORT	4/15/95	6/30/95																																				

TASK C

SSAR DEVELOPMENT

SEPTEMBER TEST CRUISE

The two SSAR drifting buoy configurations "Snubber" and "Standard" (Figure C.1) were deployed in September 1993 off Bermuda for a one week functional test. Both configurations performed without mechanical or electrical failures, and allowed recording of a variety of sensor outputs including acceleration, tension, hydrostatic pressure, tilt, compass, and acoustic level.

The "Standard" configuration suspended the full weight of the array and connecting 500 meter long electromechanical cable directly from the surface buoy. The "Standard" uses a 50 ft nylon reinforced rubber stretch hose with 4.9 inch outer diameter as shock absorber between the surface buoy and suspended array and cable, which preload the hose with 700 lbs calm water tension.

The "Snubber" configuration supported about 80 percent of the suspended array and cable weight from a subsurface buoy, which tensioned the surface float with a net calm water tension of less than 200 lbs through a 250 ft long nylon reinforced rubber stretch hose section of 2.6 inch diameter. The "Snubber" system recorded a slow increase of its suspended weight during the one week sea test. It also showed an unexpected flattening of the hose in the lower 20-30 ft observed during retrieval of the hose. The flattening can, in hindsight, be easily explained. It was caused by a pressure differential of about 30 psi between the bottom of the hose and the surrounding sea water and is due to the low-specific gravity of the Isopar fill fluid, which is only 75 percent of that of sea water. This pressure differential pushed the 250 ft vertical fluid column inside the hose toward the top, and compressed the lower hose section.

It was decided not to deploy the "Snubber" configuration for a long-term endurance test until a solution to the hose flattening and fill fluid weight problem is found. The flattened hose recovered to its original round shape after the pressure differential was removed upon retrieval. The flattening had not affected the electrical conductors inside the hose assembly. The "Standard" hose did not suffer the flattening since its length is only 20 percent of that of the "Snubber" hose, and the internal pressure generated when the hose stretches more than offsets the outside sea water pressure.

THE NOVEMBER TEST CRUISE

The Standard version of the SSAR prototype was field tested on a second cruise offshore Bermuda in November. The purpose of these tests was to measure the high frequency motions and forces experienced by the SSAR during a short

deployment and then to release the buoy for a long-term test of the system's mechanical reliability. A secondary objective was to perform initial tests of the ultra short baseline (USB) acoustic navigation system which measures the position of the acoustic array relative to the surface buoy. These tests were performed by lowering the USB system (which is contained in/on the lower electronics pressure case) to 500m and measuring the position of the responder which was hung off the ship's rail just below the hull.

The high frequency measurements were made over an 18-hour period on 3-4 November, 1993. High quality data were collected from all systems (see the November Test Plan in fig. C.12) except for the tension cell which malfunctioned because it was binding on its mounting bracket. This problem was repaired prior to the long-term deployment. An analysis of the response of the Standard design to wave forcing was performed. This analysis showed that the Standard SSAR has about a 3-second natural period. Vertical motion of the surface buoy and lower pressure case (500m depth) were compared by double integrating the measured z-axis accelerations. This analysis (Figure C.2) showed that the Standard configuration introduces significant high frequency vertical motions and amplifies overall wave induced motions by about 25%. This result was confirmed by the analytical model of SSAR motions.

The Standard prototype was deployed on 5 November 1993 about 50 miles south of Bermuda (Figure C.3). It drifted further south for about two weeks, then reversed and went north. By 1 December it was close to Bermuda's south coast. To keep it from going aground at the 500m contour, a retrieval cruise was organized and on 5 December the SSAR was retrieved. While this retrieval was unplanned, it did give us the opportunity to check the system for mechanical problems. One potential problem was found. Excessive corrosion of the sacrificial anodes located on the end caps of the lower electronics case was found. The reason was traced to electrical contact between dissimilar metals causing a galvanic reaction. We addressed the problem on the prototype by adding four anodes to each end cap, but we have modified the design for the operational units. The SSAR was re deployed about 70 miles East of Bermuda on 9 December and has continued to operate normally since. Figures C.4 - C.6 show some of the SSAR data telemetered during December.

FATIGUE TESTING OF SNUBBER HOSE ASSEMBLIES

In order to understand performance and deterioration of the hoses under wave forcing an accelerated fatigue test program was initiated with the support of Phil Gibson, president of Tension Member Technology (TMT). TMT is a sophisticated cable and rope test company, which built a customized combined tension and flex cycling machine for hose test samples of 6 to 7 ft length. The tester allows simulation and exaggeration of the hose tether loading when suspended from a wave following surface buoy. Both flex angle and tension as well as flex and stretch frequency can be programmed to provide a full range of test conditions.

The goals of the fatigue tests are:

- Determine the failure modes of the hose under tension and bend cycling.
- Determine the cycles until failure of hose designs being evaluated for use on the SSARs.
- Improve the hose designs based on the accelerated life test results.
- Test the new design which plans the electrical conductors in the hose wall to confirm its reliability.

So far two Snubber hose assemblies of 6 ft length have been fatigue tested to failure. Both of these test samples failed near the hose termination which was subjected to cyclic flexing. The hoses were exposed to higher stretch (42.5 and 50 percent) than actual installations would have to endure. Test conditions and results are summarized in Table C.1; the load elongation behavior is shown in Figures C.7 and C.8. Figure C.9 shows the hose elongation distribution over the entire hose length at maximum load and the burst location of samples 1 and 2. The hose wall of the samples is constructed with a stretchy compliant middle section, a reduced stretch portion with extra added reinforcement close to each coupling, and a 6 to 7 inch zero stretch region at each end where the hose is molded to the steel coupling.

Both samples failed due to bursting of the hose wall at the end subjected to flexing. Bursting is the formation of tears in the hose wall due to high fill fluid pressure buildup and/or breakdown of the rubber material under flexing loads. The hoses develop considerable fill pressure due to the choking of the fill fluid by the tensioned counterhelically applied nylon tire cord reinforcement (Figure C.10).

In sample 1, the hose failed at the transition point of the hose to the molded in steel coupling after 13,761 flex cycles, while being load cycled to 50 percent elongation. In sample 2 a 0.25 inch wide opening formed at the taper of the extra reinforcement layers positioned near the flexing hose coupling at flex cycle 39,546. This hose was tension cycled to 42.5 percent elongation. At the burst location of sample 2 the tension and flex loading support changes from three pairs to a single pair of counterhelically arranged nylon cord layers. Sample 2 was constructed with the shortest taper of load supporting extra nylon cord layers, thereby creating the highest stress and elongation change.

The electrical hose functions and the reinforcing cords did not suffer damage at the burst failure, but the fill fluid was forced out of the hose. If a burst failure occurred at sea, the hose would still support the suspended cable and acoustic array, but would operate with a softer and less elastic stretch response to surface buoy excursions caused by ocean waves. Its long term survival would probably be compromised substantially.

The test results provide valuable insight which allows design improvements of the stretch hoses to be made. Additional end reinforcement will be added to increase the bending stiffness and burst resistance at the coupling interface. The end reinforcement will be tapered more gradually to minimize stress concentrations and create a more gradual change of hose elongation along its axis. Both the Snubber and Standard hose designs will be strengthened and made somewhat larger in diameter. Further fatigue tests are planned next quarter.

DEVELOPMENT OF HOSE WITH ELECTRICAL CONDUCTORS CONTAINED IN THE HOSE WALL

Current SSAR hoses have coiled electrical conductor assemblies arranged inside the hose cavity to provide the signal path between the suspended electro-mechanical cable and the surface float. The conductors are either wrapped around a stop rope and contained by an outer textile braid, or - in the case of the larger "Standard" hose form a separate conductor assembly is coiled independently of the stop rope. In either configuration the conductors could be damaged by internal abrasion or local overstretching caused by snagging, though we have not seen this problem in the tests performed to date.

It may be more advantageous to build the conductors into the hose wall where they would be surrounded by rubber and reinforcing fabric and not exposed to abrasion or overstretching. A special coupling was developed which allows stress free passage of the conductors out of the hose material. The conductor path in the compliant hose section is designed to allow hose stretch up to 50 percent without elongating the copper wires. During December 1993 the first test hose with conductors in the hose wall was built and is currently being prepared for fatigue testing. The hose is constructed with a thicker hose wall encapsulating the conductors for improved protection and burst resistance. A second conductor stretch hose will be built after some fatigue test experience is gained with the first hose.

FABRICATION AND TESTING

Final SSAR electronic and mechanical designs are nearing completion. Wiring diagrams for the electronic subsystems have been completed. The fabrication plan for the ten operational units is shown in Figure C.11. Design and implementation of system software is continuing at WHOI and Penn State.

Major SSAR tests upcoming in the next quarter include a field test of the ultra short baseline acoustic navigation system at the AUTECH range tentatively scheduled for March. A preliminary cruise plan is attached. A second major test is scheduled to coincide with the Kauai source operation. When this source is operating we plan to deploy an operational SSAR and record the output of the

acoustic array and compare it to the measurements obtained from a SOSUS station located near the test area. This test is scheduled for early April.

List of Figures

- C.1 Prototype SSAR configurations
- C.2 Standard SSAR buoy (upper) and lower pressure case (lower) motions calculated from vertical acceleration data collected in November 1993 offshore Bermuda
- C.3 Standard SSAR drift track from 5 November 1993 to 23 January 1994. Note: the SSAR was recovered on 5 December and re deployed on 9 December 1993
- C.4 Standard SSAR tension data collected during long term drift test. Upper line is maximum tension, lower line is minimum tension, and middle line is average tension
- C.5 Standard SSAR vertical acceleration data. Upper, middle, and lower lines are the maximum, average and minimum accelerations experienced
- C.6 Pressure data recorded at the lower pressure case of the Standard SSAR
- C.7 Load elongation behavior of hose sample 1.
- C.8 Load elongation behavior of hose sample 2.
- C.9 Elongation under maximum tension of test hoses.
- C.10 Elongation versus fill pressure, hose sample 1 at load cycle 100 between 0 and 1,800 lbs tension; hose sample 2 between 0 and 1,300 lbs tension
- C.11 SSAR fabrication plan
- C.12 Standard Buoy Release Plan/Data Collection Strategy - November 1993
- C.13 Task C Schedule

Table C.1 Conditions and results of hose flex and tension fatigue tests

Appendix A: SSAR Cruise Report October 30 - November 7 1993

Appendix B: SSAR Cruise Report December 5-10 1993

Appendix C: SSAR Acoustic Navigation System Test Plan

Appendix D: SSAR Progress Report entitled "Surface Suspended Acoustic Receiver (SSAR) for Mapping Ocean Temperatures"

SSAR "Standard" Drifting Buoy System

SSAR "Snubber" Drifting Buoy System

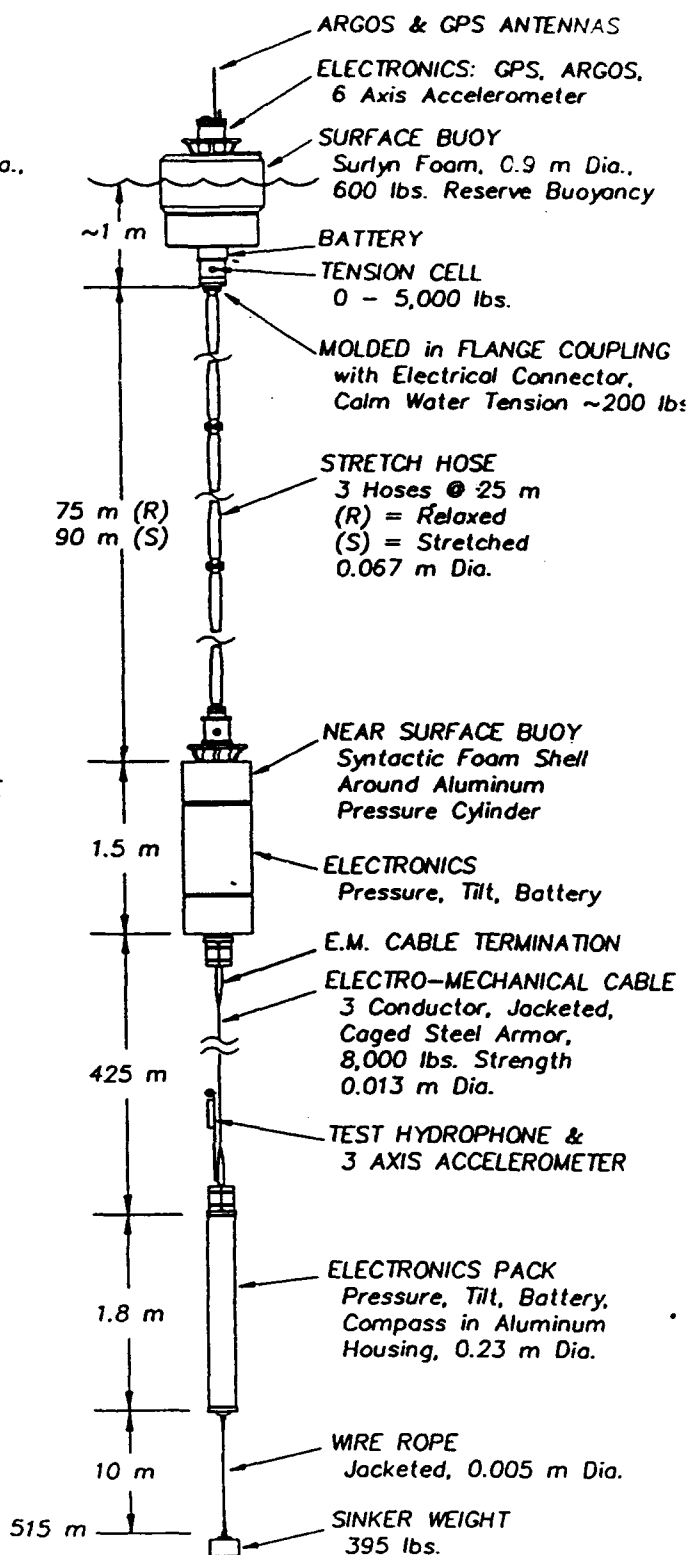
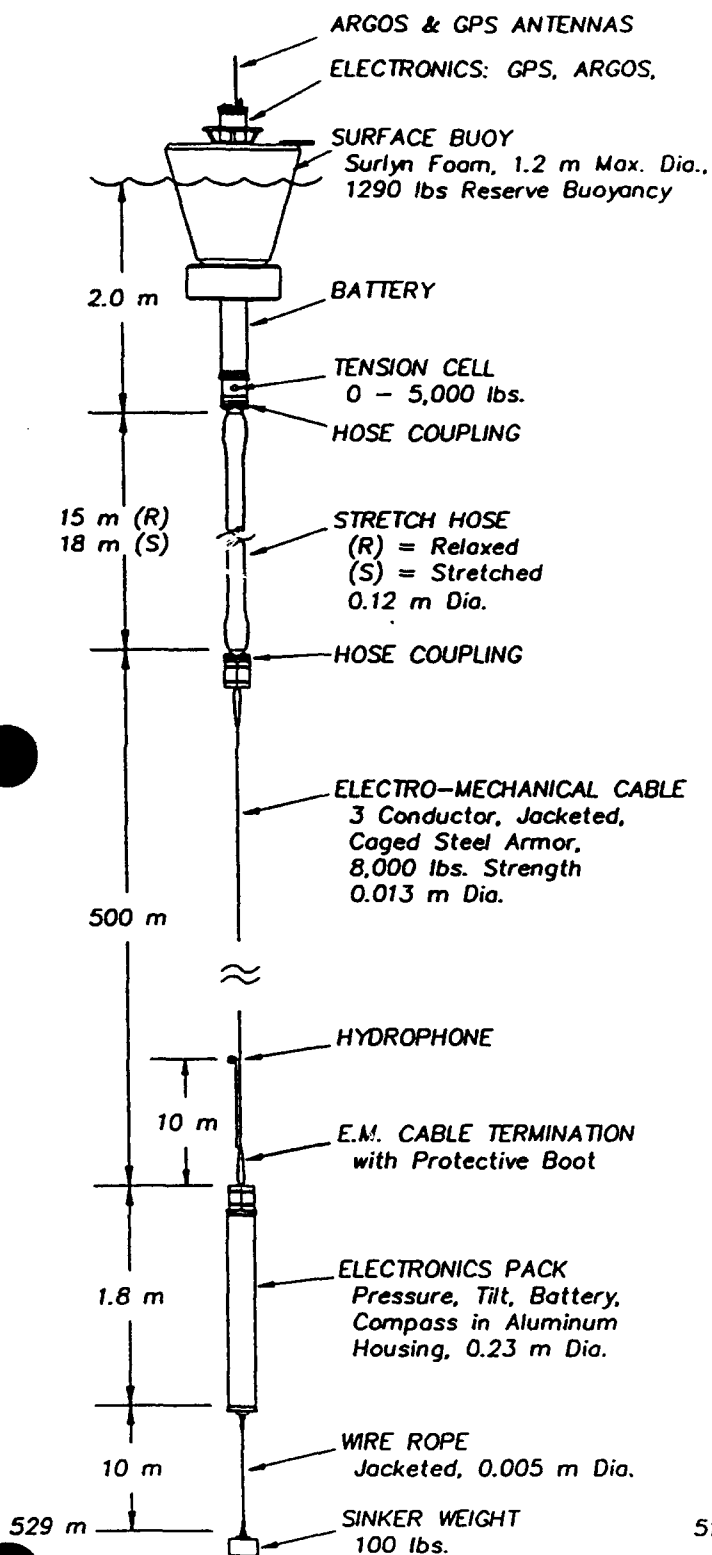


Figure C.1

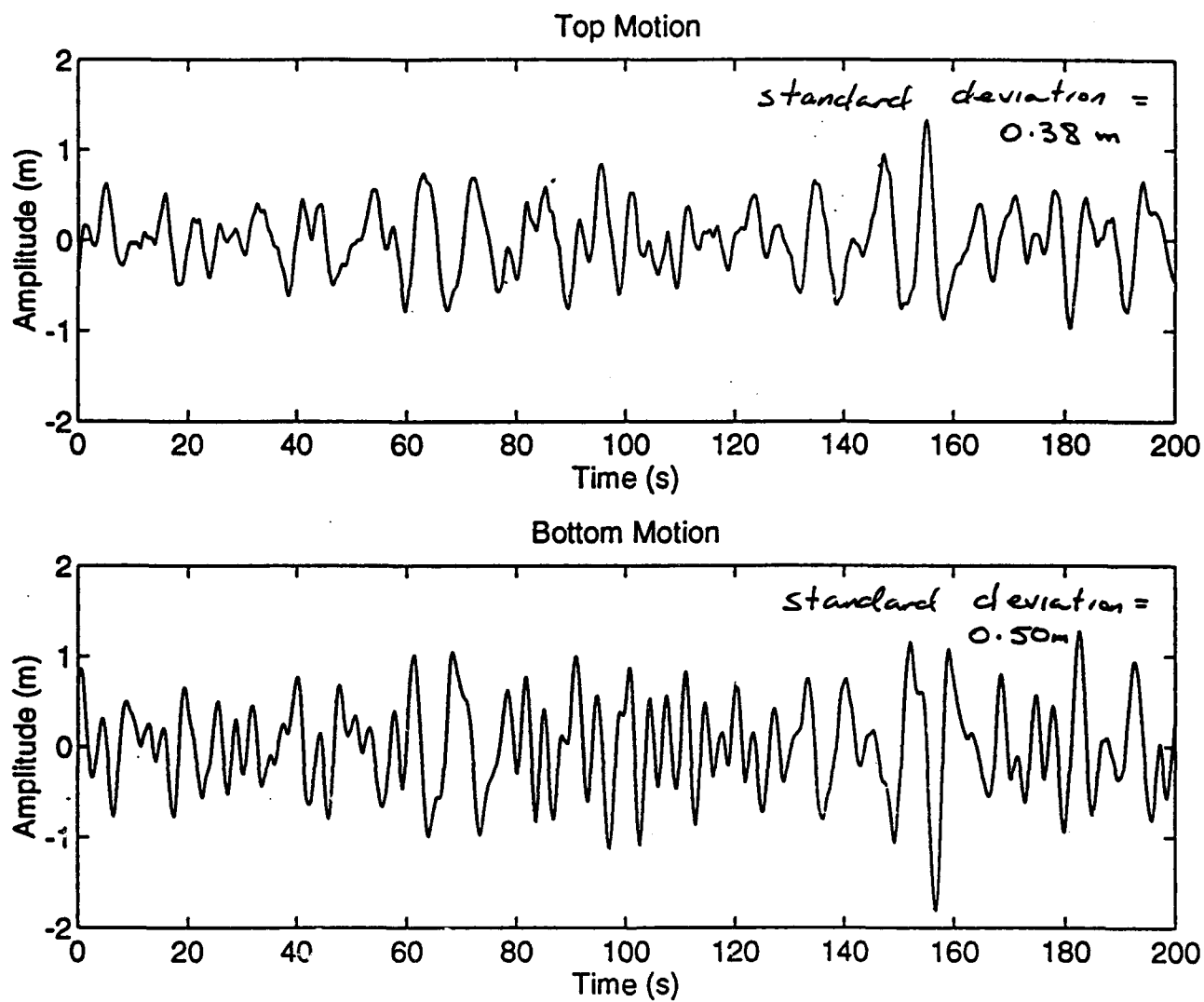


Figure C.2

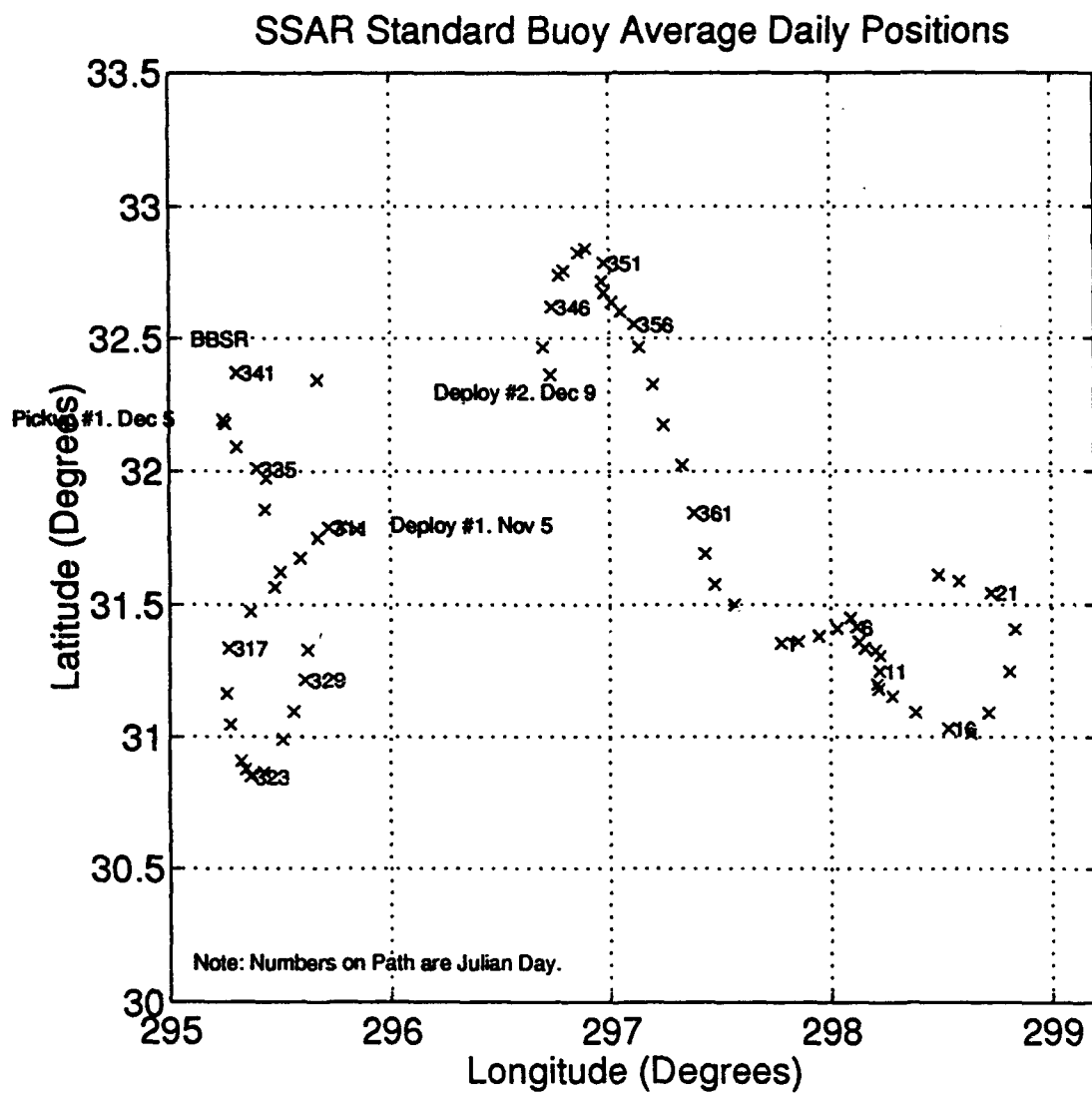


Figure C.3

Tension below Buoy

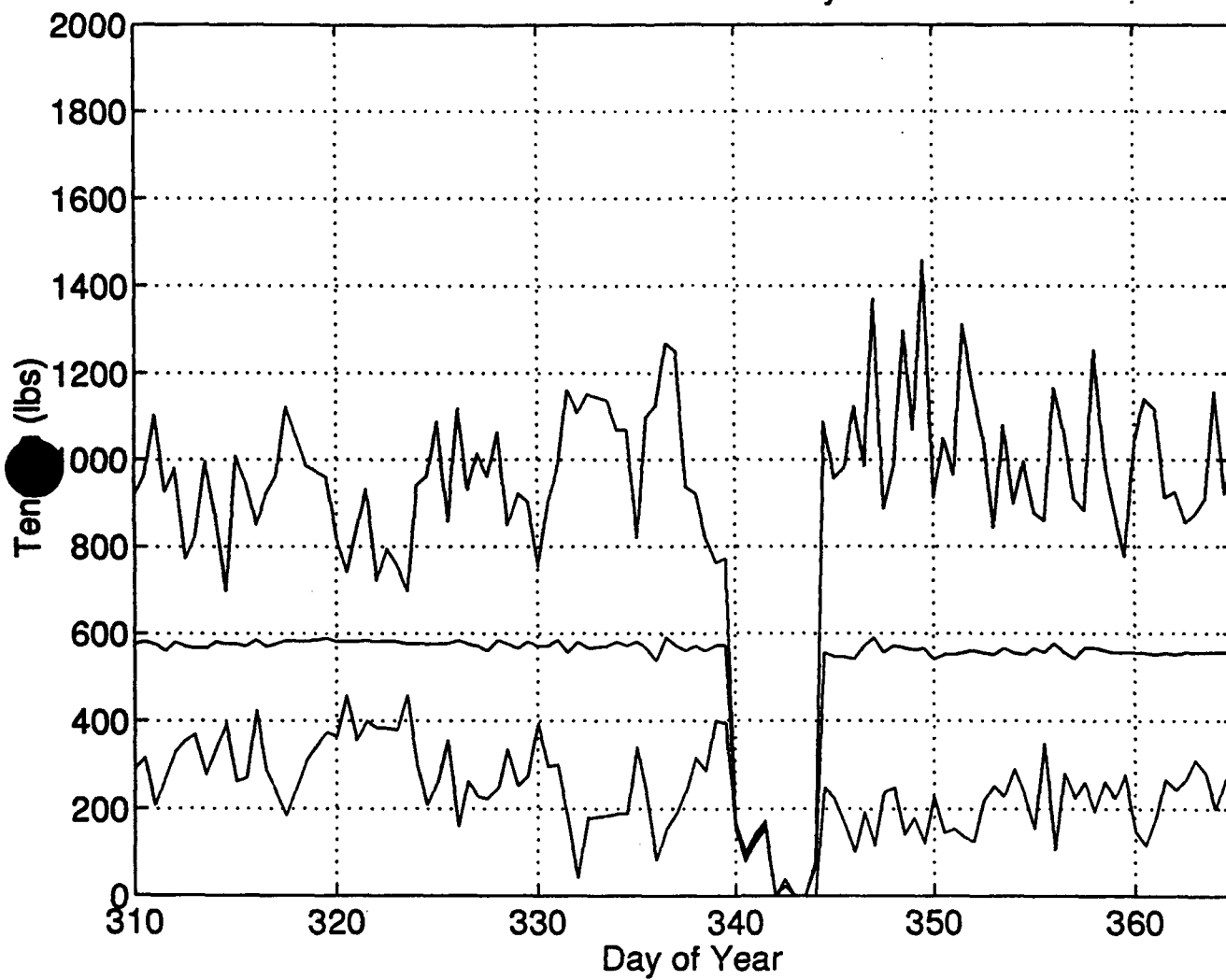


Figure C.4

Vertical Acceleration of Bottom Case

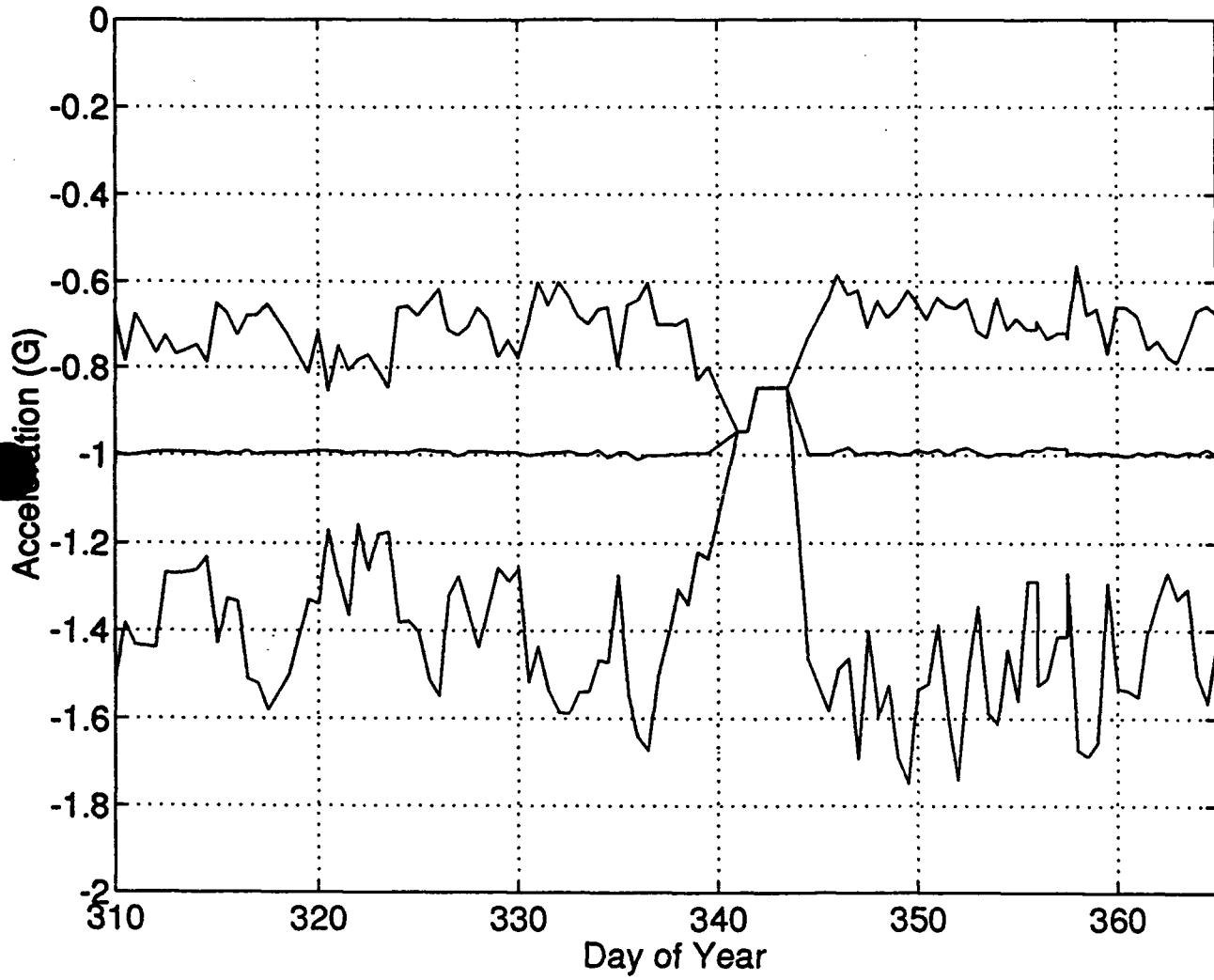


Figure C.5

Depth of Bottom Electronics

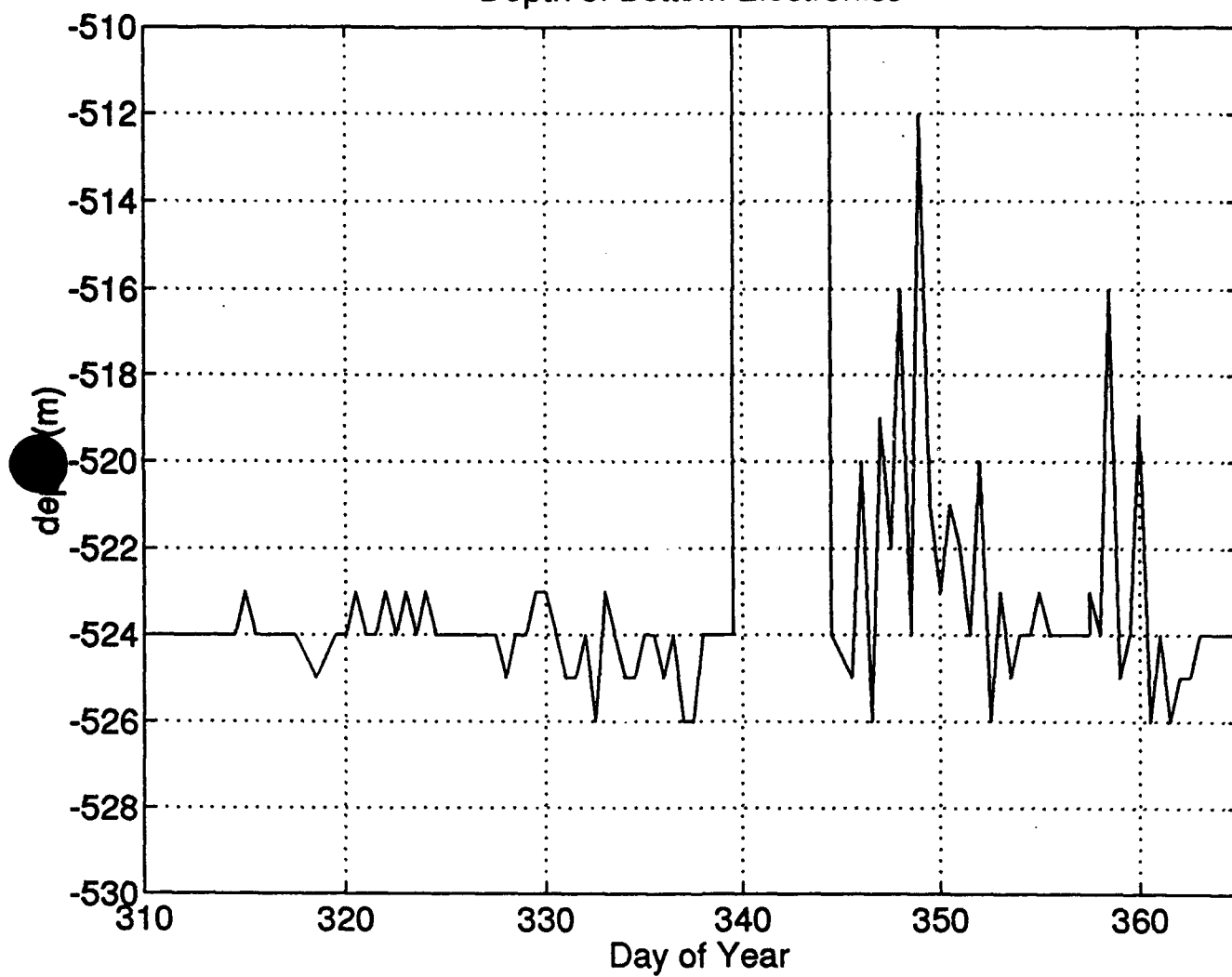


Figure C.6

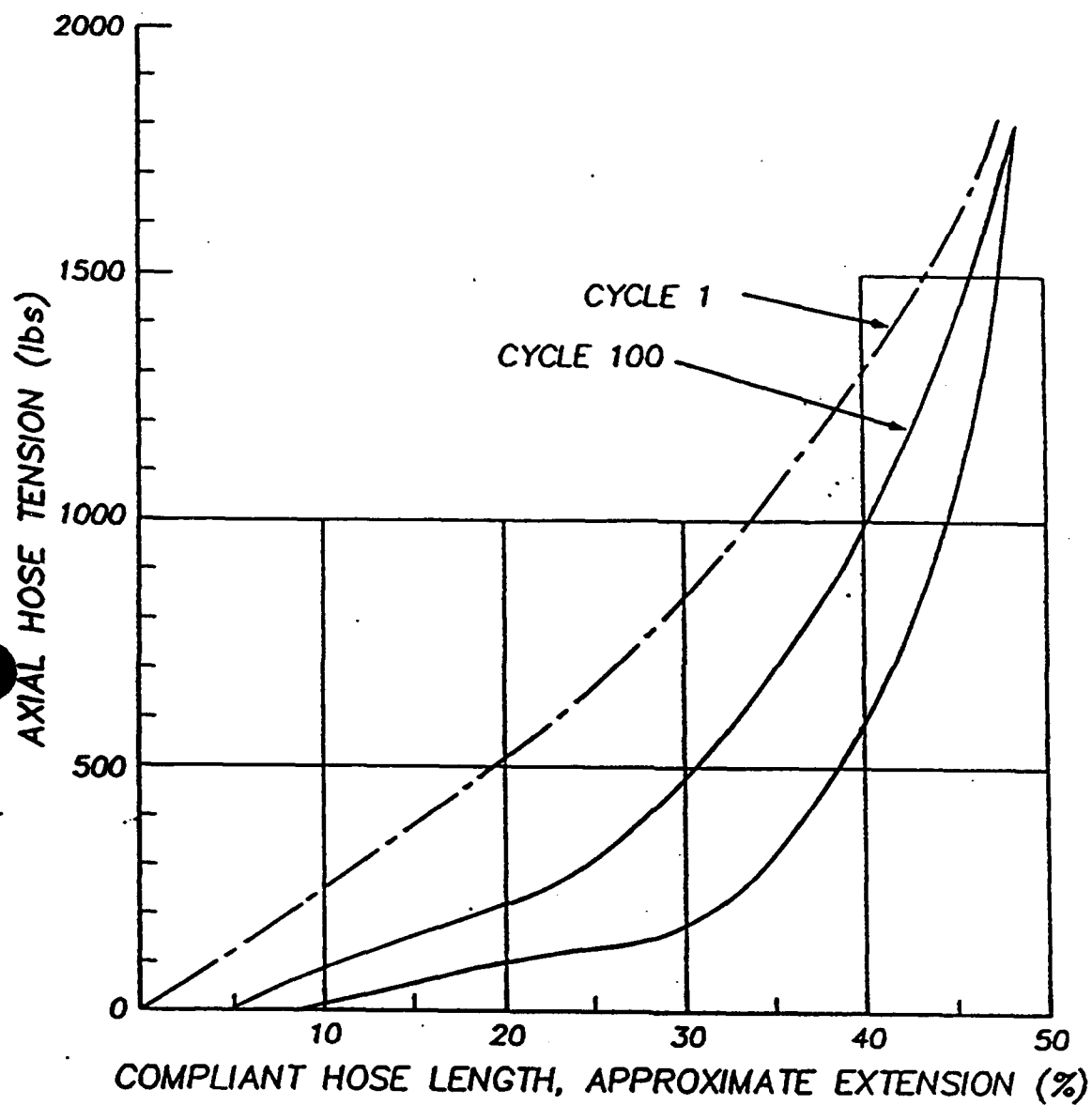


Figure C.7

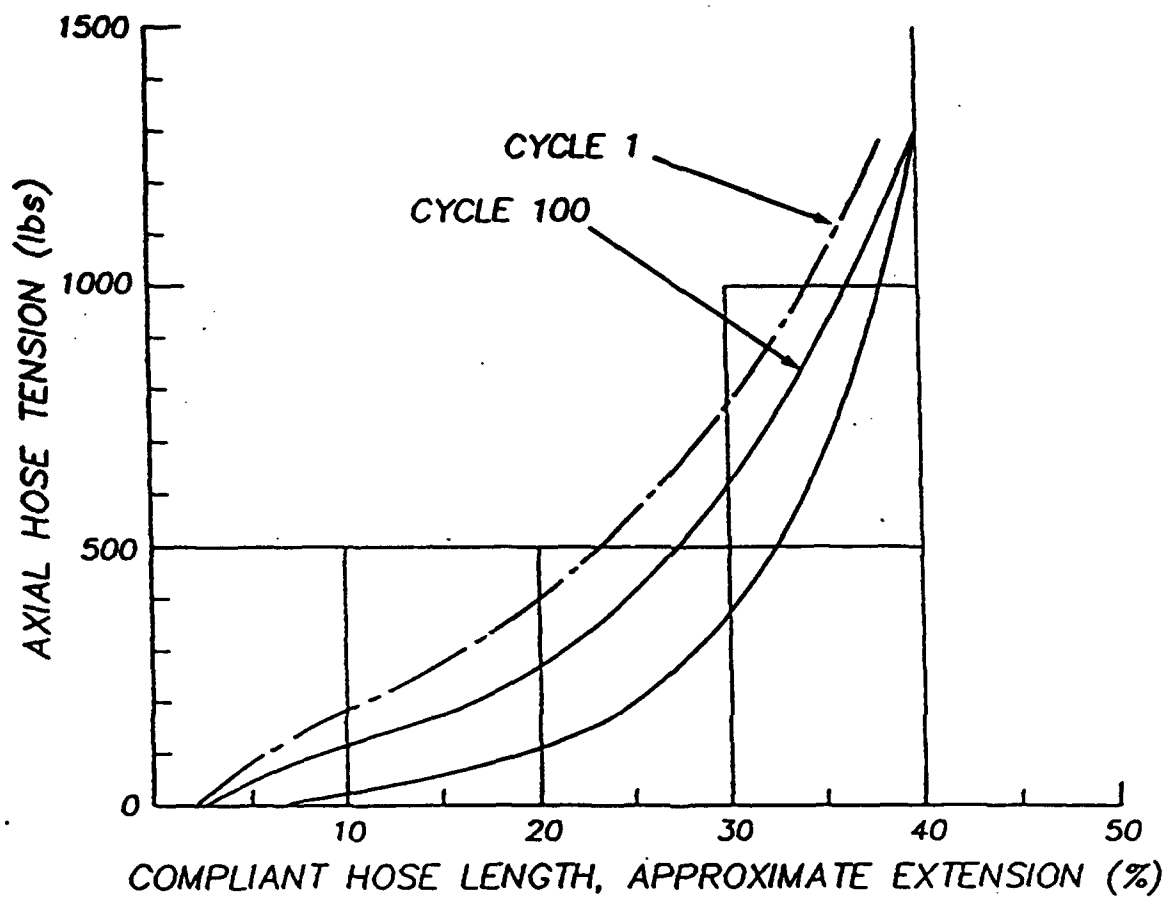


Figure C.8

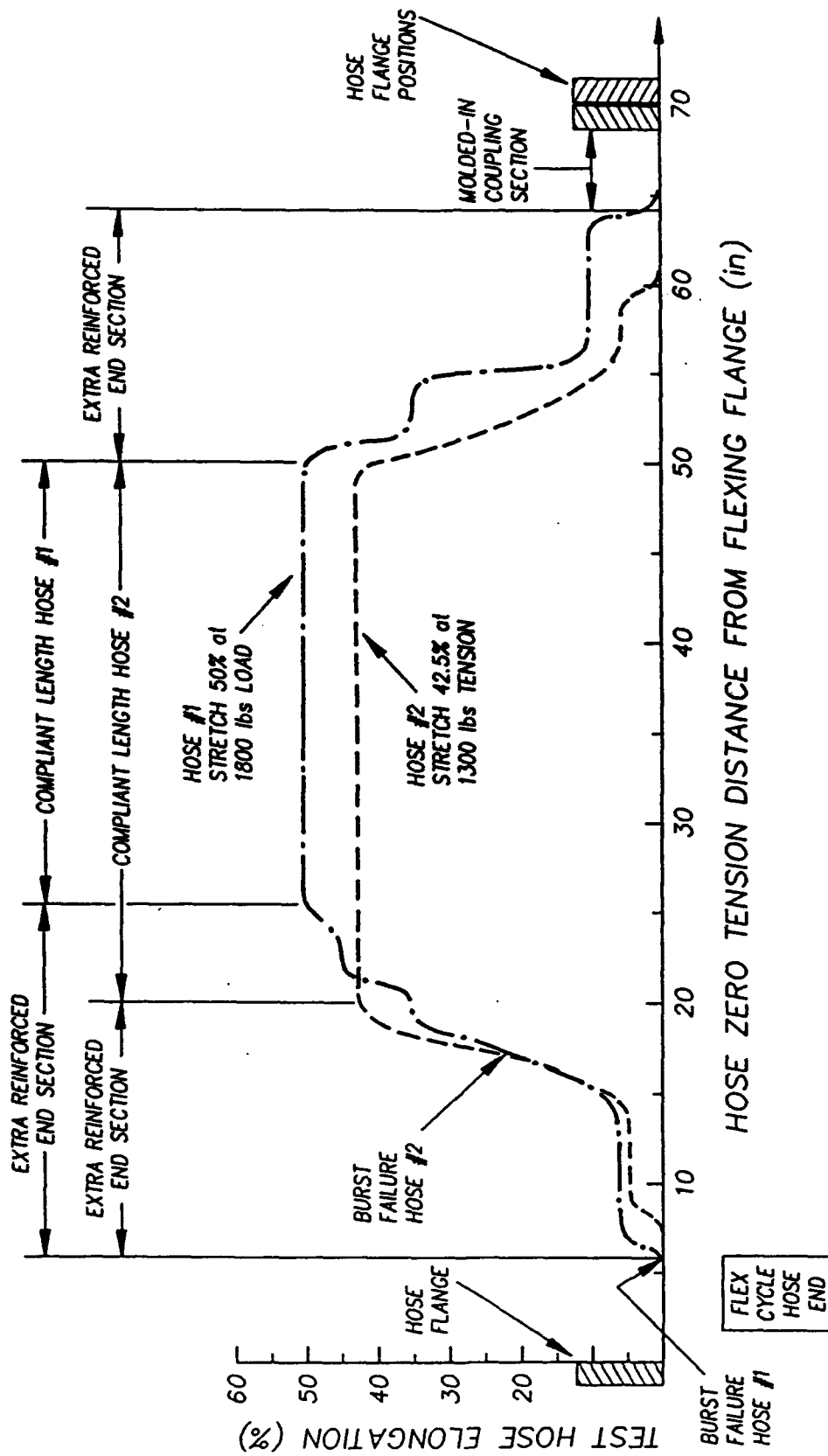


Figure C.9

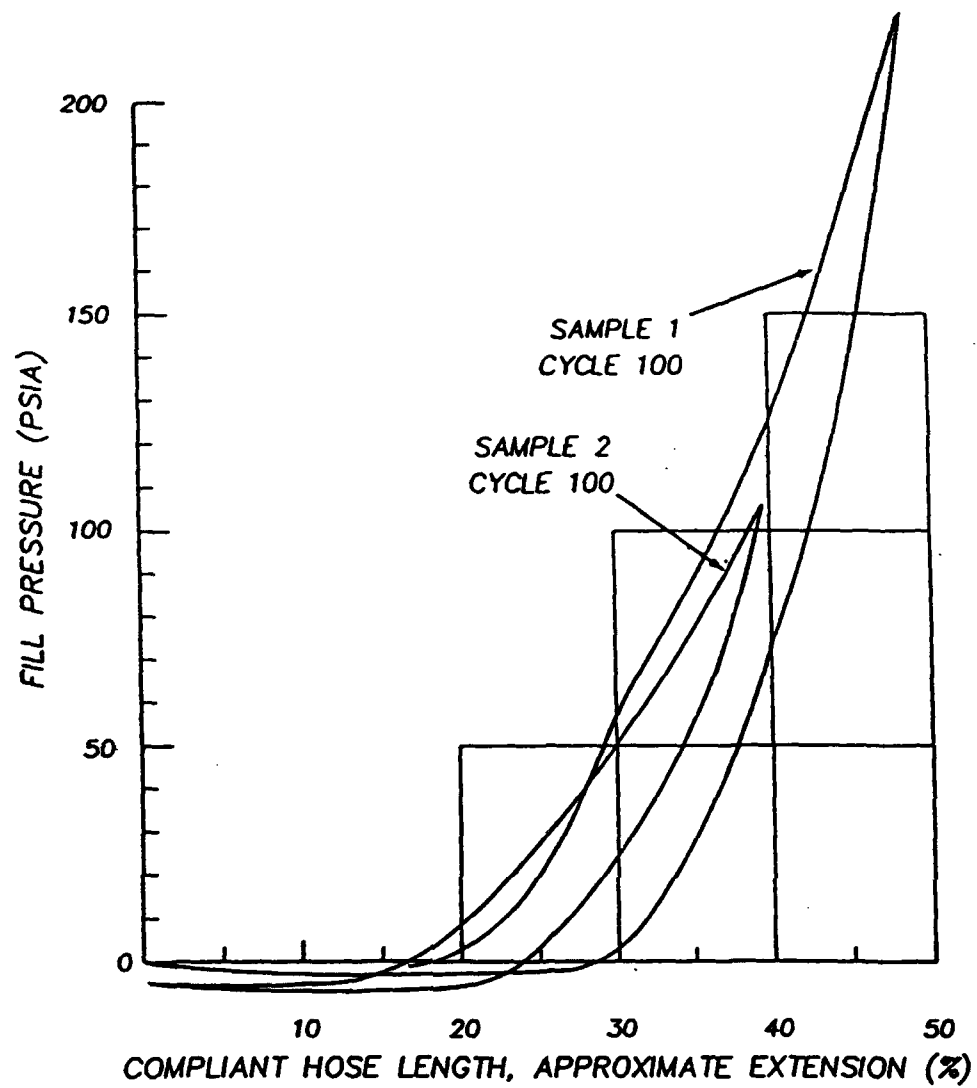


Figure C.10

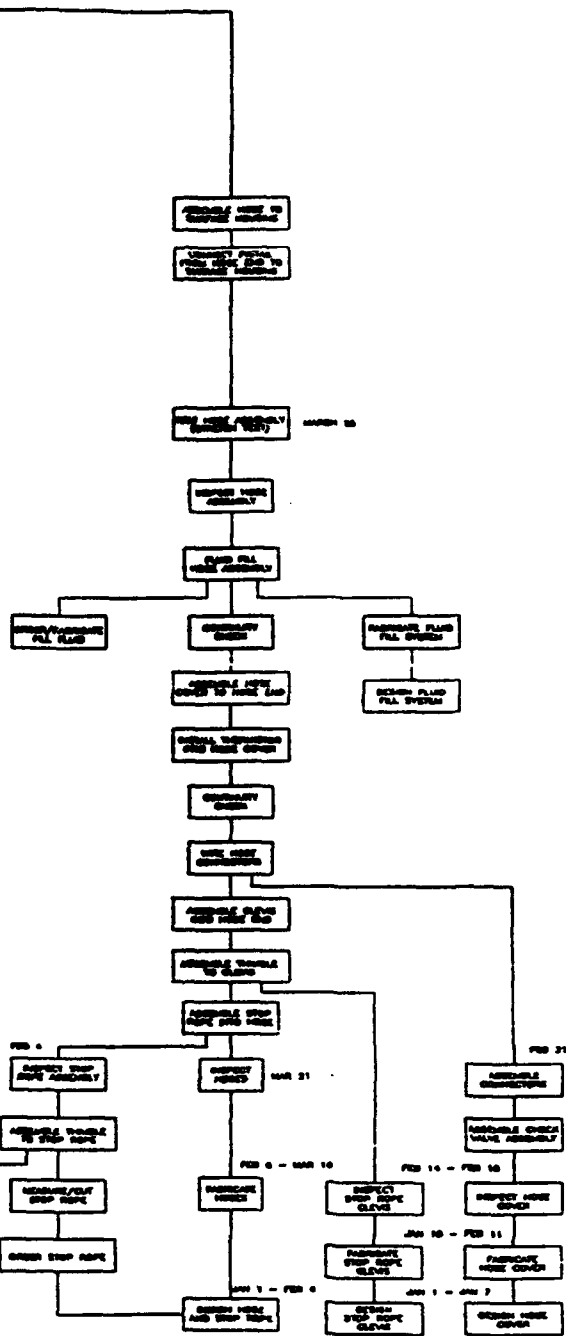


Figure C.11

3

STANDARD BUOY RELEASE PLAN - NOV. 1993

Data Collection Strategy

Release Date: November 5

Sampling: 2 times per day

Collection Period: About 10 minutes

Telemetry: 2 ARGOS transmitters each with one ID. 4 32-byte buffers each. 60 sec rep rate. Main data summaries on ID 1, time series data on ID 2.

Antennas: same as previous test, 1 patch, 1 whip

Life: Minimum life for data collect, 1 year

Sensor List:

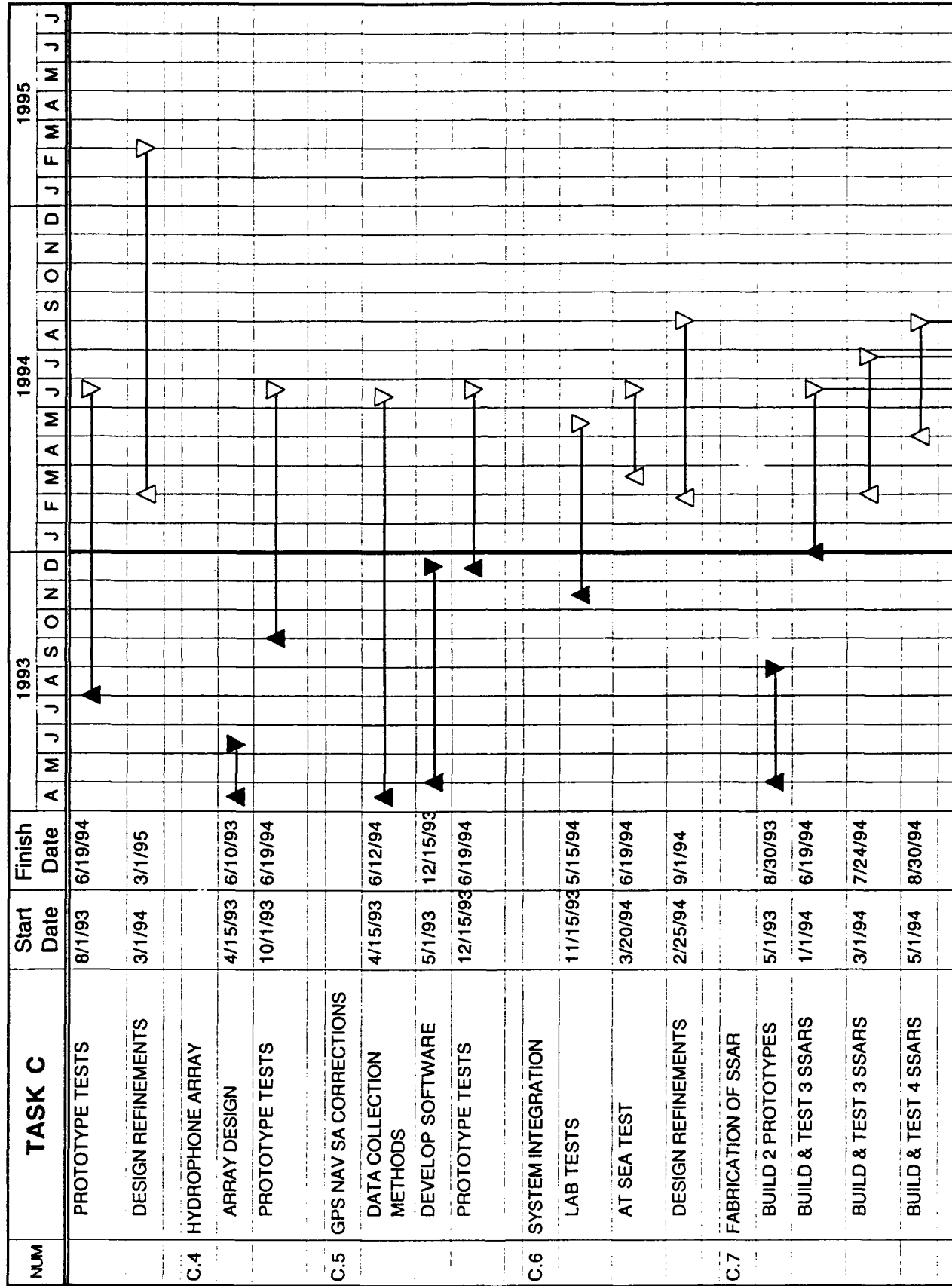
Buoy/System	Sensor	Rate	Duration	Telemeter
Top	Tension	50 HZ	600 sec max	max, min, avg, std, time series
	Tilt X,Y	50 Hz		max, min, avg, std
	Battery	n/a		1 value
	Comm Voltage	n/a		1 value
Bottom	Hydrophone	300 Hz	360 seconds	max, min, avg, std
	Tilt	300 Hz		max, min, avg, std
	Pressure	8 Hz		max, min, avg, std
	Z acc.	300 Hz		max peak - peak displ, time series
	X-Y acc	300 Hz		peak frequency and anpl of osc
	Compass			start, stop, std., avg

Figure C.12

1	2	3	4	5	6	7	8	9	10
Hose Sample #	Min and Max Load [Lbs]	Load Cycle Duration [Sec]	Elongation* at Maximum Load [Inch]	Flex Angle [degrees]	Duration of Flex Cycle [sec]	Fill fluid pressure at 4 [psi]	Load cycles till failure	Flex cycles till failure	Failure type and location
1	0 - 1,800	10	18	45'	3	220	4,152	13,761	Burst failure at end of steel coupling. Reinforcement intact.
2	0 - 1,300	9.5	14.5	25'	2.5	105	9,878	39,546	1/4" burst at taper of extra reinforcement hose otherwise intact.

*) Elongation under static tension in compliant center section of stretch hose before beginning of fatigue tests.

TABLE C.1: CONDITIONS AND RESULTS OF HOSE FLEX AND TENSION FATIGUE TESTS



[illegible]

SSAR Cruise #2 Report

Bermuda October 30 - November 7, 1993

October 30

Arrive BBSR 1300. Unpack computers and full instrumentation systems in lab. Check out of all systems. Test overnight with data log for both Argos and console. Tested both accelerometer systems and other sensors. Decided to switch over from Telonics Argos transmitter to JZ instruments version because of battery voltage mismatch with final battery configuration.

October 31

Overnight test results ok. Started checkout of long-term instrumentation. Both systems had cards dislodged, probably jarred on transit. No damage visible.

Started installation of batteries. Found that 3 of 8 will not fit into the cases. Top layers are skewed and will not fit. Decided to use 5 that will fit in surface system. One spare is left over from previous test. Total of 6 available for surface buoy. For bottom system will use the stack of three left over from test in October. Calculations of total battery life show that about 3000 WH should be left. Need about 1000 WH for 1 year for bottom system. Measured voltage was 14.7. Nominal starting voltage for these batteries is 15.2 volts.

Tested tension cell with no load, value is 85 to 90 lbs without hose attached.

Brought hose inside lab to cool in prep for potting internal connectors and topping off oil.

Installed surface electronics in buoy. Setup to run at 4 hour intervals overnight. Argos antenna placed flat in front of buoy so it will be able to hit satellite. Started log files for both the Telonics receiver and for the monitor output.

November 1

Examined Argos log files from Telonics receiver. No gaps in data from JZ Instruments PTT. Seimac PTT (4 ids with data) had several half hour gaps. 4 gaps over 10 hours (20% drop outs). Logged into Service Argos to check data. All PTT ids had data despite gaps in transmission. Passes were approximately at 00 hrs (GMT) 0710, 845, 1043, 1223.

Removed full instrumentation package from surface buoy. New collar installed on buoy.

Hose taken apart to pot connectors with socketfast. Gaskets will be replaced.

Argos antenna mounted on backing plate. Some problems with inserts. Mounted fine after replacing them.

Hose reassembled and topped off with a little less than 1 gallon of Isopar. Top and bottom systems set up for four hour updates to run overnight. Buoy is on porch, bottom system in pressure case on table inside.

November 2

AM No gaps in Argos data log file from Telonics receiver for Seimac data PTT.

Equipment loaded onto WBII

Installed new Seimac PTTs into long-term electronics and started test with Telonics receiver.

Installed surface electronics in buoy on deck of WBII. Set for four hour update rate.

Completed loading, attached hose to buoy.

November 3

0800 Depart dock, head for 1000m or greater water depth.

0900 During final electronics checkout find problem with disk controller. Pull electronics from case and replace SCSI card. Fixes problem.

0930 Purge and prepare bottom case. 1000 On station. Water depth 1860m.

1025 Tension average is -53 counts (-265 lbs). Assume due to position on deck. While on back deck buoy GPS is: 32 23.5014 N, 64 28.1149 W. Weather is mostly sunny, some waves to 3m, periods to 11-14 seconds. Prepare for launch.

1025 Hose in.

1038 Buoy in, E/M cable started out.

1115 1800m depth, E/M still going out.

1130 E/M out, preparing to mount accelerometer case.

1210 Acceleromter out, bottom case attached.

1240 Weight drop.

1248 Ship's GPS with buoy about 50m off port: 32 24.84 N, 64 28.72 W

Tension data from Argos transmission still negative. Not sure if problem is electrical or mechanical. Electrical suspected. Decision made to not retrieve system to attempt fix. Watch schedule set up to check position and operation of system through the night until 0600 hours. See watch log for details.

November 4

0615 Prepared for recovery, waiting for daylight.

0635 Buoy on recovery line.

0645 Buoy secure on deck.

0650 Hose on deck. Pickup point is 32 17.98 N, 64 31.53 W. Drift distance is about 7.5 miles.

0700 E/M cable at winch, hose and buoy rearranged on deck.

0708 E/M cable started in.

0720 At Hydrophone assembly.

0730 Bottom pressure case on deck.

0731 Weight on deck.

0740 Had to hammer off termination from pad eye.

0745 Deck secure. Headed back to BBSR. One connector on hose broken during recovery. Everything looks good otherwise.

At Dock:

Tension cell output stuck at -390 lbs. Swap signal conditioning units. New one is uncalibrated. Remove hose. Apply loads with new signal conditioning unit, not calibrated, but signal is present and changes with load change. Swap back to original unit. Check with analog scale in line with ratchet strap to deck tie-down. Force applied is within about 40 lbs of reading from tension cell. Scale is very hard to read accurately. Applied up to 1000 lbs during test. At this point have already switched over to long-term electronics system and moved original signal conditioning unit from full instrumentation unit to long-term.

Hose strung up on deck and opened to replace connector. Drilled out old one and replaced with spare. Potted as before.

Delrin ring on top of hose sanded down a lot and reinstalled. Tested with hose on by pulling straight aft. Cycled several times to make sure tension always returned to nominal zero (40 lbs). Two people pulling were able to generate up to 400 lbs force.

Logged into Service Argos to check data from long-term electronics. Both transmitters got through ok. Used spare patch antenna on chair in front of buoy.

Departed dock at 2330 hours. Very calm. Systems operating with hourly updates most of afternoon and evening. Connection from bottom case to top is via deck cable from bottom case to bottom of hose.

In preparation for deployment systems are put to sleep until 1400 GMT (1000 local), 2 hours after normal schedule. This will avoid a rush to get system in the water before update at 0800.

November 5

0600 Preparations on deck. Cases purged, deck cables removed, monitor cables removed.

0750 Buoy and hose in. Note: extra foam collar not installed. Protective cover in place at termination at bottom of hose.

0755 E/M cable started out. Weather: partly cloudy, 1.5m swell with small chop. Wind 12 knots E. NE.

0850 Begun attachment of hydrophone.

0910 Positioning bottom case in preparation for deployment and making connections at end cap.

0920 Taping up cables at top of electronics case.

0925 Bottom case over the side. Weight cable out.

0932 Weight drop. 100 lb weight used.

0944 Ship position close to buoy is 31 47.00 N, 64 07.20 W.

1010 Received 1000 update (1400 GMT) data via Argos. Data present from both top and bottom systems, tension data from top looks ok.

1030 Prep for lowering. Cable spooled to winch.

1100 Electronics with DSP for test installed in case. SCSI card fails.

1130 Replacing SCSI card.

1200 Got GPS position for buoy. Checked operation of PTTs. All working ok.

1205 Left deployment site and heading back to Bermuda.

1240 Reinstalled electronics in bottom case.

1310 Ship stopped for lowering, started down with winch.

1342 Cables connected at surface for ping trigger from bottom. Various test done with responder.

1411 Started back up.

1420 Case at surface

1425 Ship underway again.

1445 Data check. Parameters for data collection incorrect. Adjust and prepare for additional test.

1538 Ship stopped for lowering, started down with package.

1602 Responder cables connected.

1602-1637 Tests done with transponder at stern and at starboard rail at two positions.

1640 Started up with E/M cable.

1653 Case on deck. Ship under way.

1700 Checking data. Data files appear to have captured transponder pulses on all channels OK.

2030 Docked at BBSR.

November 6

WBII unloaded. Arco Lab equipment packed and prepared for shipment to WHOI.

Logged into Service Argos. Data appears OK. Summary of tension:

Day	Time	Max	Min	Avg	Std
11/5	1400	915	255	580	140
11/6	0000	940	300	590	120
	1200	990	325	595 1	40

Data checked from short test. MotionPak and bottom accelerometer data appears OK. Backed up data from buoy SCSI disks onto PC.

November 7

Container loaded with deck gear and boxes. John Kemp stays to load TSE winch on Monday when crane is available.

R. Arthur, A. Bocconcelli, E. Denton, W. Paul, L. Freitag return to WHOI.

CRUISE LOG

5 December - 10 December 1993

Objective: A prototype standard SSAR was deployed offshore Bermuda on 5 November 1993 to gather long term data on the mechanical reliability of the design. The buoy began to approach Bermuda about 1 December and a decision was made to retrieve it before it went aground and to re-deploy it if the SSAR was undamaged. Arrangements were made with the R/V Weatherbird 2 to retrieve the SSAR on Sunday, 5 December.

Sunday, 5 December 1993

0910 Frye and Bocconcelli depart Boston for Bermuda

1210 Arrive Bermuda; clear customs

1300 At Biostation - met with Captain Lee Black; install RDF equipment for locating buoy; get position update from Lee Freitag.

1400 Depart St. Georges en route to SSAR location

1645 Have SSAR in sight; begin recovery

1745 End recovery - SSAR appears undamaged.

2100 Returned to St. Georges; offloaded vessel

Monday, 6 December 1993

0630 Spoke with Chief Scientist on the cruise schedule for this morning and the second leg due to depart on Thursday, 9 December. Agreed tentatively to allow us to deploy the SSAR east of the island on the evening of the 9th.

0800 Checked buoy carefully for damage. Buoy and hose looked fine as did the E/M cable. Zines on the lower pressure case were quite corroded. Decided these needed replacement and additional anodes. Also noticed (during recovery) that the patch antenna was getting washed over about 20% of the time. We need to redesign the antenna mount to get it higher off the water. Set the SSAR up with a test cable and began a test to make sure the electronics system was functioning normally. Arranged for spare parts to be Federal Expressed from Woods Hole.

Tuesday, 7 December 1993

Checked data from overnight test - all data okay except lower case tilt - x axis. Moved case around to various attitudes. Tested E/M cable. Spare parts arrived from WHOI.

Wednesday, 8 December 1993

Checked data from overnight test - all data now okay. Installed new zines; coated end caps where anodizing scratched. Put neoprene around end plate edges to reduce corrosion near O-rings.

Thursday, 9 December 1993

Checked data from overnight test - all data normal.

0830 Boarded vessel; checked RDF gear

1200 Departed St. Georges - Biostation crew worked on BATS sampling.

1600 Steamed toward SSAR deployment site - 70 miles East of Bermuda

2030 Final data check of data collected at 2000 local time.

2100 At launch site. Begin deployment.

2235 Finished deployment @32°19.40'N and 63°16.06'W. 68.5n miles east of Bermuda. Steamed to Biostation site to recover their equipment.

Friday, 10 December 1993

0700 At the Biostation site - recovered their buoy and performed plankton net tows and CTD stations.

1000 Headed back to St. Georges

1300 At dock - unloaded equipment

1700 Depart Bermuda for Boston

1800 Arrived Boston

2000 Arrived Falmouth

SSAR Acoustic Navigation System Test Plan

NUSC AUTECH Range

Background

The SSAR (Surface Suspended Acoustic Receiver) is a free drifting buoy with an acoustic array and electronics package suspended 500 meters below on an electro-mechanical cable. The surface buoy has a GPS receiver for measuring the location of the buoy in absolute geographic coordinates. The unit at the bottom of the cable has an acoustic navigation system for locating itself with respect to the surface buoy. This is an ultra short baseline (USBL) acoustic navigation similar in principle to an ORE Trackpoint. The absolute location of the bottom electronics package and acoustic array is very important for the tomography data received on the acoustic array. The goal of the navigation system is to locate the array to within 20 meters absolute accuracy.

The surface buoy is small, 1m in diameter and less than 2 m tall. The subsurface electronics package is about 2 m long and less than 0.3 m in diameter. The height of the buoy above the water's surface when deployed is about 0.6 m. The buoy is equipped with a 6 second strobe light and reflective tape.

A very low power satellite RF link (ARGOS) will be used to get status information from the buoy. Watt and transmits once per minute for less than one second.

Objective

The objective of this test is to verify the accuracy and resolution of the SSAR acoustic navigation and GPS system by tracking the bottom electronics package and the buoy as it drifts through an instrumented acoustic range.

Requirements

The test requires the following elements:

1. Instrumented range with tracking facility providing time, x, y and z location referenced to known geographic coordinates. The accuracy of the tracking needs to be on the order of +/- 4m or better. Accuracy of +/- 2m would be preferred for system error analysis. Tracking data results are desired in digital form (ASCII file, PC diskette or other convertible electronic media, e.g. 9-track tape.).

2. Pinger capable of generating range tracking pulses which can be attached to the bottom pressure case and surface buoy. It should be self-contained or have electronics capable of fitting in an 8.5 inch ID tube with an external transducer. 15 volt power is available inside the pressure cases if needed for the pingers. The USBL system operates at 25 kHz, therefore the external pinger should be below 20 kHz or above 30 kHz. The repetition rate of the tracking pingers can be 8-16 seconds.

3. A small on-shore lab area for setting up a portable PC and GPS receiver for the shore differential station. A GPS antenna will need to be mounted within about 100 feet of the GPS receiver on an existing tower or simply on a pole clear of nearby rooftops. A surveyed reference point will be needed to locate the antenna. This requires a USGS type benchmark within a few miles of the shore differential station to be operated during the test. All GPS work including transfer of reference and survey will be completely handled by a WHOI subcontractor (University of Texas, Austin. Applied Research Lab). The differential GPS system will allow positioning of the buoy to within +/- 5 m or better.

4. Additional small area (10 by 20 feet with a few tables) for staging the electronics systems and testing prior to deploying the buoy.

5. Vessel capable of deploying the buoy and standing by during the tracking period. A winch is needed for the 500 m of electromechanical cable. A crane or A-frame is needed to deploy the buoy and electronics package. No element of the system weighs more than about 400 lbs. A few feet of bench space is needed aboard the vessel for radio monitoring equipment.

Proposed Plan of Operation

Day 1 Unpack electrical systems and test. Perform GPS survey and set up differential reference station. Prepare buoy for launch. Install and test tracking pinger.

Day 2 Complete on-shore testing, load vessel.

Day 3 0800 Depart for fine-track area in weapons range.

1000 Deploy buoy at center of fine-track area.

1200 Begin monitoring of buoy system via RF link. Start range tracking. Verify tracking status with AUTEK personnel via radio. Compare status information from buoy with tracking range location information (if available in real-time or near real-time). If system operation appears correct, continue test through the night.

If the buoy drifts outside the range area it will be towed back into the center of the fine track area or to one edge of the range as required by the current direction and magnitude.

Day 4 0800 Recover buoy completely.

1000 Transit to shore.

1200 Begin off-load of equipment

1700 Vessel off loading complete.

Day 5 Pack equipment and depart.

Contingency Notes: If problems are found with the buoy tracking system the buoy may be recovered and brought back to shore. Depending on the problem the buoy could be redeployed the next day or 1 day later. However, this also depends on the range schedule.

Summary of Required Information

1. Accuracy of acoustic tracking in the AUTEK weapons range.
2. Cost of facility use as outlined above.
3. Cost of ship use as outlined above.
4. Range availability in Jan and Feb, 1994.
5. Pinger specifications (size, weight, power, etc).
6. Data (t,x,y,z) output format after the experiment.
7. Availability of tracking data in real-time.
8. Security and classification issues (as req'd by this test).

Proposed Personnel

Dan Frye, Supervisor

Lee Freitag, Electronics Eng.

Tom Austin, Electronics & Acoustics Eng.

Deck Personnel (1 or 2)

Shaun Mckee, GPS specialist (UT-ARL)

Woods Hole Oceanographic Institution Point of Contact:

Paul Boutin, Research Specialist

Bigelow Bldg. 111

Woods Hole Oceanographic Institution

Woods Hole, MA 02543

Phone: (508) 457-2000 ext. 2212

FAX: (508) 457-2194

Technical Information:

Lee Freitag, Research Engineer

Smith Bldg, 210

Woods Hole Oceanographic Institution

Woods Hole, MA 02543

Phone: (508) 457-2000 ext. 3285

FAX: (508) 457-2195

SURFACE SUSPENDED ACOUSTIC RECEIVER (SSAR) FOR MAPPING OCEAN TEMPERATURES

**Daniel E. Frye, Woods Hole Oceanographic Institution
Lee Freitag, Woods Hole Oceanographic Institution
Walter Paul, Woods Hole Oceanographic Institution
Mark Grosenbaugh, Woods Hole Oceanographic Institution
John Spiesberger, Pennsylvania State University**

1.0 INTRODUCTION

A free-drifting acoustic receiver capable of measuring acoustic travel times across ocean basins is being developed as part of the Global Acoustic Mapping of Ocean Temperatures (GAMOT) project which is funded under the Advanced Research Projects Agency's (ARPA) Acoustic Monitoring of Global Ocean Climate Program. This program is a multi-institutional effort to develop techniques to measure and analyze changes in the heat content of the oceans [1]. The SSAR is an economical alternative to fixed receiver arrays which are cabled to shore or moored to the ocean floor. It combines a multi-element hydrophone array suspended in the sound channel with in situ data processing, acoustic and satellite navigation and near real time data telemetry. The first ten operational SSARs are scheduled for deployment in the northeast Pacific in the summer of 1994. They will receive signals generated by acoustic sources located near Hawaii and Pt. Sur, California. Anticipated lifetimes for the SSARs are one year or more.

Data collected from the operational SSARs will be used to measure acoustic travel times along many acoustic paths across the northeast Pacific. This information will be used in conjunction with similar data from fixed receiving arrays located along the U.S. West Coast, the Aleutians and in the South Pacific to investigate temperature variability over broad spatial and temporal scales. Models of the ocean's response to large scale forcing are being used to analyze the travel time data and help determine the dynamics behind the observed variability [2].

2. TECHNICAL APPROACH

MECHANICAL DESIGN: The SSAR concept is similar to a sonobuoy; suspend an acoustic array at a known depth and telemeter the received data. To be useful for long term travel time measurements across ocean basins, however, the SSAR design must extend the sonobuoy concept substantially. Table 1 shows the general requirements that a successful SSAR design must meet. The mechanical design was driven by three overriding requirements. First, a lifetime of one year was required for a drifting system with a multi-element acoustic array at 500m and a surface platform for antenna location. This requirement meant that a secure path for the data from the acoustic array had to be maintained through the air-water interface where wave

induced motions raise havoc with electrical conductors. Second, dynamic loading of the mechanical elements of the system had to be kept to a minimum to avoid fatigue related failures because millions of cycles will be experienced during the course of one year. This suggests that very conservative load factors be employed. Third, a relatively economical and easy to deploy system was required because the SSAR's utility is based at least partly on its ease of installation and low cost relative to other long term receivers.

To address these requirements a number of alternative approaches were investigated including spar buoys, nearly submerged systems, horizontal flotation techniques, standard drifting buoy designs, and compliant systems,. In addition, various techniques for telemetering data from the 500m array to the surface were also considered. These alternatives were hardwired telemetry, inductive telemetry [3] where signals are transmitted using insulated wire rope, and acoustic telemetry [4] where data are transmitted using seawater as the communication channel.

The results of the initial design investigation produced three alternative designs. Each of these three designs was capable of meeting the system mechanical requirements and each could support the use of any of the three telemetry alternatives. After further analysis, it was decided that designs 1 and 2 (Figure 1) termed "Standard" and "Snubber" would be fabricated as prototypes for laboratory and field testing with design 3 held in reserve. A preliminary decision, based on cost and reliability, was also made to use the hardwired telemetry option in these prototypes, though provision was made to allow use of another telemetry option if reliability problems were encountered during the sea tests. The decision to hold design 3 in reserve was based on the risks associated with a minimum buoyancy, horizontally positioned surface expression. These risks include marine growth, marine traffic, and high drag due to currents, winds and waves.

Two prototype SSARs have been built and tested at sea. Both have performed well. The two designs share many of the same components, differing only in the type of compliant hose used beneath the surface buoy and the distribution of buoyancy - either entirely in the surface buoy (Standard) or split between the surface buoy and a subsurface buoy located at the bottom end of the compliant hose section (Snubber). The compliant hose technology, which is an adaptation of the vibration isolation hoses used by the Navy for towing acoustic arrays and the oil transfer hoses used in the oil industry, was chosen for two reasons. First, the hoses are capable of surviving oscillating forces over millions of cycles. Since the electrical conductors are protected within the hose structure, this provides a safe passage between the electromechanical cable and the surface buoy. Second, the hoses provided compliance in the system which substantially reduces snap loads caused by wave action. These snap loads often lead to component failure in drifting systems.

In both SSAR designs a small surface buoy made of Surlyn foam supports the surface electronics package and provides a platform for the satellite antennas. An aluminum pressure case houses the electronics and is used as a central strength

member in the buoy. Lifting bales and the compliant hose section are tied directly to the pressure case. The rubber hose with its molded-in end fitting and flange is bolted to the lower end of the surface buoy pressure case. The electrical conductors inside the hose enter the pressure case through a five-pin connector. The rubber hoses used in the prototypes have been of two constructions; Standard and Snubber.

The Standard hose is 15m long and 12cm in diameter. It has a spring constant of about 1500 N/m (100 lbs/ft), allowing it to stretch about 3.0 meter elastically at 4,500 N (1,000 lbs) tension. The Standard hose supports the weight of the suspended cable, electronics housing, and acoustic array, and provides compliance to minimize snap loads.

The Snubber hose is 30m long and 6.6cm in diameter. It is a much softer tether with a spring constant of only 120 N/m (8 lbs/ft), stretching about 10m at 900 N (200 lbs) load. Its lower end connects to a subsurface buoy, which supports all but 450 N (100 lbs) of the tension of the suspended array, thereby keeping the static hose tension low. The purpose of the Snubber design is to provide a softer, more compliant response to wave frequency motions than is possible with the stiffer Standard design.

Both hoses are constructed of nitrile butadiene and neoprene rubber and counterhelically arranged and embedded layers of nylon and Kevlar tirecord reinforcement. Additional reinforcement is built up at each hose end to increase ruggedness. The nylon reinforcement controls the load-elongation behavior of the hose which the Kevlar reinforcement is added for better cut resistance against fishbite. The hose terminations consist of steel flanges to which pipe sections are welded. The reinforcing layers and nitrile butadiene rubber material are built up over the pipe sections locked on by steel wire wrapping, covered with neoprene rubber, and consolidated and adhered to the pipe section by vulcanization (Figure 2). The 80m Snubber hose length is made from three equal sections which are butted together at the flanges, while the Standard hose is a single unit. Fitted end plates are bolted to the upper and lower hose flanges, and commercial gaskets are used to seal between those flange and end plate. Inside the hoses is an initially slack stop rope with considerably higher spring constant and strength than the hose, which limits the total hose stretch to a prescribed limit, typically 30 percent. Also inside the hose is an electrical conductor assembly, coiled and arranged with enough slack to prevent conductor stretch even at maximum hose elongation. The hose is fluid filled to resist crushing and to maintain a circular cross section under applied tension and external hydrostatic pressure. Electrical penetrators are built into the end plates together with valves to allow filling of the hose with fluid.

Below the hose section of the Standard design is a 500m shot of electromechanical three-conductor cable. This is a two layer steel armor construction with an outer polyurethane jacket. Through the use of an outer spaced armor layer the cable features a high degree of torque balance as well as maximized anchoring of the outer jacket to the cable armor. The 10mm diameter cable has a breaking

strength of 36,500 N (8,200 lbs). The EM cable terminates at the lower electronics case which contains the acoustic array receiver, A/D board, processor and related sensors and batteries. Suspended from the lower pressure case is a six-element hydrophone array, 50m in length. The array consists of a Kevlar strength member with individually wired hydrophones. A lead weight is suspended beneath the array to help maintain a vertical orientation.

Below the hose section of the Snubber design is the subsurface buoy and a 425m long shot of EM cable. Except for the subsurface buoy, a shorter EM cable, and a difference in the sinker weight the lower portion of the Snubber and Standard designs are identical.

ELECTRONIC DESIGN:

Sensors and Subsystems Overview: The SSAR buoy payload is centered around the tomography receiver and the systems required to support it. The primary subsystems are the tomography receiver, buoy and array navigation system, and the control, power and telemetry modules. System operation follows two primary schedules. The main schedule is for tomography reception and processing. Tomography receptions are synchronized to the source transmission schedules and offset by the estimated travel time from the source to the current receiver position. The second system schedule is for uploading data into the Argos transmitter. This schedule varies in order to maximize the data throughput. The sections below describe each of the major subsystems and the general operation of the buoy as it drifts.

Description of Operation: The acoustic sources the SSAR will listen to transmit at least 6 times per day. The SSAR will listen to each source (currently plans call for two or three sources in the Pacific) on a different day. Before a source is due to transmit the system comes out of low-power state and turns on the GPS receiver. With the current time and position from the GPS the estimated travel time from the source is computed using a database of average sound speed. This time, approximately 30 minutes for a basin-scale path, is used to set the precise point for the tomography data collection to begin.

While it waits for the tomography data collection to begin, the system reverts to low-power mode. At the appointed time the surface buoy controller wakes up, turns on the GPS receiver and then initializes the subsurface system. Precise time is transferred over the communication cable to the bottom using the one pulse per second hardware output of the GPS receiver. The bottom system then knows exactly when to begin collecting acoustic data, and that time is saved with the output data and sent back via Argos.

The navigation system is activated after the subsea unit is initialized. This includes the GPS receiver at the surface and an ultra-short baseline (USBL) acoustic positioning system at the bottom. The USBL system tracks the x-y offset and range of

the subsea package from the surface buoy and does so at a time synchronized with the GPS. This is later processed to yield an exact geographic position.

After the position fix is obtained, the tomography system begins collecting data from the array. After reception is complete the analog system is turned off and the signal processing subsystem activated. The tomography data is beamformed, match-filtered and processed for Doppler shift on the DSP. Peaks are picked from the processed data and their arrival time, signal to noise ratio and arrival angle recorded. This output is compressed to an absolute minimum and stored for later transmission back to shore via Argos. After these tasks are completed the source schedule is consulted to obtain the next time to record data and the system returns to low-power mode.

Control, Communication and Power Systems: Identical control computers are used at the surface and subsea. They are configured differently to handle their sensors and subsystems. Key features include low power sleep mode, real-time clock wake-up, solid-state power switching for all external devices and a number of configurable serial ports for communication with external devices. At the surface the control computer has to handle the GPS receiver and the Argos transmitter as well as telemetry to the bottom package. Communication to the bottom is single-duplex, but high bandwidth data throughput is easily obtain using differential RS-422. Large batteries are available at the top and bottom. Topside power consumption is governed primarily by the Argos transmitter and the GPS receiver. Subsea the data collection and processing units take similar amounts of power (several watts maximum).

Tomography System: The most important sensor on the buoy is the low-frequency array suspended at the subsea pressure case 500 meters below the surface. The 6 element array is 50 meters long. The size and the number of elements is a trade-off between cost, reliability and performance. Many factors were considered in the design including array gain, beamforming capability, directional noise, aliasing and physical aspects such as deployment and longevity.

The hydrophone elements are wired into the subsea case to an analog front-end and digitizing subsystem. The elements are 2-wire current mode and one twisted pair is required in the array cable for each element. At the midpoint of the array is a two-axis tilt sensor. This is included in order to calculate the approximate arrival angles of the acoustic multipaths observed at the array. The array will tilt depending on the local current shear. The hydrophone array cable has a Kevlar outer jacket with breaking strength selected to match the main EM cable to the surface.

The tomography digitizer is a separate subsystem that loads data into the control computer for later processing by the DSP. It is isolated as much as possible to reduce coupling of electrical noise into the low-amplitude acoustic signals. The data are direct transferred to processor memory and then to a non-volatile SRAM disk. After the tomography sampling is finished, the DSP is used to process the data as described above.

Navigation System: The buoy navigation system is as complex as the tomography data processing system. Components of the system include the GPS receiver at the surface and the USBL acoustic system subsea.

The GPS receiver is a standard off-the-shelf unit whose output is enhanced from the standard specification of 100 meters (with Selective Availability turned on), to better than 20 meters through use of post-processing on shore. Raw satellite data from the receiver on the buoy is sent back via Argos. This data is then used to reconstruct the range data (which would be too much for the available Argos bandwidth). The range data is then corrected and combined with other information to produce the corrected positions. Some of this post-processing must be performed in a classified facility.

In order to determine where the tomography array is with respect to the surface buoy, an ultra-short baseline acoustic positioning system is used. An acoustic responder at the buoy is triggered by command from below to transmit a coded ping to a high-frequency array. This array is a small encapsulated unit mounted just above the pressure case located at the bottom of the cable. This unit has its own analog front-end and digitizer, and the data is processed on a floating-point DSP. The output of the USBL is azimuth, elevation and acoustic travel time. Several other sensors are used to convert the acoustic information to actual x-y-z offset. To determine the attitude of the high frequency array, a two-axis tilt sensor is used, and rotation is measured by a digital flux-gate compass. Temperature and pressure sensors are used to make sound speed and depth estimates respectively. The sensor data is combined with the acoustic data to transform coordinate systems and optimally estimate the x-y-z offset given that the problem is overdetermined.

3. INITIAL RESULTS

ANALYSIS: Static and dynamic analyses have been performed on the SSAR prototype designs to determine their response to steady state current shear and their response to dynamic wave forcing. The static current shear case was investigated by developing a model which derived the shape of the suspended elements based on their drag characteristics. This model was run for the anticipated current shear profiles and predicted the corresponding tilts at the array. The size of the weight located beneath the array was chosen to keep the array tilt below 5° for most anticipated situations.

The dynamic analysis was performed by solving the equations of motion of the array cable in the frequency domain using a finite difference scheme. The input to the program is a specified wave spectra. The surface buoy is assumed to be a wave follower so that the input motion at the top of the array is equal to the wave motion. The hydrodynamic forces which are modeled with an "equivalent linearized" coefficient. Since the value of this coefficient depends on the response, the solution must be found by iteration.

The computer codes were checked against data collected during the field trials for the Standard (Figure 4) and Snubber (Figure 5) prototypes. The sea conditions during both tests were comparable with a wave-height standard deviation of 0.50m and a peak frequency of 0.12 Hz. The motion at the bottom of the array is amplified in the Standard SSAR. This is explained by the fact that the natural frequency of the system, which is associated with the elastic stiffness of the hose, is a 0.3 Hz. For the Snubber SSAR, the motion at the bottom of the array is damped. Here, the natural frequency associated with the hose is approximately 0.09 Hz. Numerical predictions of the tension at the surface buoy for the given wave conditions yield a standard deviation of 885N (200 lbs) for the Standard SSAR and 362N (80 lbs) for the Snubber SSAR.

Also, calculations were performed using a sea state corresponding to a strong gale. Inputting a standard deviation of 3.5m at the surface buoy and a peak frequency of 0.06 Hz, predicted motion at the bottom of the Standard SSAR will have a standard deviation of 3.6m and the tension at the surface buoy will have a standard deviation of 2,500N (540 lbs). For the Snubber SSAR, the standard deviation of the bottom motion is 1.8m and the standard deviation of the top tension is 1,000N.

LABORATORY TESTING: A program of laboratory testing has been initiated to test short sample hoses under conditions that mimic the most extreme ocean conditions they must survive. These tests are being performed at a commercial testing laboratory using equipment that stretches the hose sample slowly while bending one end back and forth at a higher frequency. To date two short Snubber style hoses have been tested to destruction with the results shown in Table 3. While both of these test hoses failed after only a few tens of thousands of cycles, the forces on them and their elongation as a percentage of unstretched length were considerably higher than those expected at sea. In addition, because they were short and their compliant sections were even shorter, the forces were concentrated to a degree not expected in a much longer hose. These results, however, have pointed out where improvements need to be made and new Snubber and Standard hose samples are being prepared for testing. These new samples will be reinforced by additional layers of rubber and longitudinal cords in the vicinity of the buoy coupling and they will be somewhat larger in diameter, which increases their overall strength in tension. This will increase stiffness (and therefore bending radius near the coupling) as well as bursting resistance. The design goal is to achieve 500,000 bending cycles before failure under the anticipated maximum hose tensions.

FIELD TESTS: A series of field tests have been performed and are being planned to test all elements of the SSAR design. These tests can be categorized as mechanical, navigational, or acoustical. The mechanical field tests are partially complete. They have consisted of two series of ocean deployments. In the first series the goal was to measure the motions and forces experienced by the two prototype SSARs under actual oceanic conditions. To achieve this goal the prototype systems were instrumented to measure the motions of the surface buoy, the tensions below the surface buoy, and the position and motions of the subsurface elements.

The fully instrumented Snubber SSAR was deployed for five days offshore Bermuda in September 1993. Figure 6 is an example of data collected on the motion of the surface buoy and the acoustic array. These data were recorded every four hours at high frequency on hard disks located at the upper and lower pressure cases. They were compared to the predictions for SSAR behavior from the dynamic models.

This first at-sea test provided important data on the Snubber response to wave frequency motions and also illuminated one serious problem. The original choice of fill fluid was Isopar, an oil frequently used in towed seismic hoses. This oil, which is 25% lighter than seawater, proved unsuitable because hydrostatic pressure inside the hose was lower than the outside pressure, with the result that the lower 10-15m of the hose collapsed. No failures occurred during the five-day test, but the collapsed hose lost some of its springiness and twisted along its length like a long ribbon which could have damaged the conductors running down its center. Freshwater is now being used as the fill fluid which is almost as heavy as seawater. Since the hose generates internal pressure as a function of tension, the small difference between freshwater and seawater will not produce hose collapse.

Following the Snubber sea test, the fully instrumented Standard SSAR was deployed offshore Bermuda in early November 1993 to collect high frequency data on its response to ocean waves. Figure 7 illustrate some of the results obtained. Again, these data were used to compare with and validate the dynamic model. After retrieving the Standard SSAR, the high frequency instrumentation and recording packages were removed and the SSAR was released for a long term drift test. The purpose of this test was to see if a SSAR prototype mechanically similar to an operational model would survive for one year at sea. The prototype was equipped with sensors to monitor tilt and vertical acceleration of the surface buoy tension beneath the buoy and vertical acceleration, pressure, orientation, tilt and acoustic noise at the lower pressure case (500m). These data are being telemetered via Service Argos twice per day. Figure 8 shows the track of the buoy to date. Time series of the tension at the top of the hose and the vertical accelerations at the bottom pressure case are shown in Figures 9 and 10, respectively. On December 5, 1993, the buoy approached Bermuda and to avoid having it going aground, it was retrieved and redeployed on December 9 about 130 km east of Bermuda.

The Standard SSAR has continued to operate normally during this time. Maximum tensions have been about 7000N (1600 lbs) during periods of strong winds and seas. While no major wind events (i.e. hurricanes) have occurred during this time, the buoy has been exposed to a number of winter storms with sustained winds over 15 m/s (30 knots).

NAVIGATION TESTS: During the September field trials the GPS correction technique was tested by comparing the GPS positions after removal of selective availability with differential GPS data collected on site. Results of this comparison is

shown in Figure 11. These data show that the position of the SSAR surface buoy can be determined to within about 10m well within the 20m requirement for buoy position accuracy.

Field tests of the other half of the navigation system, the ultrashort baseline acoustic navigation system are scheduled for March 1994. These tests will be conducted at the U.S. Navy's AUTECH range located at Andros Island in the Bahamas. In this test a fully configured SSAR buoy will be tracked independently by the AUTECH acoustic tracking system and the combined GPS and USB system. Absolute positions will then be compared to obtain a very accurate estimate of the position errors for the operational SSAR.

ACOUSTIC TESTS: Field tests of the SSAR acoustic systems are planned for April 1994 in the Pacific offshore California. These tests will involve receptions of a signal generated by a 70 Hz source installed offshore Hawaii. A fully operational SSAR will be deployed for several days in the vicinity of a SOSUS station so that data quality between the fixed and drifting receivers can be compared. Both moored and free-drifting SSAR configuration will be used to investigate the ability of the SSAR to resolve and track acoustic multipaths.

4. SUMMARY AND CONCLUSIONS

Design of the SSAR mechanical and electrical systems is nearing completion. Most parts and components have been ordered for the fabrication of ten operational units. A final decision between the Snubber and Standard mechanical designs has not been made, but all systems except the hoses and buoys are identical between the two designs. The electronic systems are nearing completion, but critical tests of the ultrashort baseline acoustic navigation system and the hydrophone array sensitivity and noise immunity are still to be done. The results of these tests, particularly the acoustic noise immunity, may have a bearing on which mechanical design is used for the operational systems.

Besides increasing the reinforcing in the critical hose coupling areas, a design enhancement in hose construction is being pursued for the operational systems. The enhanced design incorporates the electrical conductors into the hose wall rather than coiled in the middle of the hose. By building them into the hose wall they are protected from abrasion on the inside wall of the hose and from tangling and snagging on the stop rope, either of which could lead to failure. The problems with this new approach are threefold. First, the conductors must be designed so that they are not stressed when the hose elongates under load; second, they must be capable of surviving the vulcanizing process where temperatures of 150°C occur which causes problems with some insulating materials; and third, a method for taking the conductors out of the hose wall at the termination must be developed. Test hoses with conductors built into the wall will be tested under cyclic tension and bending in the laboratory to see if these goals have been met.

The operational SSARs are scheduled for deployment in the northeast Pacific between July and October 1994. Present schedules have three SSARs installed in July, three more in August, and the last four units deployed in October. The installation locations have yet to be determined, but will be designed to both stay in the area of interest for as long as possible and to create the best acoustic paths possible given source locations offshore Hawaii and California.

SSAR costs in this program are estimated at \$50,000-\$70,000 not including the initial engineering design and testing. Of these costs about 70% are hardware and 30% are labor for fabrication and assembly. The program goal is to develop a system that could be built for \$25,000 per unit in large quantity. Considering the fact that the present design is optimized for reliability rather than cost, this goal is probably achievable.

5. ACKNOWLEDGMENTS

The SSAR development program has been funded by the Advanced Research Projects Agency on the Acoustic Monitoring of Global Ocean Climate program directed by Dr. Ralph Alewine. This work relates to the Defense Advanced Research Projects Agency Grant MDA972-93-1-0004 issued by the Contracts Management Office. The United States Government has a royalty-free license throughout the world in all copyrightable material contained herein. The authors would like to acknowledge the efforts of the following individuals who have contributed to the SSAR development: Richard Arthur, John Kemp, Ken Prada, Alessandro Bocconcelli, Tom Austin, Henri Berteaux, Carter Ackerman, Mark Leach, and Phil Gibson.

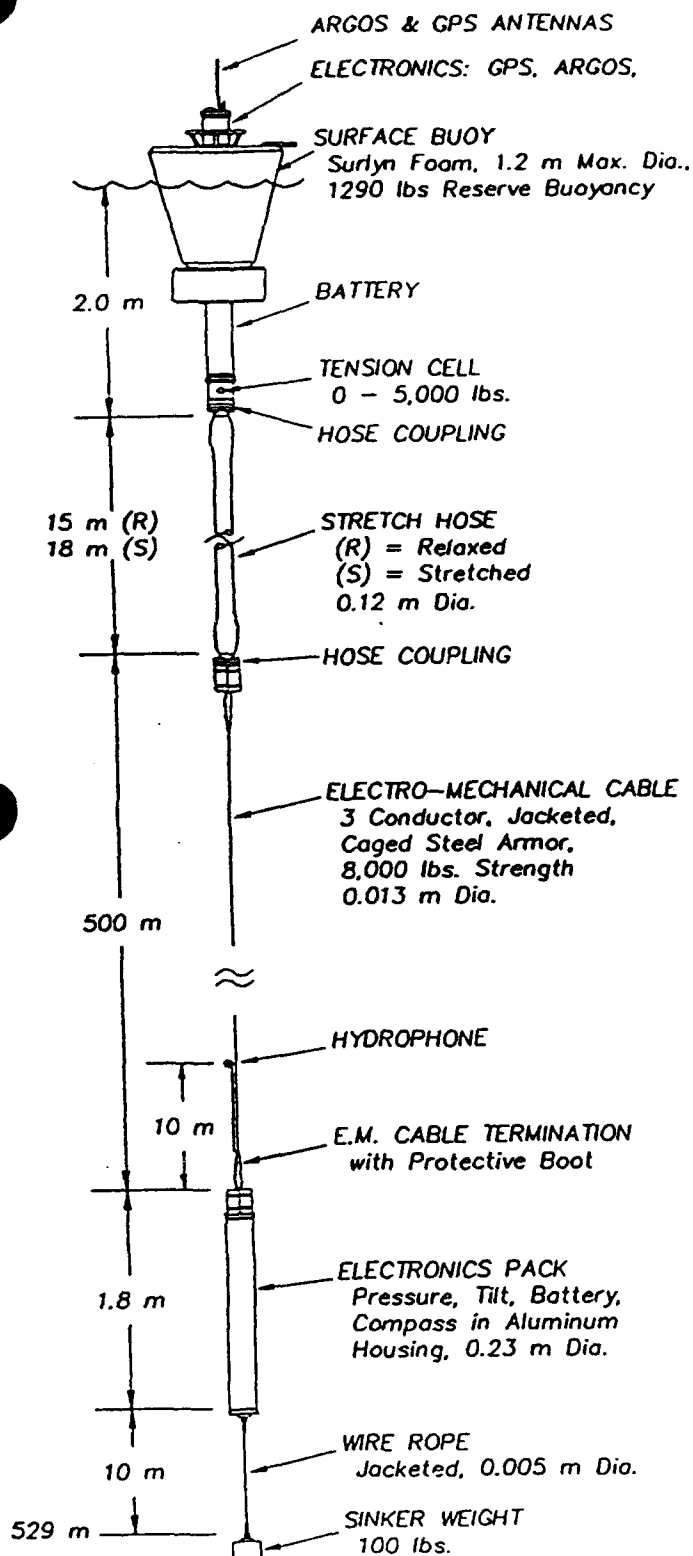
6. REFERENCES

- [1] J. L. Spiesberger, D. E. Frye, J. O. O'Brien, H. Hurlburt, J. W. McCaffrey, M. Johnson, and J. Kenny, "Global acoustic mapping of ocean temperatures (GAMOT)," IEEE Oceans '93 Proceedings, I-253-I-257, 1993.
- [2] J. Shriver, M. Johnson, and J. O'Brien, "Analysis of remotely forced oceanic Rossby waves off California," J. Geophys. Res., Vol. 96, 749-757, 1991.
- [3] A. J. Fougere, N. L. Brown, and E. Hobart, "Inductive modem for ocean data telemetry," Proceedings Oceans '91, 1165-1170, 1991.
- [4] L. E. Freitag, J. S. Merriam, D. E. Frye, and J. A. Catipovic, "A long-term deep-water acoustic telemetry experiment," Proceedings Oceans '91, 254-260, 1991.

LIST OF FIGURES AND TABLES

- Figure 1: Standard and Snubber prototype SSAR designs as used during the at-sea tests.
- Figure 2: Rubber hose construction.
- Figure 3: Block diagram of SSAR data collection, processing and telemetry systems.
- Figure 4: Measured and calculated power spectra for the motion at the bottom of the Standard SSAR for the following sea-state conditions: wave height standard deviation = 0.5m and peak frequency = 0.12 Hz.
- Figure 5: Measured and calculated power spectra for the motion at the bottom of the Snubber SSAR for the following sea-state conditions: wave height standard deviation = 0.5m and peak frequency = 0.12 Hz.
- Figure 6: Snubber motions compiled from vertical accelerations measured at the surface buoy and the acoustic array at 500m depth.
- Figure 7: Standard SSAR motions computed from vertical accelerations measured at the surface buoy and the acoustic array at 500m depth.
- Figure 8: SSAR Standard drift track from 5 December 1993 to 23 January 1994.
- Figure 9: Tension measured at the top of the Standard SSAR during December 1993. The top line is maximum tension, the bottom line is minimum tension, and the middle line is average tension. The buoy was on shore from Day 340 to 344.
- Figure 10: Maximum (upper), minimum (lower), and average (middle) vertical acceleration measured at the lower pressure case of the Standard SSAR during December 1993.
- Figure 11: GPS error plotted versus time for the Standard SSAR. (Figure provided by Applied Research Laboratory - University of Texas).
- Table 1: General SSAR requirements.
- Table 2: SSAR sensors and systems specifications summary.
- Table 3: Conditions and results of hose flex and tension fatigue tests.

SSAR "Standard" Drifting Buoy System



SSAR "Snubber" Drifting Buoy System

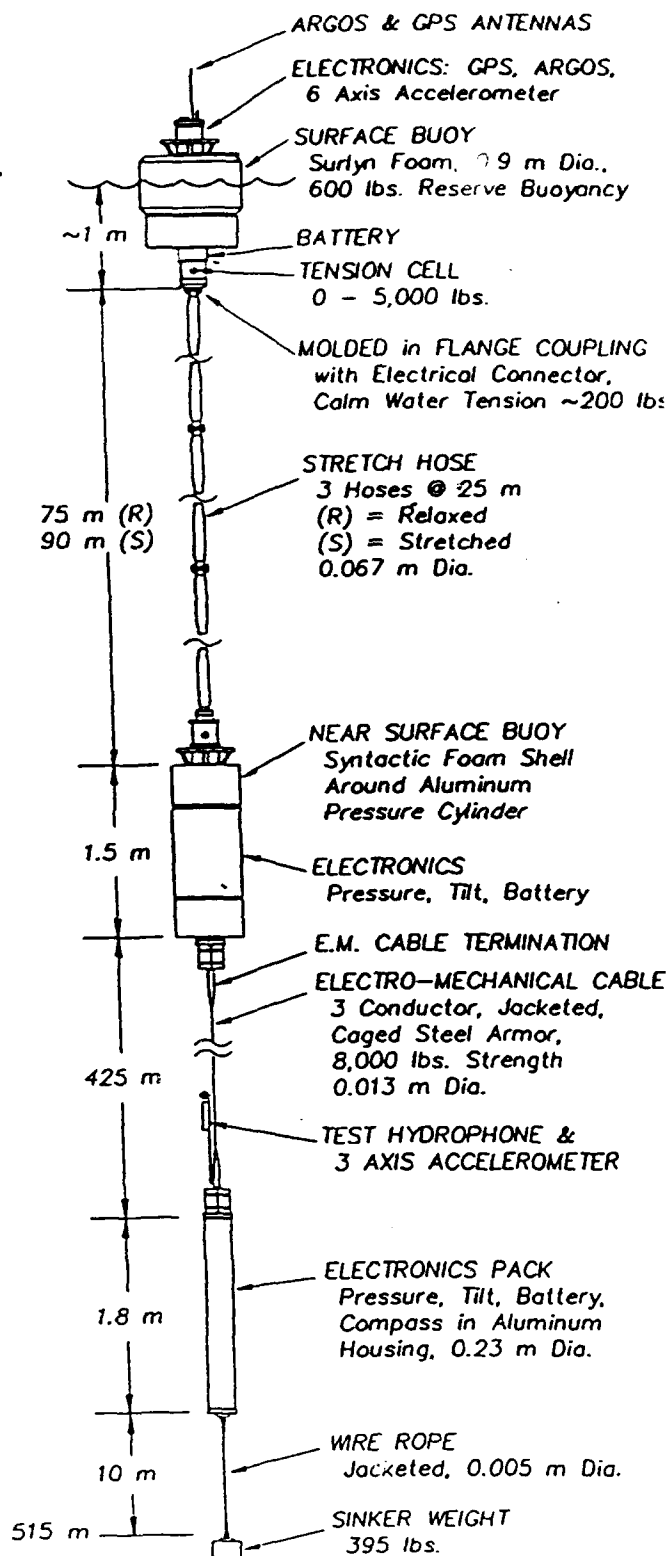
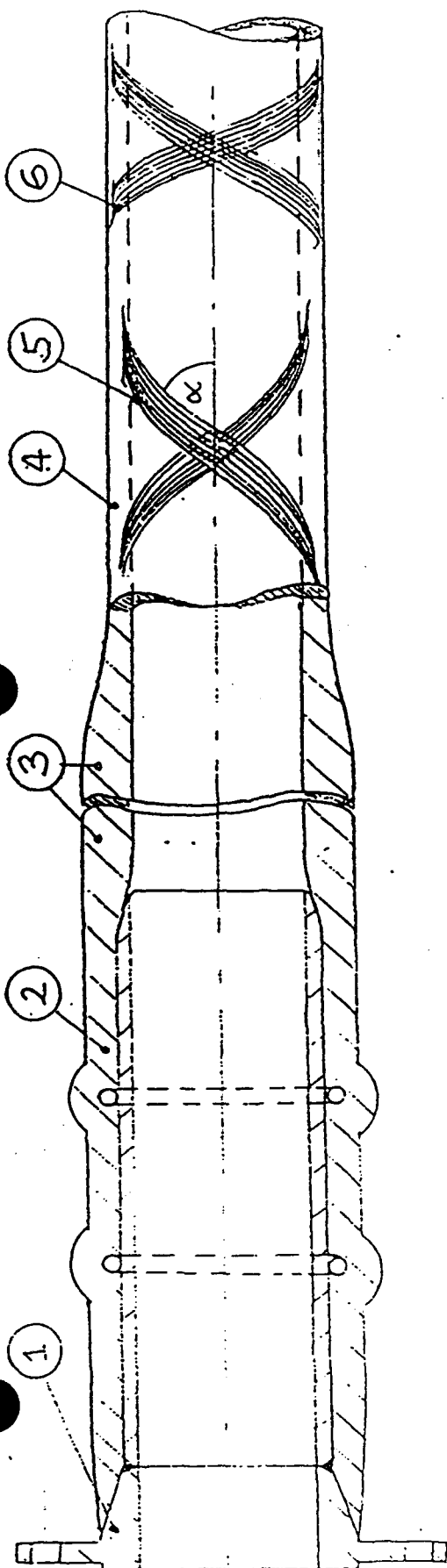


Figure 1

Standard and Snubber prototype SSAR designs as used during



- ① Standard offshore fuel hose coupling
- ② Hose body with extra reinforcement buildup at coupling
- ③ Bend limiting section of hose
- ④ Stretch section of hose
- ⑤ Counterhelical nylon reinforcement to control hose stretch
- ⑥ Fishbite protective counterhelical layer of Kevlar fabric

Figure 2

Rubber hose construction.

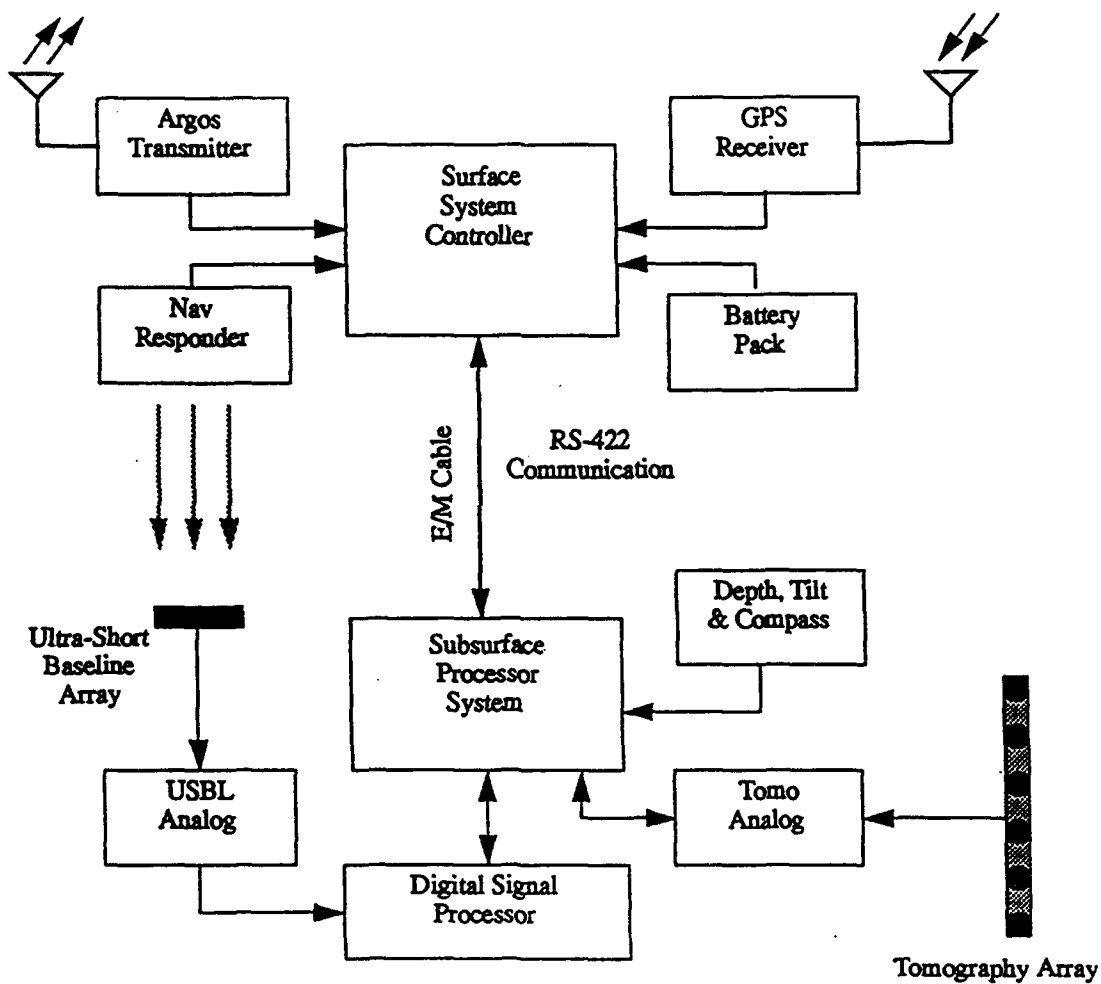


Figure 3

Block diagram of SSAR data collection, processing and telemetry systems.

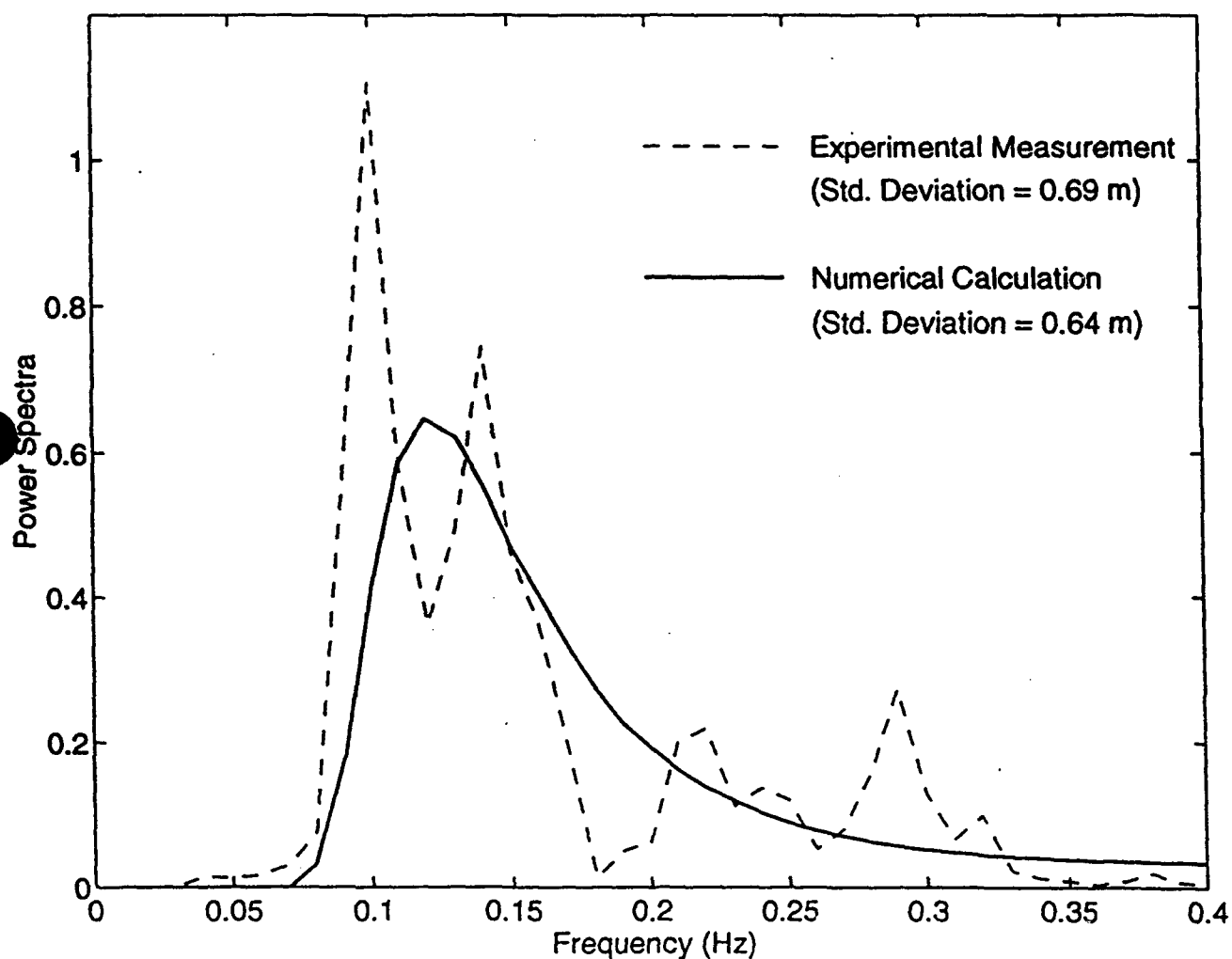


Figure 4

Measured and calculated power spectra for the motion at the bottom of the Standard SSAR for the following sea-state conditions: wave height standard deviation = 0.5m and peak frequency = 0.12 Hz

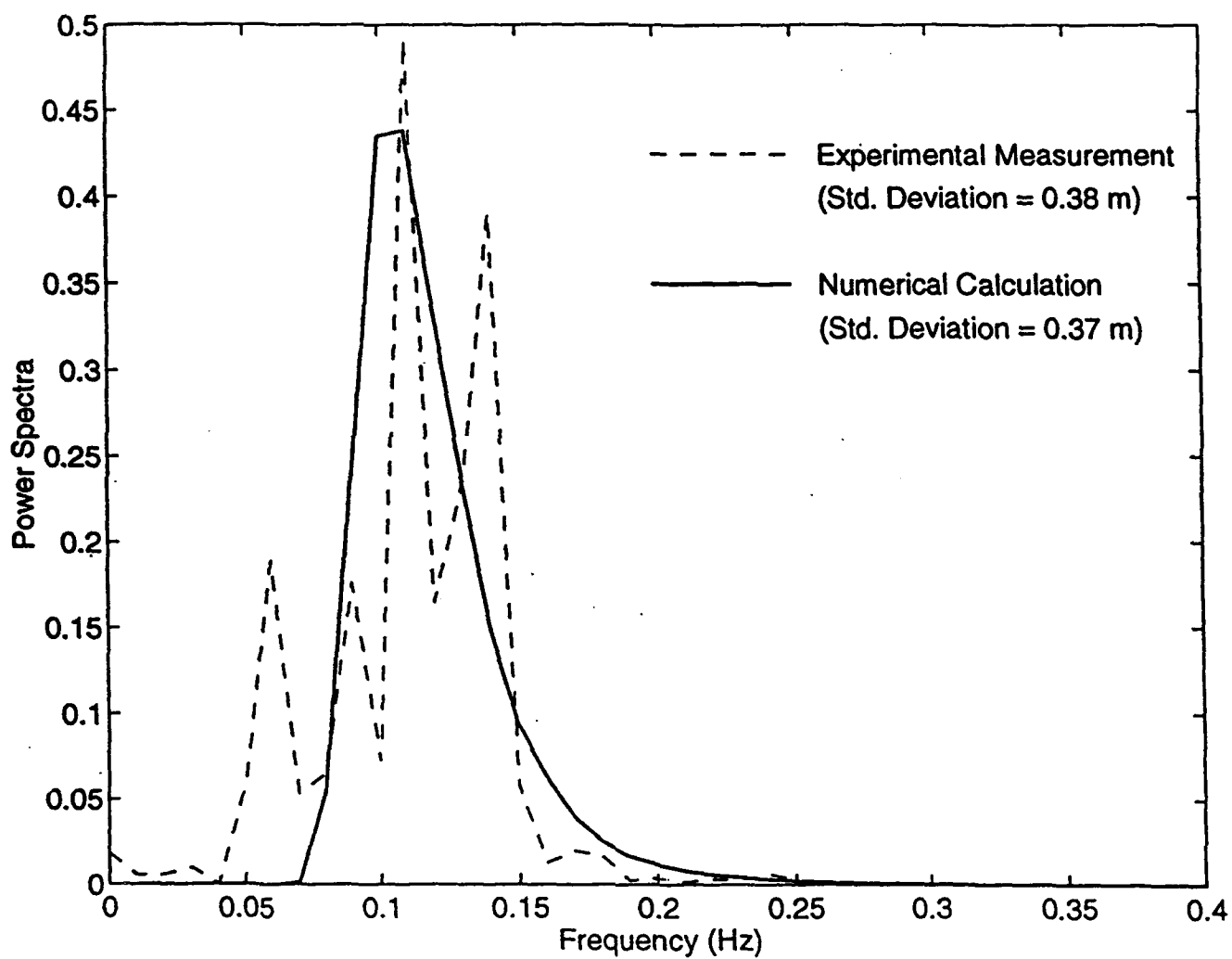


Figure 5

Measured and calculated power spectra for the motion at the bottom of the Snubber SSAR for the following sea-state conditions: wave height standard deviation = 0.5m and peak frequency = 0.12 Hz.

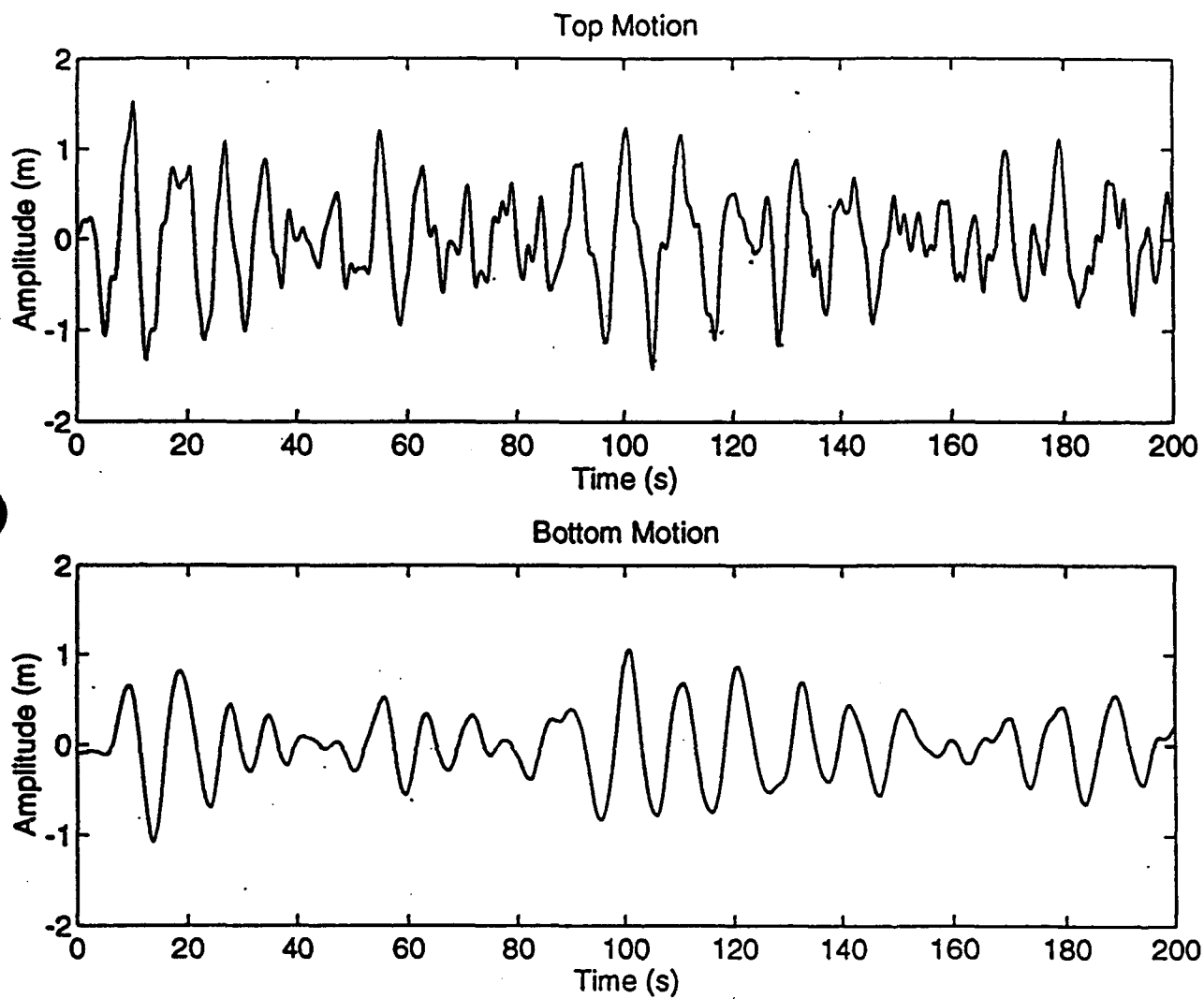


Figure 6

Shubber motions compiled from vertical accelerations measured at the surface buoy and the acoustic array at 500m depth.

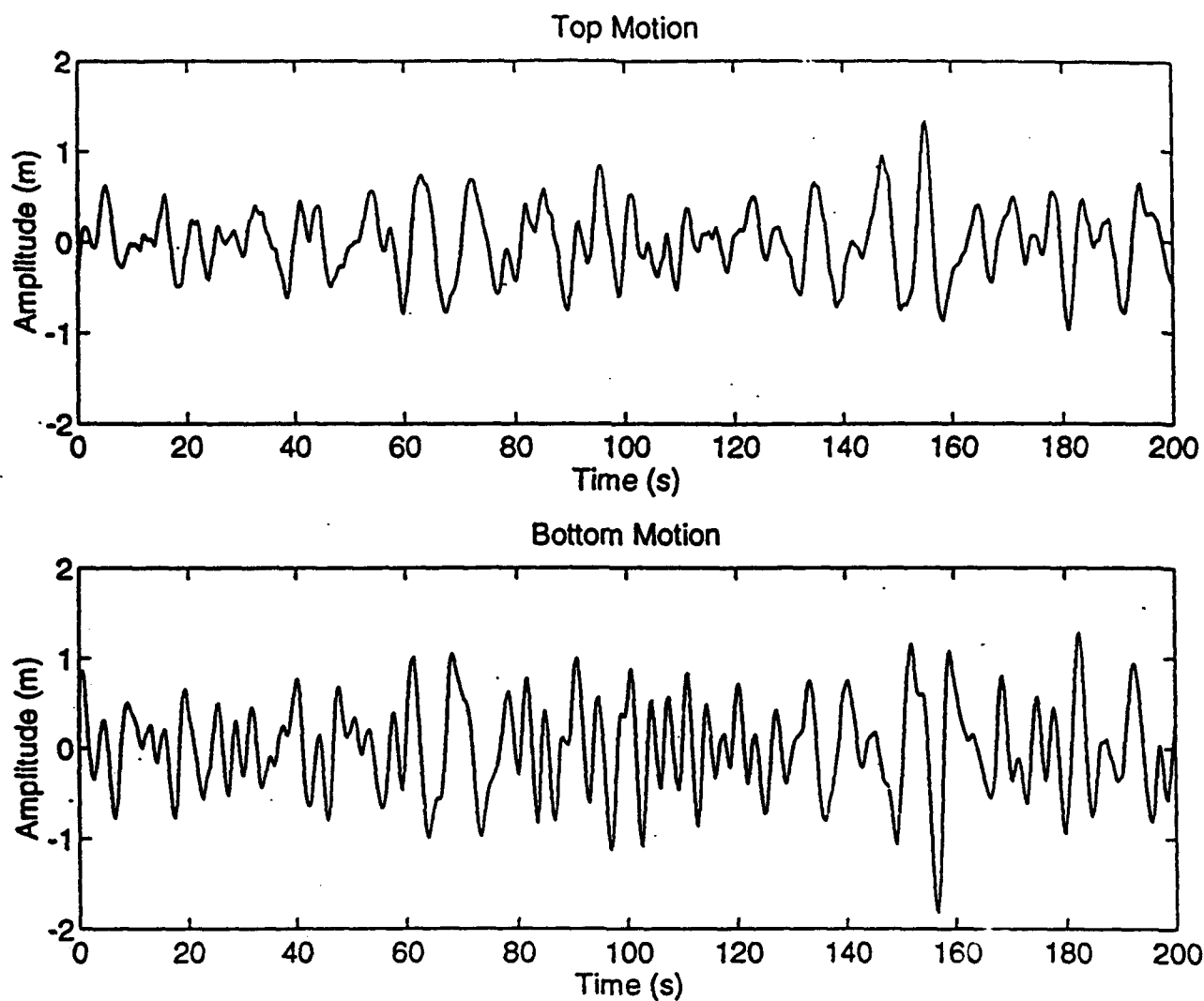


Figure 7

Standard SSAR motions computed from vertical accelerations measured at the surface buoy and the acoustic array at 500m depth.

SSAR Standard drift track from 5 December 1993 to 23 January 1994.

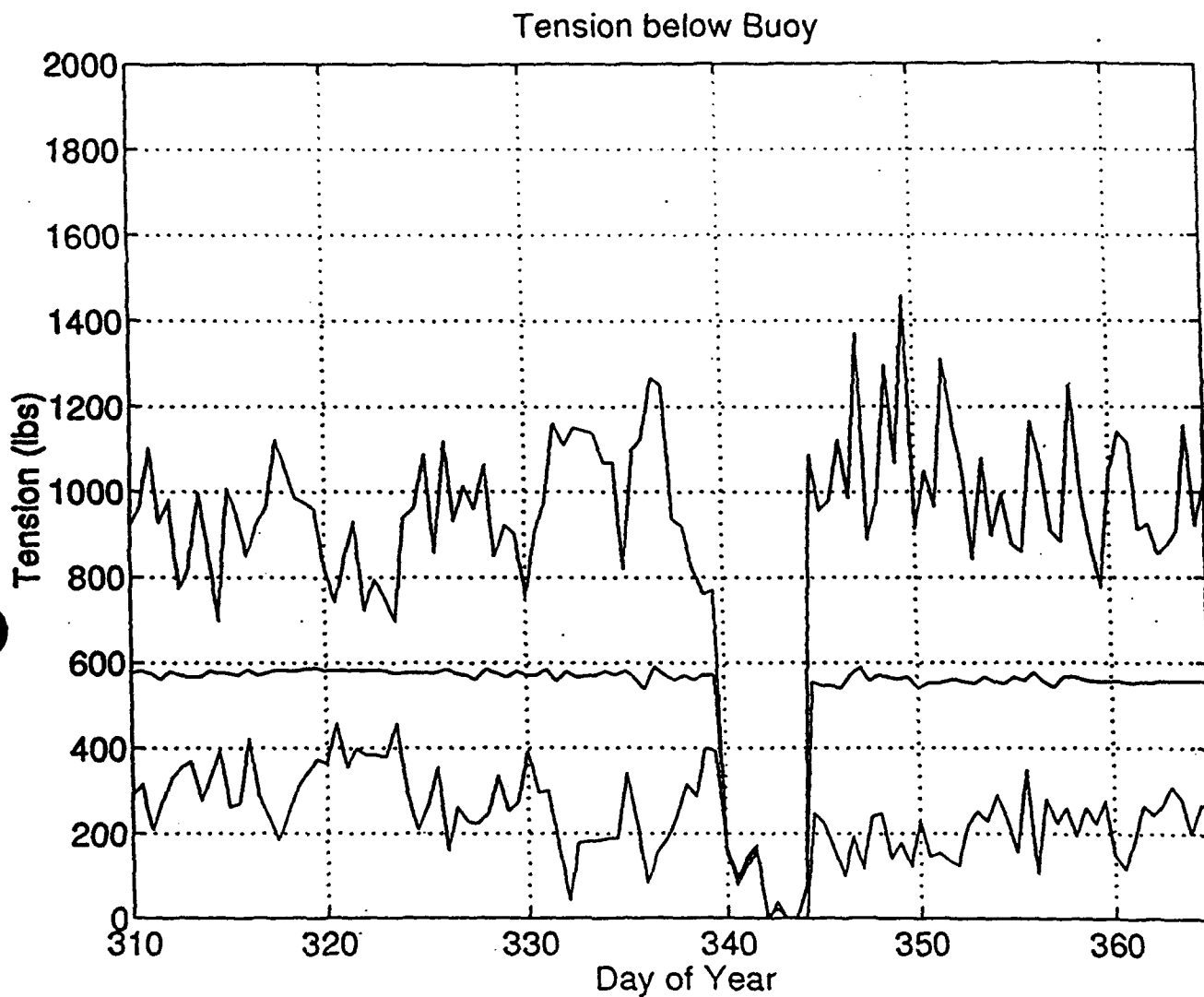


Figure 9

Tension measured at the top of the Standard SSAR during December 1993. The top line is maximum tension, the bottom line is minimum tension, and the middle line is average tension. The buoy was on shore from Day 340 to 344.

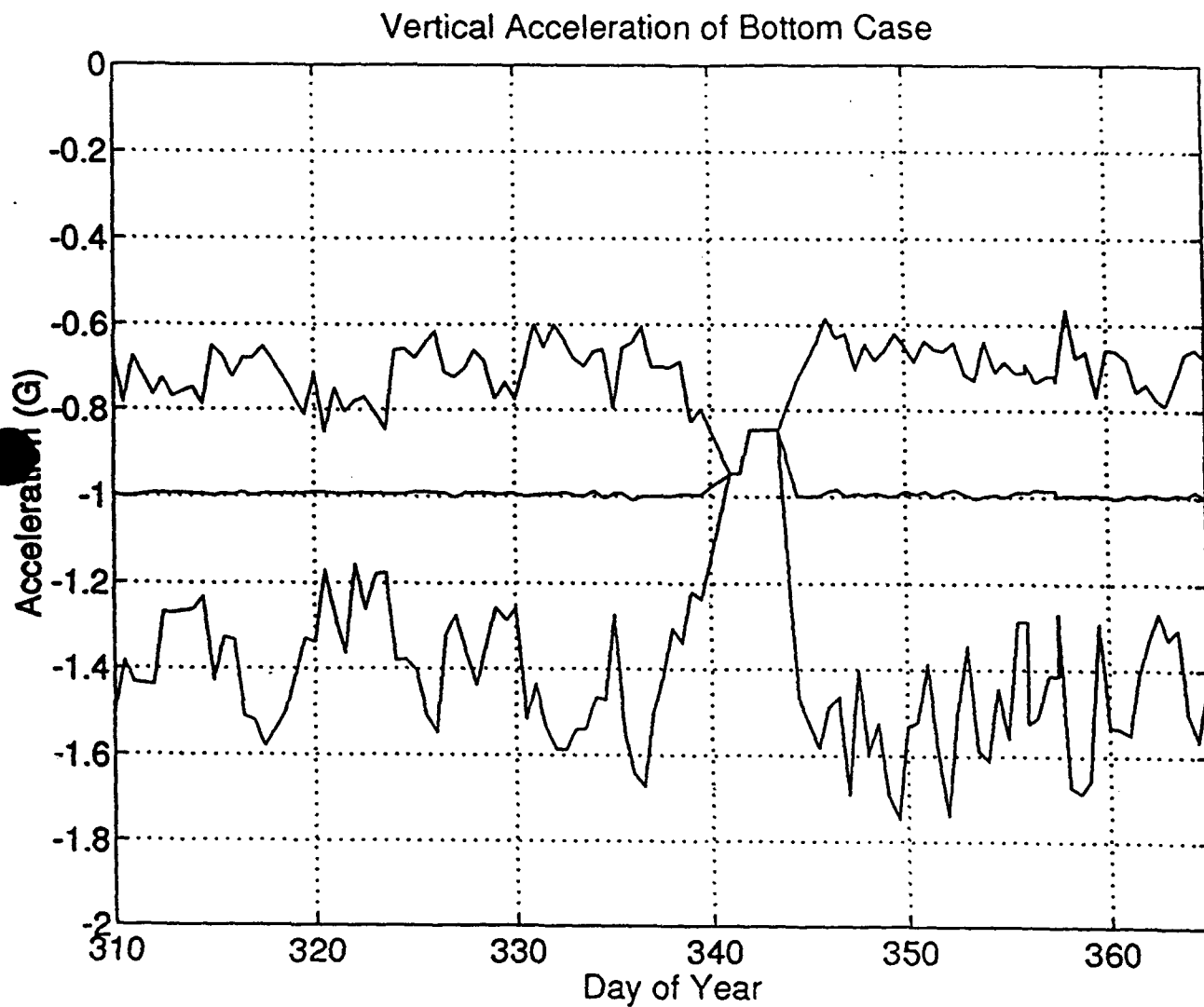


Figure 10

Maximum (upper), minimum (lower), and average (middle) vertical acceleration measured at the lower pressure case of the Standard SSAR during December 1993.

SA Corrected Solution - DGPS Solution (2D RSS)
Standard Buoy, 0000 hr, Day 262

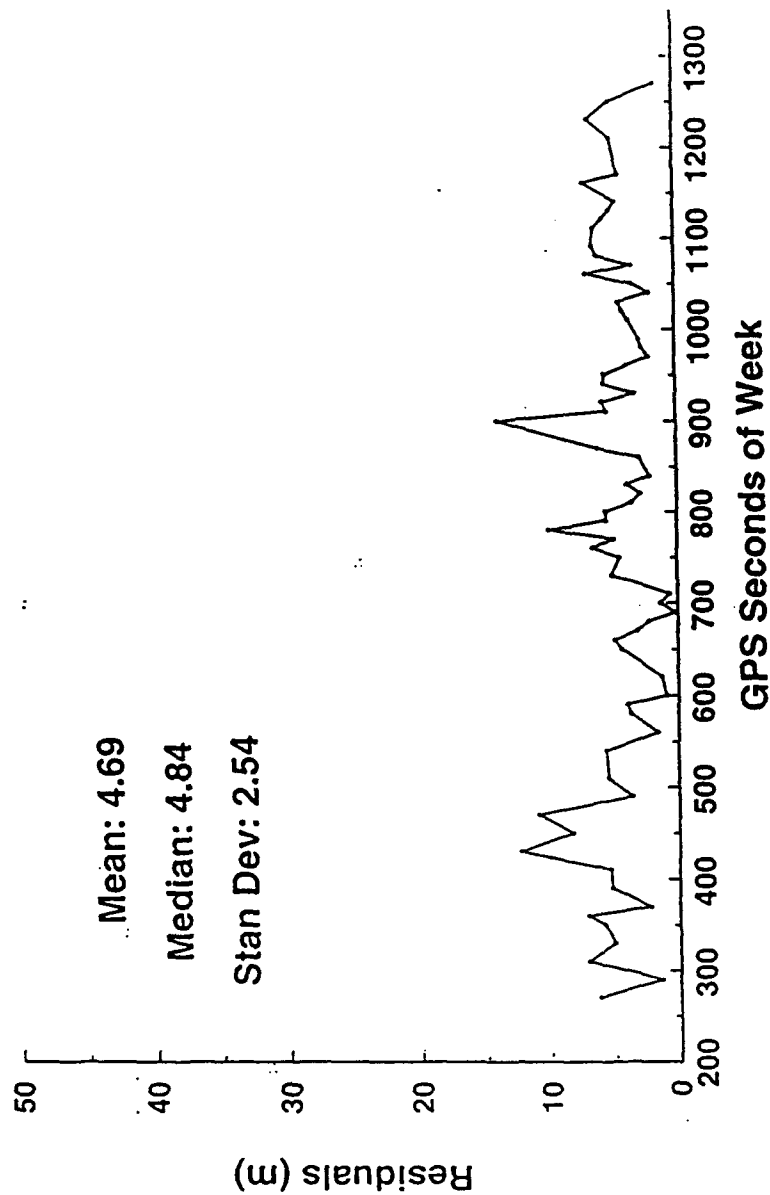


Figure 11

GPS error plotted versus time for the Standard SSAR. (Figure provided by Applied Research Laboratory - University of Texas).

Lifetime	1 Year
Position Accuracy - Buoy	± 20 meters
Position Accuracy Array	± 10 meters
Timing Accuracy	± 1 msec
Power Usage	1 watt average
Array Depth	500 meters
Array Tilt	± 10 degrees
Data Telemetry Requirement	500 bytes per reception
Data Processing Requirement	25M Flops
Array Motion	≤ 10 m vertical over 10 seconds ≤ 3 m horizontal over 10 seconds (after mean velocity removed)

Table 1
General SSAR requirements.

Item	Specification or Description
Surface Processor	DOS-based miniature PC with 1 MB memory, 2 MB non-volatile (PCMCIA) disk. Quiescent power drain less than 20 mW. Real-time clock and scheduler.
GPS Receiver	Ashtech OEM unit. 12 channels, L1 band, 1 pulse-per-second TTL output, 4 W power. Aircraft style antenna with LNA built into buoy endcap to withstand 40 psi.
Argos Transmitter(s)	Supports 2 Seimac SmartCat PTTs with integral data buffering and multiple IDs. Automatically cycles through 16 buffers and up to 4 IDs. Antenna is whip style, through-bolted to endcap and requires no additional connector.
Surface-Bottom Telemetry	RS-422 (differential plus ground) over 3 conductor E/M cable. Max rate 115 Kbits per second.
Battery Power	15 Volts. 6000 Watt-Hours capacity
Status and Housekeeping	Monitors tension between buoy and hose, battery voltage, water temperature at bottom of hose.
Item	Specification or Description
Subsurface Processor	DOS-based miniature PC with 1 MB memory, 4 MB non-volatile (PCMCIA) disk. Quiescent power drain less than 20 mW. Real-time clock and scheduler.
Subsurface Co-processor	AT&T DSP32C signal processor running at 50 MHz. 512 KB memory. Power switched.
Low-frequency Acoustic Array	6 elements with 10m spacing, -185 dB re uPa response, 2 wire current-mode interface. Kevlar outer braid with 8000 lbs breaking strength.
Low-frequency Analog Processing	4 pole high-pass and low-pass filters and programmable gain. 300 Hz per channel sampling with direct DMA transfer to processor. Optically isolated interface.
High-frequency Ultra-short Baseline Acoustic Array.	4 element encapsulated array less than 4 inches in diameter
High-frequency Analog Processing	4 channel analog front-end with programmable gain. 100 KHz per channel simultaneous sampling. with 12 bit A/D converter directly into DSP coprocessor.
Heading sensor	KVH digital compass with 0.5 deg accuracy (max)
Internal tilt sensors	2 orthogonally mounted Lucas Accustar clinometers sampled at 0.2 degrees resolution.
Array tilt sensors	Integrated 2-axis tilt sensor mounted in external pressure case at array midpoint.
Pressure sensor	0.1 percent of full scale
Temperature sensor	Platinum RTD with 0.01 deg C accuracy
Battery Power	15 Volts. 4800 Watt-Hours capacity
Status and Housekeeping	Monitors battery voltage

Table 2

**TABLE 3: Conditions and results of hose flex
and tension fatigue tests**

Hose Sample #1		Hose Sample #2
Min and Max Load	0-1,800 lbs	0-1,300 lbs
Load Cycle Duration	10 sec	9.5 sec
Elongation* at Maximum Load		14.5"
Flex Angle	45°	25°
Duration of Flex Cycle	3 sec	2.5 sec
Fill Fluid Pressure at Max Tension	220 psi	105 psi
Load Cycles till Failure	4,152	9,878
Flex Cycles till Failure	13,761	39,546
Failure Type and Localization	Burst failure at end of steel coupling. Reinforcement intact.	1/4" burst at taper of extra reinforcement hose; otherwise intact.

Table 3

Conditions and results of hose flex and tension fatigue tests.

TASK D

THE AUTONOMOUS MOORING

Last quarter ARPA directed the GAMOT Principal Investigators to submit a proposal to increase the scope of Task D (procure a 70 Hz source which could be moored autonomously) and gave the following guidelines:

- the frequency of the source will be 70 Hz.
- the schedule could be extended to accommodate the additional engineering and source procurement lead time.
- consider sources capable of transmitting m-sequences and FM codes.
- initially a dual design study could be undertaken.
- the proposal should contain go/no-go milestone decision points to ensure effective funding control.
- more than one option for each type of coding may be submitted along with recommendations as to the best course of action to follow.

Seven contractors responded to the RFP and their responses were evaluated based on the criteria listed below in the order of importance (first being the most important):

- time resolution and source level
- efficiency
- size and weight
- technical risk
 - level of development
 - contractor experience
 - contractor capabilities/facilities
- reliability
 - underwater service life of similar designs
 - reliability of design
 - maintainability
- initial development and unit costs, and
- schedule.

Site visits were conducted and additional questions asked to ensure that there was sufficient information available to fairly evaluate all of the responses.

At a meeting at WHOI in December 1993, the responses were weighted and the field of contenders was reduced to the two most promising responses.

The procurement specifications and statements of work are being finalized. The proposal will be presented to ARPA in early February 1994. A revised schedule, milestones and deliverables which reflect the increased scope of Task D will be included in the next quarterly report.

DELIVERABLES

Four deliverables were delivered during this quarter:

1. Source depth recommendation.
2. Range of acceptable SSAR depths
3. Demonstration of connection between observed climate data and ocean climate models.
4. SSAR progress report.

One deliverable is due during the next quarter:

1. Array motion compensation software..

Figure:

Fig. 1 GAMOT Deliverable Master Schedule

[illegible]

[illegible]

[illegible]

